Scuola Dottorale di Ateneo
Graduate School

Dottorato di ricerca / Doctorate
in Environmental Science

Ciclo XXVII / *28th Cycle*
Anno di discussione / *Year of defense 2016*

*Titolo/*Title

Inorganic and Organic Pollutants in Atmospheric Aerosols: Chemical Composition and Source Apportionment

SETTORE SCIENTIFICO DISCIPLINARE DI AFFERENZA: CHIM/12

Tesi di Dottorato di / *PhD thesis of Md. Badiuzzaman Khan*
matricola 956030

Coordinatore del Dottorato   **Tutore del Dottorando**

Prof. Gabriele Capodaglio   **Prof. Bruno Pavoni**

Forward

This work is the first one conducted in Veneto region, Italy with collaboration of ARPAV including important organic (OC/EC and PAHs) and inorganic pollutants (trace elements), which were characterized for longer period of time in order to quantify the source contributions of $PM_{2.5}$ at regional scale (Veneto) using receptor modelling [Factor Analysis, Positive Matrix Factorization (PMF). This dissertation has provided a general introduction and methodology for organic and inorganic pollutant. Then this research work has described the results related to chemical composition of pollutants, their seasonal and spatial vairations and meteorological factors controlling their composition in Chapter 4 (carbonaceous particulate matter), Chapter 5 (polycyclic aromatic hydrocarbons) and Chapter 6 (trace elements). Finally, the possible sources of particulate matter have been characterized in chapter 7.

The outcome of this research work has been presented in different Conferences:

1. **Poster Presentation**

i) Attended **European Aerosol Conference**, during 6-11 September, 2015, University of Milan, Italy

    Title: Organic compounds in fine particulate matter across the Veneto region, Italy: Spatial-temporal variations and meteorological influences.

    Authors: Md. Badiuzzaman Khan, Mauro Masiol, Gianni Formenton, Alessia Di Gilio, Gianluigi de Gennaro and Bruno Pavoni

ii) PhD students exhibit's research, Venezia, Gradute School, Università Cà Foscari Venezia, Convegno: PhD students exhibit's research, 14 November, 2014

    Title: Chemical Composition and Source Apportionment of Atmospheric Particulate Matter in the Veneto Region, Italy

    Authors: **Md. Badiuzzaman Khan**, Francesca Benetello, Mauro Masiol, Gianni Formenton, Bruno Pavoni (2014)

2. Oral presentation for Seminar and Conference and others

i) Attended YISAC 2014 (21st Young Investigator's Seminar on Analytical Chemistry), during June 25-28, 2014 University of Pardubice, Czech Republic.

Title: *Primary and secondary carbonaceous species in atmospheric fine particles in the Veneto region, Italy*

Author: **Md. Badiuzzaman Khan,** Mauro Masiol, Gianni Formenton, Alessia Di Gilio, Gianluigi de Gennaro, Bruno Pavoni (2014).

ii) Attended RICTA-2014, the 2nd Iberian Meeting on Aerosol Science and Technology, Universitat Rovira I Virgili, in Tarragona, Spain, during 7-9 July 2014.

Title: *Characterization of carbonaceous particulate matter and factors affecting its variations in the Veneto region, Italy.*

Author: **Md. Badiuzzaman Khan**, Mauro Masiol, Gianni Formenton, Alessia Di Gilio, Gianluigi de Gennaro, Claudio Agostinelli, Bruno Pavoni (2014).

iii) Attended XXV Congresso Nazionale della Società Chimica Italiana, during 7-12 September, 2014, Universita Della Calabria.

Title: *Spatial and seasonal variations of carbonaceous particulate matter in the Veneto Region, Italy*

Author: **Md. Badiuzzaman Khan**, Mauro Masiol, Gianni Formenton, Alessia Di Gilio, Gianluigi de Gennaro, Claudio Agostinelli, Bruno Pavoni (2014), .

iv) Attended AsiaFlux training & seminar on methane flux and carbon cycle in February, 2014, Bangladesh Agricultural University, Bangladesh.

Title: **Methane and Carbon Dioxide Flux from Peat soils and Rice fields.**

v) Worked as a researcher in "professional services for non-employee resident abroad" from October 17, 2015 – November 26, 2015 at the Ca Foscari University of Venice.

Title: Experimental data processing and scientific manuscript writing

3. **Printed Manuscript**

a) **Khan MB,** Masiol M, Hofer A, Pavoni B. 2014. Harmful Elements in Estuary and Coastal Systems. In: Bini C, Bech J (Eds.). PHEs, Environment and Human Health. Springer, Dordecht. pp. 37-83.

b) Islam MF, Majumder SS, Mamum AA, **Khan MB,** Rahman MA, Salam A. 2015. Trace metals concentrations at the atmospheric particulate matters in the Southeast Asian mega city (Dhaka, Bangladesh). Open Journal of Air Pollution 4, 86-98.

c) **Khan MB,** Masiol M, Formenton G, Di Gilio A, de Gennaro G, Agostinelli C, Pavoni B. Carbonaceous $PM_{2.5}$ and secondary organic aerosol across the Veneto region (NE Italy). Science of the Total Environment 542, 172-181.

ACKNOWLEDGEMENT

CONTENT

LIST OF TABLES

TABLE NO.	TITLE OF THE TABLE	PAGE NO.

Introduction

Methodology

Characterization of Meteorological parameters

4	**Carbonaceous particulate matter**	

Polycyclic aromatic hydrocarbons (PAHs)

TABLE NO.	TITLE OF THE TABLE	PAGE NO.

Polycyclic Aromatic Hydrocarons (PAHs)

Trace elements

CHAPTER 1

INTRODUCTION

1.1. Definition of atmospheric aerosols

The term aerosol was first used by the physical chemist Frederick G Donnan in 1918 (Whytlaw-Gray et al., 1923) and it was introduced into scientific literature as similar to the term hydrosol, a stable liquid suspension of solid particles in 1920 by A. Schmauss (Schmauss, 1920), the director of the Meteorological Central Station in Munich, Germany (Spurny, 2001, Clobeck and Lazaridis, 2010). Aerosol which as generally referred to as particulate matter is the suspension of fine solid or liquid particles in a gas (Seinfeld and Pandis, 2006). In this thesis, the terms particle/particulate matter have been used instead of aerosols.

1.2. Particle sizes and size distribution

The size of the particles determines the behaviour of particulate matter in the atmosphere, its transport and deposition in the respiratory tract and residence time. The size distribution of the particulate matter is important to understand the effects of particles on human health and visibility and to estimate the magnitude of particulate matter-climate effects. The particle distribution by number, surface area and volume is given in Figure 1.1. Atmospheric particulate matter ranges in size from a few nanometers (nm) to tens of micrometers (µm) in diameter (Seinfeld and Pandis, 2006). Generally atmospheric particles have been categorized into three distinct size classes (or modes) (Hester and Harrison, 2009) such as ultrafine (diameter: 0.01-0.1 µm or 10-100 nm), fine (diameter: 0.1-2.5 µm) and coarse mode (diameter: >2.5 µm) particles. All the three distinct size classes have different chemical composition, optical properties and deposition pattern. Moreover, their origin, transformation and removal mechanisms are also different.

Atmospheric particles have four different modes (Figure 1.2) such as nucleation mode/nuclei (Particles with diameters up to about 10 nm), aitken mode (Particles range between 10 nm to 100 nm in diameter), accumulation mode (Particles with sizes between 0.1 to 2.5 µm) and coarse mode (Particles with sizes larger than 2.5 µm). Particles both in nucleation and aitken modes are predominant in number due to their small size. Nucleation mode is the fresh aerosol formed in-situ by nucleation from gas phase. Accumulation and coarse phase modes are predominant in volume or mass distribution in most of the areas.
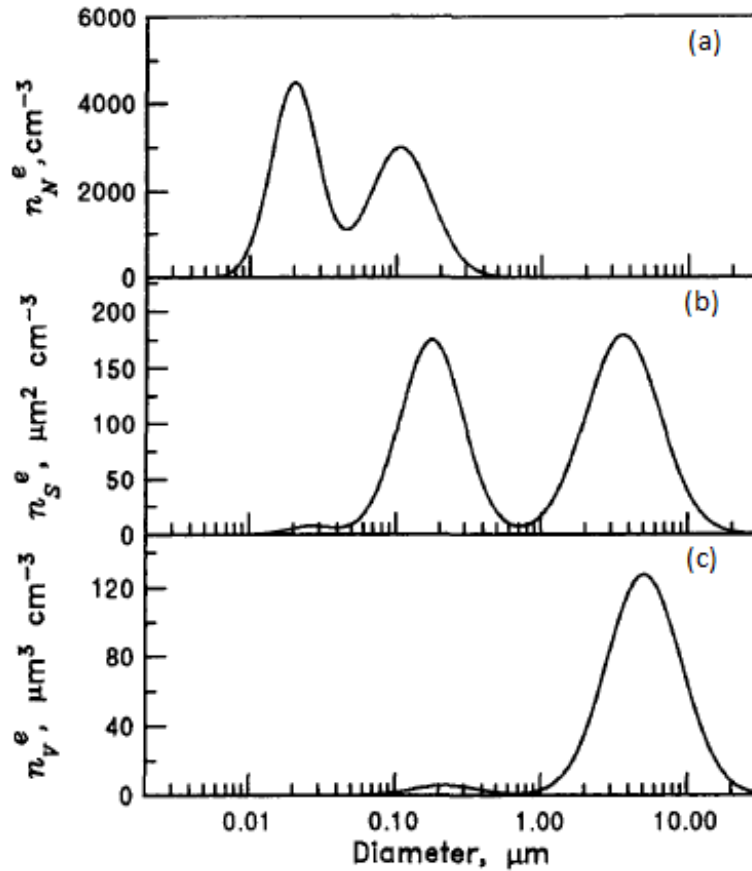
Figure 1.1. Size distribution of atmospheric particles; (a) number (b) surface (c) volume [source: Seinfeld and Pandis, 2006].

Accumulation mode particles are mainly formed due to the primary emission (condensation of secondary sulphates, nitrates and organics from gas phase; and coagulation of smaller particles). Coarse-mode particles are generally formed by mechanical processes such as wind or erosion and may be primary and secondary. Accumulation mode has two sub-modes such as condensation mode (produced from the emission of primary particles and coagulation and vapour condensation of smaller particles) and droplet mode (created during cloud processing). The size of the aerosol distribution could be characterized by number concentration (expressed as $dN/dlogD_p$ versus $logD_p$, with N the number concentration and D_p the particle diameter), surface distribution and volume or mass size distributions ($dM/dlogD_p$ versus $logD_p$, M is the mass concentration) (Figure 1.2).
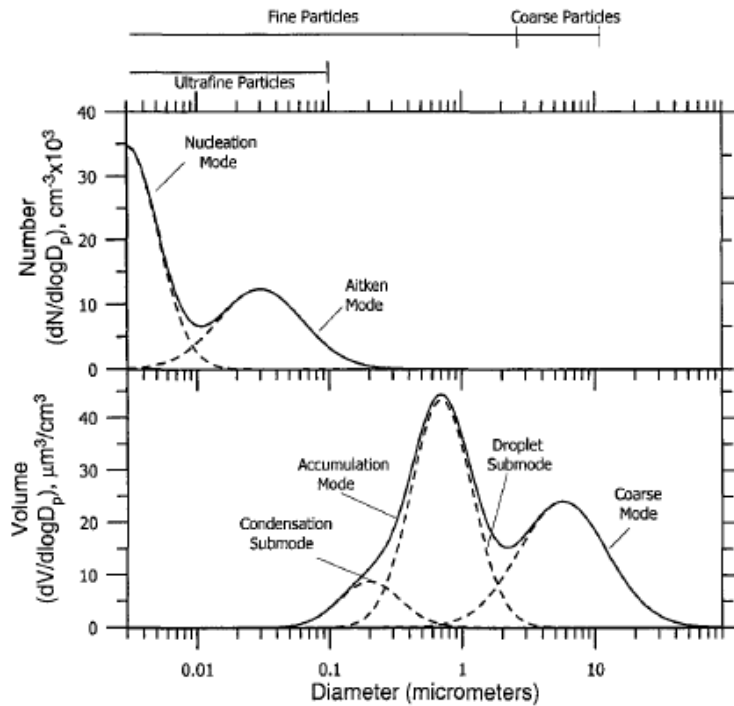
Figure 1.2. Typical number and volume distribution of atmospheric particles with the different modes (Seinfeld and Pandis, 2006).

1.3. Sources of atmospheric particulate matter

Atmospheric particulate matter has both natural and anthropogenic sources. Main natural sources are soil and rock debris (terrestrial dust), volcanic eruption, sea spray, biomass burning, forest fires, biological sources (pollen, bacteria, fungal spores etc) and reactions between natural gaseous emissions. Anthropogenic activities responsible for the emission of particles are fuel combustion, industrial processes, non-industrial fugitive sources (roadway dust from paved and unpaved roads, wind erosion of cropland, construction etc.) and transportation. Approximately, 10% of the particulate matter comes from anthropogenic sources. A significant fraction of particulate matter is secondary inorganic particles (formed from the oxidation of primary gases such as sulphur and nitrogen oxides and produced ammonium sulphate and ammonium nitrate) and organic particles [produced from the reaction of biogenic emitted species (volatile organic components)]. Particles emitted from both natural and anthropogenic sources are given in Table 1.1.

Table 1.1. Natural and anthropogenic sources of primary and secondary aerosols in global scale [based on Maenhaut, 1996; Raes et al., 2000; Mather et al., 2003; Jaenicke, 2005]. Adapted from Wang (2010).

Source		Particle size (µm)	Emission (Tg/yr)
Natural			
Primary	Soil dust (mineral aerosols)	D <1	110
		D =1-2	290
		D =2-20	1750
	Sea to air flux of sea salt	D <1	54
		D=1-16	3290
	Biogenic organic matter	Coarse	1000
	Volcanic ash	Fine	20
Secondary	Sulphate from aerosols from marine biogenic gases (mainly DMS)	Fine	16-32
	Sulphate aerosols from terrestrial biogenic gases	Fine	57
	Nitrate aerosols from NO_x (lightning, soil microbes)	Mainly coarse	3.9
	Organic matter from biogenic gases	Fine	16
	Sulphate aerosols from volcanic SO_2	Fine	9-21
Natural subtotals		**At least**	**6600**
Anthropogenic			
Primary	Aerosols from all kinds of fossil fuel burning, cement manufacturing, metallurgy, waste incineration, etc	Coarse and fine	100
	Soot (black carbon) from fossil fuel burning (coal, oil)	Fine	8
	Soot from biomass burning	Fine	5
	Biomass burning without soot	Fine	80
Secondary	Sulphate from SO_2 (mainly from coal & oil burning)	Fine	140
	Nitrate aerosol from NO_x (fossil fuel and biomass combustion)	Mainly coarse	36
	Organic matter from anthropogenic gases	Fine	5
	Organic matter from biomass burning	Fine	54
	Organic matter from fossil fuel burning	Fine	28
Anthropogenic Subtotal			**460**
Total			**7100**

1.4.   Effects of atmospheric particulate matter

1.4.1. Impacts of atmospheric particulate matter on human health

Various epidemiological and toxicological studies have provided evidence that particulate matters are correlated with severe health impacts especially, respiratory, allergic, cardiovascular diseases and even mortality (Bernstein et al., 2004; Katsouyanni et al., 2001; Pope et al., 2004; Samet et al., 2005). A correlation between daily mortality and changes in particulate matter has been found from daily time-series data [Schwartz and Dockery, 1992; Schwartz, 1994]. Lung cancer and cardiopulmonary mortality increase with the increases of fine particulate matter $PM_{2.5}$ (Dockery et al., 1993; Pope et al., 1995; Schwartz et al., 1996; Pope et al., 2002). About 6% cardiopulmonary and 8% lung cancer risk are increased for every 10 µg m^{-3} elevation in fine particulate air pollution. Long-term exposure to atmospheric aerosols may have an association with cardiovascular problems, respiratory morbidity and mortality particularly for infants and elderly people.
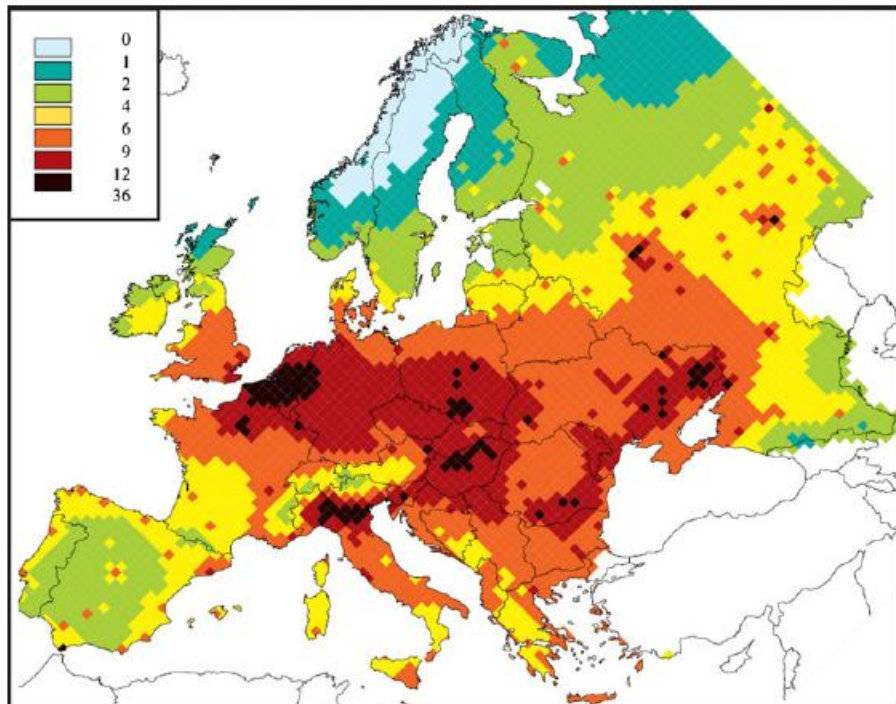
Figure 1.3. Loss of life expectancy due to ambient aerosols in Europe in 2000. Calculation results for the meteorological conditions of 1997 (CAFÉ 2011).

However, strong correlation is also observed between short-term exposure to ambient particles and hospital admissions or consultations of physicians (Hauck et al., 2004, Schulz et al., 2005; Tie et al., 2009). A recent research reported approximately 22,000-52,000 annual deaths in the United States (from 2000) and ~370,000 premature deaths in Europe during 2005 due to particulate matter pollution (Mohapatra and Biswal, 2014). Loss of life expectancy in Europe due to ambient aerosols (PM_{10}) has been delineated in Figure 1.3 which is prepared by the CAFÉ (Clean Air For Europe) steering group of the European Commission from meta-analysis of epidemiological data and the measured mass concentration of $PM_{10.}$

Particle size is the main factor that determines where the pollutant will deposit in the respiratory tract of human body. Particulate matter, PM_{10} penetrates thorough the upper airways (nose, mouth, nasopharynx and larynx) and can be settled in conducting airways (bronchi and upper part of lungs). Particulate matter, $PM_{2.5}$ can be deposited in gas-exchange part (deep) of the lung, whereas ultrafine particles (< 100 nanometers) deposit in alveoli and may penetrate through the lungs to infect other organs (Hester and Harrison, 2009). Respiratory deposition of the particulate matter in human body is shown in Figure 1.4.
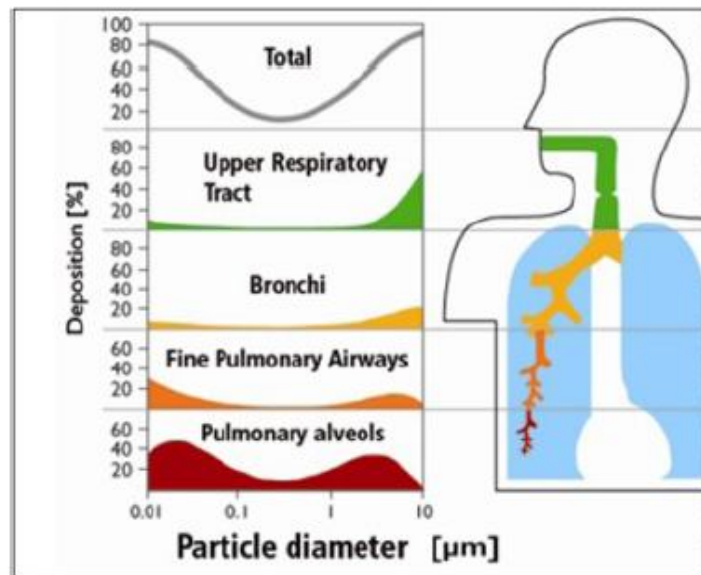
Figure 1.4. Deposition of different sized particles in the respiratory system (ICAO, 2005).

According to the Figure 1.4, approximately 40% of the ultrafine particles ($PM_{0.1}$, particles with a diameter up to 0.1 µm) can deposit in the pulmonary alveoli while 60% of the particle $\leq$ 10 µm (PM_{10}) can be retained in the upper respiratory tract.

The occupational health community has classified airborne particles into different aerosol fractions based on the penetration of particles in the various regions of the respiratory tract (Figure 1.5). This convention has classified particles into inhalable ($D_{ae} \leq$100 µm; they enter the respiratory tract including head airways), thoracic (D_{ae} <30 µm; they penetrate into trachea-alveolar region of the lung; lung airways and the gas-exchange regions of the lung) and respirable particles (D_{ae} <10 µm: they penetrate into the alveolar region of the lung; gas-exchange region of the lung (Wilson et al., 2002).
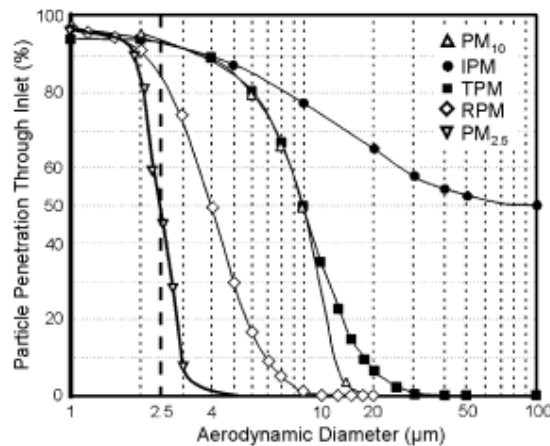
Figure 1.5. Occupational health size-cuts (Wilson et al., 2002)

However, penetration and deposition position of the particles in the respiration systems are dependent on not only their size but also on their shape and chemical composition (Harrison and Yin, 2000). Various aerosol pollutants have toxicological effects. Several trace elements especially lead (Pb), cadmium (Cd), manganese (Mn) and arsenic (As) present in the particulate matter are hazardous to human health (Manahan, 1993). Nowadays scientists are concerned about organic pollutants found in atmospheric particulate matter especially polycyclic aromatic hydrocarbon (PAHs) and dioxins for their toxicity and carcinogenicity (Poschl, 2002, Hu et al., 2007; Viana et al., 2008a).

Bio-aerosols such as viruses, bacteria, spores, pollen and insect parts (i.e. house dust mites) cause diseases or allergenic reactions in humans (Matthias-Maser et al., 2000). Major health impacts associated to biogenic fractions are inflammation and irritation (Fujii, 2002). Although many studies have proved that atmospheric particulate matter have strong impact on human health, but due to a limited knowledge on sources, composition, properties and processes, the actual effects of particulate matter on human health and their mechanisms are not fully understood (Poschl, 2005). Several possible mechanisms by which atmospheric particles may affect human health are given here below (Bernstein et al., 2004).

- Pulmonary inflammation induced by PM or O_3.

- Free radical and oxidative stress generated by transition metals or organic compounds (e.g. PAHs).

- Covalent modification of key intracellular proteins (e.g. enzymes).

- Inflammation and innate immune effects induced by biological compounds such as endotoxins and glucans.

- Adjuvant effects in the immune system (e.g. DPM and transition metals enhancing responses to common environmental allergens).

- Procoagulant activity by ultrafine particle accessing the systemic circulation.

- Suppression of normal defense mechanism (e.g. suppression of alveolar macrophages functions).

1.4.2. Effect of atmospheric particulate matter on climate

Both greenhouse gases and particulate matter (microscopic airborne particles or droplets) can alter global radiation budget and hence climate [IPCC (Intergovernmental Panel on Climate Change), 2007]. However, the mechanism behind the global climate change due to atmospheric aerosols is more complicated and far less understood. Greenhouse gases absorb or trap infrared radiation at the top of the atmosphere, while aerosols increase the reflection of solar radiation back to the space through various radiative and physical processes (Ramanathan, 2001). Moreover, atmospheric particles are also capable of heating the lower atmosphere when they contain light absorbers likely elemental carbon and mineral dust (Andreae, 2001). The warming effects caused

by black carbon may be neutralized or balanced by the cooling effect of the sulphate aerosols (Jacobson, 2000). Greenhouse gas forcing has global significance while the aerosol forcing in mainly regional and seasonal (Bengtsson et al., 1999). The Climate is influenced by atmospheric particles in both directly (by the scattering and absorption of solar radiation) and indirectly (as cloud condensation nuclei).

Radiative forcing components

	RF Terms		RF values (W/m²)	Spatial scale	LOSU
Anthropogenic	Long-lived greenhouse gases	CO_2	**1.66** [1.49 to 1.83]	Global	High
		N_2O / CH_4 / Halocarbons	**0.48** [0.43 to 0.53] **0.16** [0.14 to 0.18] **0.34** [0.31 to 0.37]	Global	High
	Ozone	Stratospheric / Tropospheric	**-0.05** [-0.15 to 0.05] **0.35** [0.25 to 0.65]	Continental to global	Med
	Stratospheric water vapour from CH_4		**0.07** [0.02 to 0.12]	Global	Low
	Surface albedo	Land use / Black carbon on snow	**-0.2** [-0.4 to 0.0] **0.1** [0.0 to 0.2]	Local to continental	Med -Low
	Total Aerosol — Direct effect		**-0.5** [-0.9 to -0.1]	Continental to global	Med -Low
	Total Aerosol — Cloud albedo effect		**-0.7** [-1.8 to -0.3]	Continental to global	Low
	Linear contrails		**0.01** [0.003 to 0.03]	Continental	Low
Natural	Solar irradiance		**0.12** [0.06 to 0.30]	Global	Low
	Total net anthropogenic		**1.6** [0.6 to 2.4]		

Radiative Forcing (W/m²)

Figure 1.6. Global average radiative forcing (RF) (Wm^{-2}) for the period from pre-industrial (1750) to 2005. (IPCC, 2007)

Positive or negative changes in energy balance because of GHGs (Greenhouse gases) and aerosols, land cover and solar radiation are expressed as radiative forcing used to evaluate warming or cooling effects on global climate change (IPCC, 2007). Changes imposed on the Earth's radiation balance are known as radiative forcing (Seinfeld and Pandis, 2006). IPCC (2007) defined it as "the change in net (down minus up) irradiance (solar plus longwave; in W m^{-2}) at the tropopause after allowing for stratospheric temperatures to readjust to radiative equilibrium, but with surface and tropospheric temperatures and state held fixed at the unperturbed values". Changes happen from

scattering and absorption of ambient aerosols is known as direct radiative forcing. Contribution of aerosol to radiative forcing arises from sulphate aerosols, fossil fuel, soot and biomass burning (Penner et al., 1993; Robock 1991). IPCC (2007) has calculated radiative forcing considering anthropogenic aerosols (primary sulphate, organic carbon, black carbon, nitrate and dust) and found total direct radiative forcing is -0.5 (-0.9 to -0.1) W m^{-2} while indirect cloud albedo effect is -0.7 W m^{-2} (-1.8 to -0.3 W m^{-2}). Estimated radiative forcing from beginning of the Industrial Era to 2005 from quantifiable natural and anthropogenic forcing sources is given in Figure 1.6 (IPCC, 2007).
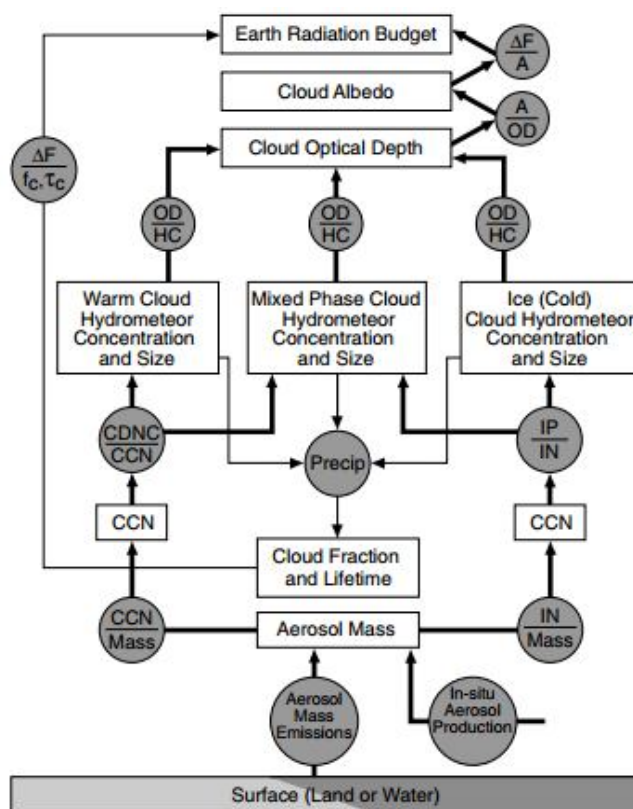
Figure 1.7. Flow chart showing the process linking aerosol emissions or production with changes in cloud optical depth and radiative forcing. Bars indicate functional dependence of the quantity on the top of the bar to that under the bar. Symbols: CCN (Cloud condensation nuclei, CDNC (Cloud droplet number concentration), IN (Icc Nuclei), IP (Ice particles), OD (Optical depth), HC (Hydrometeor concentration), A (Albedo), f_c (Cloud fraction), τ_c (Cloud optical depth), ΔF (Radiative forcing). (IPCC, 2001)

11

Broadly, indirect forcing may be defined as the process by which aerosols perturb the Earth-atmosphere radiation balance by modifying cloud albedo and cloud amount (IPCC, 2001). A diagram of the processes involve in indirect forcing linking several intermediate variables such as aerosol mass, cloud condensation nuclei (CCN) concentration, ice nuclei (IN) concentration, water phase partitioning and cloud optical depth is shown in Figure 1.7. As an indirect effect, aerosols in the lower atmosphere can modify the number and size of the cloud droplets (Kaufman et al., 2002) or cause effects on precipitation efficiency (Poschl, 2002). Indirect effect arises when aerosol number concentration increases from anthropogenic sources which lead to the formation of cloud condensation nuclei. Cloud droplets formed on atmospheric particles, known as cloud condensation nuclei, lead to the increase in the number of cloud droplets with smaller radii, which in turn form more scattering of shortwave radiation i.e higher cloud albedos (Seinfeld and Pandis, 2006). This phenomenon is known as first indirect effect or Twomey effect (Cloud albedo effect). Changes in the number concentration of aerosols lead to the variations/reduction of the size of cloud droplets. This process increases cloud lifetime by decreasing or suppressing precipitation, known as the cloud lifetime aerosol effect or second indirect effect or Albrecht effect. Effectiveness of aerosol particles to work as a nucleus for the formation of water droplet (to become activated as a CCN) depends on its size and response to water (IPCC, 2001). Sulphates, sodium chloride and other water-soluble salts and inorganic acids are efficient as CCN (Hudson and Da, 1996).

1.4.3. Visibility

Visibility degradation is the most observable impact of air pollution and considered as a primary and general index of ambient air quality in an urban area (Watson, 2002). The term visibility (also known as "visual range") may be defined as the farthest distance an object can be seen against the sky from the horizon (Seinfeld and Pandis, 2006). This depends on several factors such as optical properties of the atmosphere, amount and distribution of light, characteristics of the objects and properties of the human eye (Seinfeld and Pandis, 2006). Visibility is reduced by the absorption and scattering of solar radiation by both gas molecules and aerosol particles (Figure 1.8).
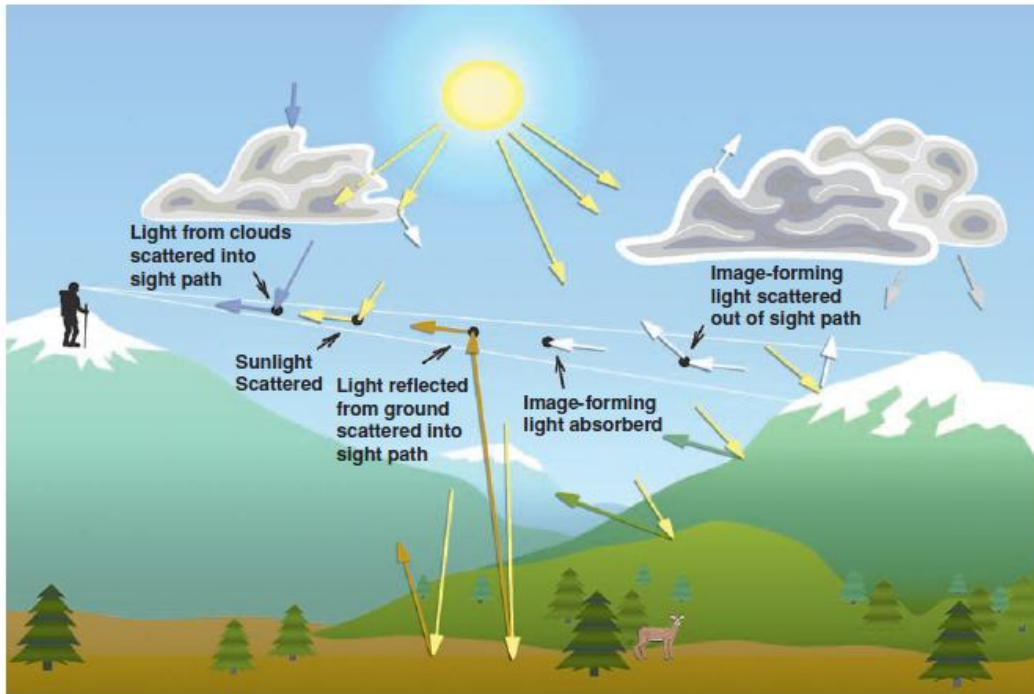
Figure 1.8. Processes by which particles and gases in the atmosphere affect visibility (Adapted from Malm, 2000).

These two processes, scattering (changes the direction of photon) and absorption (removes the photon from the beam by conversion to thermal or electronic energy) are collectively known as light extinction and responsible for visibility reduction. Atmospheric light extinction is characterized by the extinction coefficient (b_{ext}) and can be divided into four components: absorption by gases (b_{ag}), scattering by gases (b_{sg}), absorption by particles (b_{ap}) and scattering by particles (b_{sp}).

$b_{ext} = b_{ag} + b_{sg} + b_{ap} + b_{sp}$ ……………………. (1.1)

Nitrogen oxide is the only light-absorbing gas present in the troposphere. Gaseous scattering (known as Rayleigh scattering) has minor contribution to visibility reduction in urban areas whereas scattering and absorption by atmospheric particles (known as Mie scattering) have been found to be more prominent reason of light extinction in urban areas (Chan et al., 1999). Accumulation mode aerosol particles (0.1 to 1 µm) are more effective in reducing light than nucleation or coarse mode particles. (Seinfeld and Pandis, 2006).

1.5. Removal mechanism

Atmospheric particles are taken away from the atmosphere by following two mechanisms such as dry deposition (deposition at the Earth's surface) and wet deposition (incorporation with cloud droplets during formation of precipitation) (Seinfeld and Pandis, 2006). Atmospheric cycling of atmospheric particles has been given in Figure 1.9.
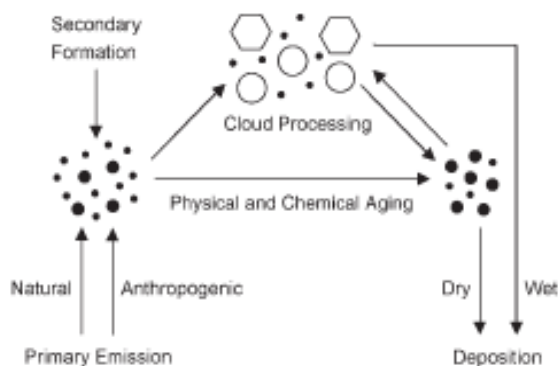
Figure 1.9. Atmospheric cycling of particulate matter (Adapted from Poschl, 2005).

1.5.1. Dry deposition

Dry deposition is the moving of gaseous and particulate matter from the atmosphere to the surface in the absence of precipitation. The main factors affecting particles of dry deposition are i) level of atmospheric turbulence, ii) the chemical properties of the depositing species, iii) the nature of the surface itself (Seinfeld and Pandis, 2006). The level of atmospheric turbulence is the layer closest to the ground which regulates the rate of the species, which are transported down to the surface. Solubility and chemical properties affect the uptake of gaseous species at the surface, while size, density and shape decide the captured position by the surface of the particles. Bounce-off of the particle may be higher in smooth surface, whereas highly variable vegetable surface accelerates dry deposition.

The dry deposition process of gases and particles includes three steps such as i) aerodynamic down transport through the atmospheric surface layer to a very thin layer of stagnant air just adjacent to the surface, ii) molecular (gases) or Brownian (for

particles) transport across this thin stagnant layer of air, known as quasi-laminar sublayer, to the surface itself and iii) uptake at the surface (Seinfeld and Pandis, 2006).

Deposition velocity is defined as,

$$V_d = 1/r_t = 1/(r_a + r_b + r_a r_b v_s) + v_s \quad \ldots\ldots\ldots\ldots\ldots\ldots(1.2)$$

Where, r_a is the aerodynamic resistance, r_b is quasi-laminar layer resistance and v_s is the particles settling velocity. Settling velocity v_s is generally expressed by the following equation,

$$V_s = \rho_p D^2_p C_c / 18\mu \quad \ldots\ldots\ldots\ldots\ldots\ldots\ldots\ldots\ldots\ldots\ (1.3)$$

Where,

ρ_p = density of the particles

D = particle diameter

μ = viscosity of air

C_c = slip correction

1.5.2. Wet deposition
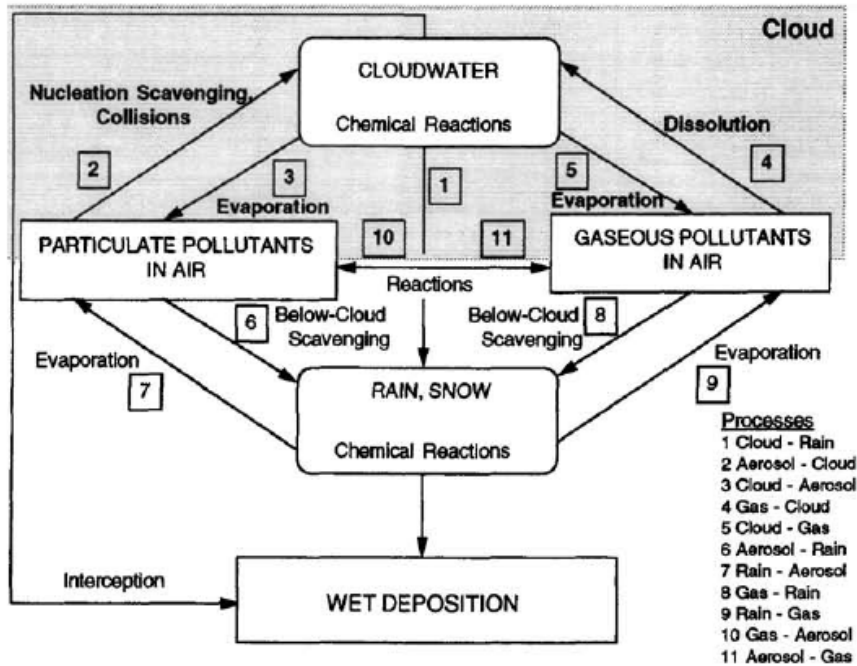
Figure 1.10. Conceptual framework of wet deposition processes [Seinfeld and Pandis, 2006]

Wet deposition is a natural process where particles are removed by atmospheric hydrometeors (cloud and fog drops, rain, and snow) and thus delivered to the Earth's surface (Seinfeld and Pandis, 2006, Fig. 1.10). Several terms are related to the wet deposition such as precipitation scavenging, wet removal, washout and rainout. Rainout is the in-cloud scavenging, whereas washout is the below-cloud scavenging by falling rain, snow and so on. All the processes follow three steps during wet removal of a material especially i) species should be brought into the presence of condensed water, ii) species must be scavenged by hydrometeors and finally iii) delivered to the Earth's surface. However, the compound may undergo chemical transform during each one of the above steps. The wet deposited steps are delineated in Figure 1.10.

1.6.   Chemical components of particulate matter

Atmospheric aerosols consist of various organic and inorganic compounds such as ions, organic carbon and elemental carbon, trace elements, polycyclic aromatic hydrocarbon, n-alkanes, dicarboxilic acids, water soluble compounds etc. (Alves, 2008)

1.6.1. Inorganic ions

Besides ammonium, sulphate and nitrate, various other water-soluble inorganic ions are also present in atmospheric aerosols. They include Cl^-, Na^+, Ca^{2+}, K^+, Mg^{2+} and phosphate. Although these ions are often only responsible for a minor fraction of the PM mass, these inorganic species are of importance for aerosol mass closure balance and as tracers for source apportionment. Sea spray is a major source of Cl^-, Na^+ and Mg^{2+} and Ca^{2+} has contribution from marine aerosols. In continental aerosols, Ca^{2+} and coarse K^+ have often important contribution from mineral dust disposal. Fine K^+ is a good indicator for biomass burning and mineral incinerators as its strongly enriched in biomass smoke.

1.6.2. Carbonaceous aerosols

Carbonaceous compounds are an important fraction of atmospheric aerosols, contributing annually 20-45% of $PM_{2.5}$ and 20-35% of PM_{10} (Putaud et al., 2010; Yttri et al., 2007). In European urban areas carbonaceous compound accounts for 30-50% to $PM_{2.5}$ (Putaud et al., 2004). In recent years, scientists all over the world have paid much attention to the carbonaceous particulate matter because it has great influences on

16

global radiation budget, cloud microphysics (Seinfeld and Pandis, 1998; Lyamani et al., 2006), global climate change (Hitzenberger et al., 1999; Dan et al., 2004) and human health (Na et al., 2004). Moreover, cardiovascular mortality and morbidity is associated with increased levels of urban carbonaceous particulate matter (Ito et al., 2011). Furthermore, several organic compounds such as PAHs and PCBs are found in OC mixtures which have carcinogenic and mutagenic effects (WHO, 2000).

Carbonaceous particulate matter is classified into two main types such as organic carbon (OC) and a refractory light-absorbing component commonly referred to as soot (Baumgardner et al., 2012; Bond and Bergstrom, 2006). Soot is produced from incomplete combustion of organic material from traffic, residential heating, industrial activities and energy production using heavy oil, coal or biofuels (Sandrini et al., 2014). Based on empirical determination, soot is referred to as elemental carbon (quantified by thermal optical method) and equivalent black carbon (EBC, quantified by optical measurement).

According to EEA (European Environmental Agency) (2013a), "Soot, the product of incomplete combustion of fuels, can be determined using different methodologies. When its light-absorbing properties are measured, soot is referred to as BC (Black carbon). When its concentration is measured by thermal-optical techniques, soot is known as elemental carbon (EC)".

1.6.2.1.   Elemental Carbon (EC)

EC is the primary pollutants released in the particle phase from the incomplete combustion of carbon-containing fuels. The main sources of elemental carbon are biomass burning and fossil fuel combustion (Gelencser, 2004). Out of the two sources, the first one is predominant in Europe and in the continental mid-latitude northern hemisphere (Hamilton and Mansfield, 1991) whereas biomass burning (savana fires, forest fires, agricultural burning and domestic biofuel burning) is predominant in tropical and equatorial regions. The EC or black carbon has significant impact on reducing visibility because of its light absorption properties in the atmosphere. In addition, EC is a potential carrier of toxic compounds into human and animal respiratory systems (Novakov et al., 1997).

1.6.2.2.   Organic Carbon (OC)

OC includes thousands of organic compounds (such as aliphatic, aromatic compounds, carboxylic acids and carboxylic compounds with polar substituents etc.) with widely varying chemical and physical properties. It may be emitted directly from sources such as combustion, industrial, and natural sources (primary OC) or formed in the atmosphere from gas to particle conversion of semi- and low-volatility organic compounds (secondary OC). The quantification of contribution of primary and secondary organic carbon is quite difficult through direct chemical analysis, as OC is a complex mixture of many compounds. Several indirect methods have been used to estimate secondary organic carbon. Among them, EC tracer method is a widely accepted technique where EC is used as a tracer of primary organic carbon (POC) (Turpin and Huntzicker, 1995; Castro et al., 1999, Lim and Turpin 2002; Cabada et al., 2004; Harrison and Yin, 2008). Particles containing OC may also pose a significant risk to human health (Mauderly and Chow, 2008).

1.6.3. Trace elements

Trace elements are introduced into the atmosphere from various natural and anthropogenic sources (Borbely-Kiss et al., 1999; Pakkanen et al.. 2001). Humans play a significant role in trace element pollution by different ways especially combustion of fossil fuels and biomass, industrial processes and waste incineration (Rajsic et al., 2008). However, there are some natural sources which contribute trace elements to the atmosphere such as erosion, dusts from aerolian processes and weathering, volcanic activity, oceans, forest fires and sea spray near coastlines (Allen et al., 2001; Hester and Harrison, 2009; Karanasiou et al., 2007). In an urban area, key source of trace elements in a particular day depend on anthropogenic activities and national regulations such as limits in gasoline, emissions from coal fired power plants and industry (mainly, metallurgic and chlor-alkali processes) (Hester and Harrison, 2009).

From various epidemiological studies, it was revealed that atmospheric particulate matter with diameters less than 2.5 micrometers, is strongly correlated with human morbidity and mortality (Huang et al., 2012; Pope and Dockery, 2006; Poschl, 2005). It is quite difficult to remove fine particles after being entered into the pulmonary systems (Donaldson et al., 2002). Although trace metals represent a small fraction of

PM, high concentration and/or long exposure of metals may cause harmful effects on human health, (Berggren et al., 1990; Devries et al., 1996) and long-term burden on the biogeochemical cycling in the ecosystem (Adriano, 2001; Hu et al., 2012). Several metallic elements are highly toxic (V, Cr, Mn, Ni, Cu, Zn, Cd, Hg and Pb) (Campen et al., 2001; Donaldson et al., 2002; Garcon et al., 2006) and referred to as human carcinogenic (Cr, As, Cd, Ni). Particulate matters containing transitional metals such as Cu, Fe, and Zn are responsible for cellular inflammation because metals favour free radicals releasing in lung fluids (Donaldson et al., 1997).

Trace particles in the ambient atmosphere have been of greater interest because they give a high surface area-to-volume ratio, leading to higher toxicity and reactivity (Dockery et al., 1994; Peters et al., 1997; Oberdörster, 2000). Determination of metals composition of inhalable particles is important in determining their potential impact on human health (Allen et al., 2001). Many research works have been conducted on atmospheric particulate matter in different parts of the world and found variations and inequalities among the trace elements components (Sohrabpour et al., 1999; Bilos et al., 2001; Gupta et al., 2007; Hao et al., 2007; Ayrault et al., 2010). Fluctuation of the concentration and size distribution of metal aerosols depend on emission sources, rates of wet and dry deposition and physical and chemical transformation (Gu et al., 2008). Moreover, long-range transport of aerosols also influences the concentration and size distribution of metals (Xu et al., 2008). Generally, the accumulation type particles have long residence time and are able to be transported over a long distance influencing remote regions from sources. Therefore, size-resolved metal concentration will provide information on the toxicity level of metals, as well as on transport behavior in the ambient atmosphere and on inhalation characteristics of the human respiratory system.

1.6.3.1. The elements in the particulate and their origin

A large number of elements (about 70) are responsible for pollution, but from the air pollution point of view the most important are only twenty (Ministry of Environment, 2013).

The trace metals of natural origin transported into the atmosphere have a concentration that varies greatly over time because events that spread them are usually sporadic and brief. The concentration of man-made elements, instead, is more consistent over time,

since it is based on continuing operations in the year (Molinaroli and Masiol, 2006). The metals from natural sources are related to the geological composition of the earth's crust and their re-suspension in the air is in agreement with chemical, physical, biological and meteorological factors, such as resuspension of soil particles by the action of wind, volcanic emissions, sea spray and forest fires. The major and trace elements classified as natural are: Na, Mg, K, Ca, Si, Al, Cl, Fe, Ti (Brunelli, 2009; Farao, 2014).

The anthropogenic sources, related mostly to high temperature processes, release certain metals in vapor form which can then form particles by condensation reactions or conversion to gas-particle. They are responsible for more than 50% of total emissions of Cr, Mn and V and for 20-30% of the annual release of Cu, Mo, Ni, Pb, Sb, As, Se, Hg, Sn and Zn into the atmosphere (Farao, 2014). Various metals are used as marker for the indentification of emission sources as discussed below (Mitra et al., 2002; ARPA, 2005; ARPAV, 2007) and also given in Table 1.2 and Table 1.3 (Calvo et al., 2013).

- Aluminum (Al), iron (Fe), calcium (Ca), silicon (Si), titanium (Ti) and manganese (Mn) are primarily derived from soil and rocks (crustal elements). The oxides of aluminum, calcium, iron and silicon are the main components of the fly ash of the natural combustion processes. Other elements also present in fly ash combustion are C, Mg, S, Ti, K and Na.

- Sodium (Na), chlorine (Cl), magnesium (Mg), sulfur (S) are elements that come from marine aerosols.

- Arsenic (As), cadmium (Cd), manganese (Mn), lead (Pb), nickel (Ni), antimony (Sb), selenium (Se), vanadium (V), and zinc (Zn) can volatilize during the process of high temperature combustion of fossil fuels and, when the temperature decreases, condense on the surface of suspended ash (fly ash). In particular, As, Cd, Cu, Ni, Zn are also indicators of metallurgical processes.

- Bromine (Br), lead (Pb), barium (Ba), iron (Fe), copper (Cu), zinc (Zn), cadmium (Cd) are good indicators of emissions from transport vehicles. The concentrations of bromine and lead, in particular, have decreased compared to

the past due to the use of "green" gasoline. Sb, Cu and Ba are mainly originated from brake wear, whereas Zn and Cd are primarily derived from abrasion of the tires; in fact, such elements are used as additives for plastics and rubbers and therefore are emitted in the combustion of these substances.

- Bromine (Br), lead (Pb), zinc (Zn), copper (Cu), sulfur (S) are elements emitted from various industrial activities.

- Vanadium (V) and nickel (Ni) derive from combustion of fuel oils and particularly they are used as indicators of anthropogenic pollution. These elements are also present in traces in the primary particles of oil-fired power stations; Vanadium is also returned from diesel vehicles.

- Zinc (Zn), antimony (Sb), copper (Cu), cadmium (Cd), mercury (Hg) are present in the elements emissions from the incineration of wastes.

- Selenium (Se), arsenic (As), chromium (Cr), cobalt (Co), copper (Cu) are present in the primary particles of coal-fired power stations.

- Nickel (Ni), vanadium (V), manganese (Mn), copper (Cu) are often issued in fusion processes.

Table 1.2. Inorganic marker elements associated with various emission sources (Calvo et al., 2013)

Emission sources	Characteristic element emitted
Road transport	
Motor vehicle emissions	Br, Pb, Ba
Industrial facilities	
Oil fired power plants	V, Ni
Coal combustion	Se, As, Cr, Co, Cu, Al
Refineries	V
Non-ferrous metal smelters	As, Ni smelting, Cu
Iron and steel mills	Mn
Plant producing Mn metal and Mn chemicals	Mn
Cu refinery	Cu
Small combustion	
Refuse incineration	Zn, Sb, Cu, Cd, Hg
Use of pesticides	As

Table 1.3. Inorganic tracer elements associated with different emission sources (Adapted from Calvo et al., 2013)

Secondary aerosols		SO_4^{2-}, NO_3^-, NH_4^+
Sea salt		Cl, Na^+, Cl^-, Br, I, Mg and Mg^{2+}
Crustal or geological tracers		Elements associated with feldspars, quartz, micas and their weathering products (mostly clay minerals), i.e. Si, Al, K, Na, Ca, Fe and associated trace elements such as Ba, Sr, Rb, and Li. In addition, there will be accessory silicates (notably zircon, titanite and epidote), and representatives from the minority non-silicate mineral groups, namely carbonates, sulphates, oxides, hydroxides and phosphates.
Technogenic tracers	Steel industry	Cr, Ni and Mo
	Copper metallurgy	Cu and As
	Ceramic industries	Ce, Zr and Pb
	Heavy industry (refinery, coal mine, power stations)	Ti, V, Cr, Co, Ni, Zn, As and Sb
	Petrochemical industry	Ni and V
	Oil burning	V, Ni, Mn, Fe, Cr, As, S and SO_4^{2-}
	Coal burning	Al, Sc, Se, Co, As, Ti, Th, S, Pb and Sb
	Iron and steel industries	Mn, Cr, Fe, Zn, W and Rb
	Non-ferrous metal industries	Zn, Cu, As, Sb, Pb and Al
	Cement industry	Ca
	Refuse incineration	K, Zn, Pb and Sb
	Biomass burning	K and Br
	Firework combustion	K, Pb, Ba, Sb and Sr
	Vehicle tailpipe	Platinum group elements, Ce, Mo and Zn
	Automobile gasoline	Ce, La, Pt, SO_4^{2-} and NO_3^-
	Automobile diesel	S, SO_4^{2-} and NO_3^-
	Mechanical abrasion of tyres	Zn
	Mechanical abrasion of brakes	Ba, Cu and Sb

1.6.4. Polycyclic Aromatic Hydrocarbons (PAHs)

The most important part of the organic compounds are the polycyclic aromatic hydrocarbons (PAHs), which are normally emitted from human activities such as industry, vehicles emissions, incineration of waste and wood burning, domestic heating, oil refining, asphalt production, agricultural burning of biomass, shipping and flying (Ravindra et al., 2008). There is an increasing concern about aerosols especially with a diameter of 10 μm or less because of their inhalation into the deeper respiratory tract region without difficulty (Kameda et al., 2005). Probably this is one of the major reasons for considering the particle-bound PAHs as the most hazardous chemicals to human health. Although polycyclic aromatic hydrocarbons represent a small part of the particulate matter, they are ubiquitous organic pollutants, some of which are known as mutagenic and /or carcinogenic (Omar et al., 2006; Fang et al., 2002) and are mainly generated by incomplete combustion and pyrolysis of organic material (Manahan, 2009). Polycyclic aromatic hydrocarbons in atmospheric particles have obtained a great deal of attention because of having carcinogenic effects of some of these compounds especially benzo(a)pyrene, benzo(a)anthracene, chrysene, benzo(e)pyrene, benzo(e)acephenanthrylene, benzo(j)fluoranthene, and indenol. However, the most important one is benzo(a)pyrene because the body can easily metabolize to a carcinogenic form (Bahry 2007). Polycyclic aromatic hydrocarbons is the complex organic chemicals, consist of two or more fused benzene rings containing only hydrogen and carbon (Ravindra et al., 2008; Seinfeld and Pandis, 2006). PAHs found in the atmosphere both in lower and higher molecular weight. The lighter PAHs are found in the atmosphere in gas phase, whereas the heavier PAHs are totally adsorbed on to the particles. The carcinogenicity of PAH increases with the increases of molecular weight, whereas acute toxicity decreases (Ravindra et al., 2008).

1.6.4.1.   Formation of PAHs

The main mechanisms that explicate the formation of PAHs are pyrosynthesis and pyrolysis. PAHs form from lower hydrocarbons through pyrosynthesis. Free radicals are formed when carbon-hydrogen and carbon-carbon bonds are broken down at a temperature higher than 500 ^{0}C. These free radicals join with acetylene and produce PAHs after condensation (Figure 1.11). The formation of PAHs from hydrocarbon by pyrosynthesis process varies in the order – aromatics> cycloolefins> olefins> parafins

(Manahan, 1994). Some controls such as type of fuels, oxygen amount and temperature influence the rate of production and fate of combusted-derived PAH in the environment (Lima et al., 2005).
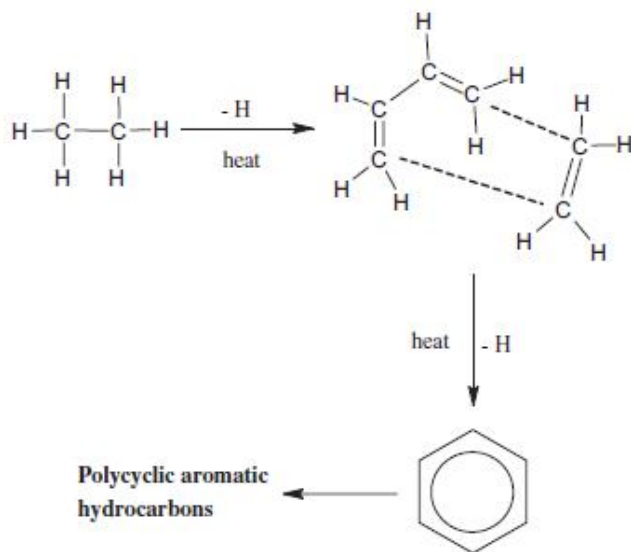
Figure 1.11. Pyrosynthesis of PAHs starting with ethane [Adapted from Ravindra et al., 2008].

1.6.4.2. Priority PAHs

The United States Agency for Toxic Substances and Disease Registry has given priority to 17 PAHs based on their toxicological profile specially availability of the information, harmfulness and exposure (ATSDR, 1995). On the contrary, based on toxicity, potential to human exposures, frequency of occurrence at hazardous waste sites and availability of information, United States Environmental Protection Agency (USEPA) has categorized 16 of the PAHs as priority-pollutants (ATSDR, 2005). They are listed in Table 1.4. Working groups of International Agency for Research on Cancer (IARC) also categorized agent or pollutant into four groups depending on their carcinogenicity.

Group 1: Carcinogenic to humans

An agent may be placed in this category when there is sufficient evidence of carcinogenicity in humans.

Group 2: Probably carcinogenic to humans (2A) and possibly carcinogenic to humans (2B)

An agent may be included in this group when the degree of evidence of carcinogenicity in humans is almost sufficient. This group also considers the evidence of carcinogenicity in experimental animals when there is unavailability of human data. This group is further divided into Group 2A (probably carcinogenic to humans) or Group 2B (possibly carcinogenic to humans) based on epidemiological and experimental evidence of carcinogenicity and mechanistic and other relevant data.
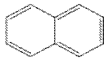
Group 3: Not classifiable as to its carcinogenicity to humans
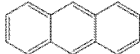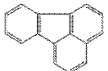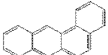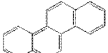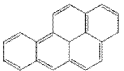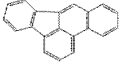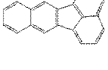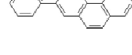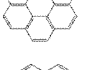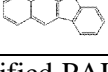
Agent listed for which the evidence of carcinogenicity is inadequate in humans and inadequate or limited in experimental animals.

Group 4: Probably not carcinogenic to humans

Agents for which there is evidence suggesting lack of carcinogenicity in humans and in experimental animals.

Table 1.4. USEPA's 16 priority-pollutant PAHs and selected physico-chemical properties (ATSDR, 2005).

PAHs		Particle/gas phase	Molecular weight (g/mole)	Solubility (mg/L)	IARC category
Napthalene		gas	128.17	31	2B
Acenapthene		gas	154.21	3.8	3
Acenapthylene		gas	152.20	16.1	

Fluorene		gas	166.22	1.9	3
Anthracene		Particle-gas	178.23	0.045	3
Phenanthrene		Particle-gas	178.23	1.1	3
Fluoranthene		Particle-gas	202.26	0.26	3
Pyrene		Particle-gas	202.26	0.132	3
Benzo (a) anthrance		particle	228.29	0.011	2B
Chrysene		particle	228.29	0.0015	2B
Benzo (a) pyrene		particle	252.32	0.0038	1
Benzo (b) fluoranthene		particle	252.32	0.0015	2B
Benzo (k) fluoranthene		particle	252.32	0.0008	2B
Dibenz (a,h) anthracene		particle	278.35	0.0005	2A
Benzo (g,h,i) perylene		particle	276.34	0.00026	3
Indeno[1,2,3-cd] pyrene		particle	276.34	0.062	2B

USEPA has classified PAHs in italics as probable human carcinogens (NTP, 2005)

1.6.4.3.   PAHs distribution

PAHs exhibit a bimodal distribution (0.01-0.5 μm diameter) mode in ambient urban aerosol, with an additional mode in the 0.5-1.0 μm diameter range (Venkataraman and Friedlander, 1994, see Figure 1.12).
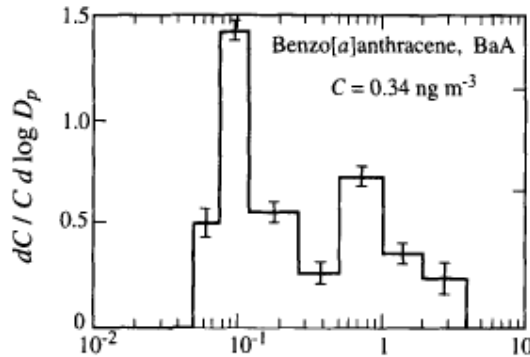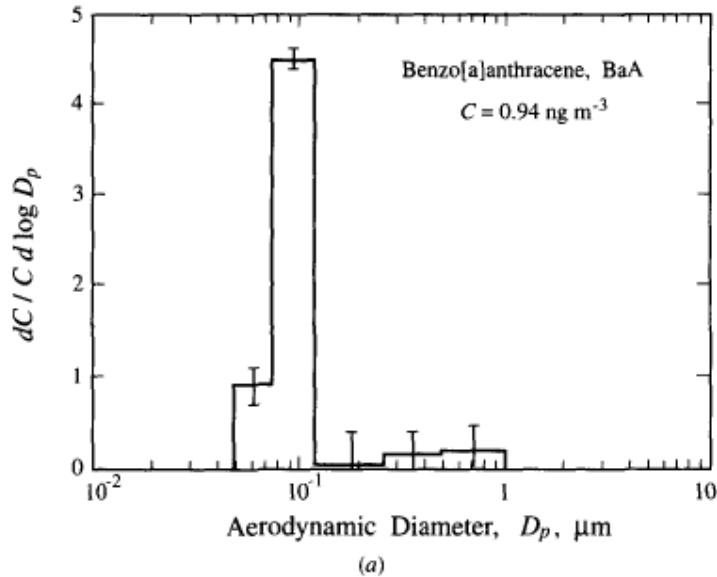
Figure 1.12. Size distribution of benzo[a] anthracene a) measured inside a tunnel and b) the ambient atmosphere of southern California.

1.6.4.4.   Partitioning between gas and aerosol phase

Polycyclic aromatic hydrocarbons remain in the atmosphere either as particulates or in the form of gases because their vapour pressures vary over several order of magnitude. Generally lower molecular weight PAHs are present in the atmosphere in gaseous phase, while the higher molecular weight PAHs remain as particulate PAHs. There is a rule of thumb proposed by Baek et al (1991) that 2-3 ring PAHs (naphthalene, fluorene,

phenanthrene, anthracene) are predominantly in the gas phase, four-ring PAHs (pyrene) remain in both phases, while 5-6 ring PAHs exist mainly in the aerosol phase. The distribution of PAHs between gas and particle phases can be calculated using the partitioning constant K_p (Yamasaki et al., 1982; Pankow, 1987).

$$K_p = \frac{C_{aer}}{M_t C_g} \dots\dots\dots\dots\dots\dots\dots\dots\dots\dots\dots \quad (Eq.\ 1.4)$$

Where,

K_p = Temperature-dependent partitioning coefficient ($m^3\ \mu g^{-1}$)

C_{aer} = Aerosol-phase concentration of the species ($\mu g\ m^{-3}$)

M_t = Total ambient aerosol mass concentration ($\mu g\ m^{-3}$)

C_g = Gas-phase concentration of the species ($\mu g\ m^{-3}$)

1.6.4.5. Sources of PAHs

PAHs are formed mainly from incomplete combustion and pyrolysis of fossil fuels or wood and from the release of petroleum products (Manahan, 1994). There are also other sources such as petroleum spills, oil seepage and diagenesis of organic matter in anoxic sediment. Broadly, there are five major emission sources of PAHs such as domestic, mobile, industrial, agricultural and natural (Ravindra et al., 2008).

1.6.4.5.1. Domestic Emission

This includes burning of coal, oil, gas, garbage and other organic substances such as tobacco or char broiled meat (Smith, 1987). Several wastes used mainly in developing countries such as wood, dried animal-dung-cake and crop waste (agricultural residue) are also responsible for domestic emissions (WHO, 2002). During 45-60 minutes of cooking, the concentration of 16 USEPA PAHs were 2.0 $\mu g\ m^{-3}$ (wood), 3.5 $\mu g\ m^{-3}$ (wood/dung), and 3.6 $\mu g\ m^{-3}$ (dung-cake).

1.6.4.5.2. Mobile Emissions:

Emission from transportation is the main sources of mobile emissions such as aircraft, shipping, railways, automobiles, off-road vehicles and machinery. Emissions from these sources depend on engine types, load and age, fuel type and quality (such as aromaticity).

1.6.4.5.3. Industrial Emissions

The main industrial sources of PAHs are primary aluminium production (plant using Soderberg process), coke production (part of iron and steel production), creosote and wood preservation, waste incineration, cement manufacture, petrochemical and related industries, bitumen and asphalt industries, rubber tire manufacturing and commercial heat/power production (PAHs Position paper, 2001).

1.6.4.5.4. Agricultural Sources

Burning of agricultural waste is another major source for PAHs which includes stubble burning, open burning of moorland heather for regeneration purposes, and open burning of brushwood and straw.

1.6.4.5.5. Natural Sources:

a. Terrestrial origin: Terrestrial origin includes non-anthropogenic burning of forest, woodland, and moorland due to lightning strikes (Baumard et al., 1999). In nature, PAHs generally form in three ways such i) high-temperature pyrolysis of organic materials, ii) low to moderate temperature diagenesis of sedimentary organic material to form fossil fuels and iii) direct biosynthesis by microbes and plants (Neff, 1979).

b. Cosmic origin: Carbonaceous chondrites originated in the main asteroid belt and are not associated with life (Halasinski et al., 2005).

1.6.4.6. Ambient air quality standards for PAHs

Although there is no mandatory air quality standard for PAHs, Many countries have included PAHs to their hazardous air pollutants list (Table 1.5).

Table 1.5. Non-mandatory ambient air quality standard for the B[a]P (Adapted from Ravindra et al., 2008)

Countries	Limit value[a] (ng m^{-3})	Guide value (annual average) (ng m^{-3})
Australia	-	1.0
Belgium	1.0	0.5
Croatian	2.0	0.1
Germany	-	10.0
India[b]	-	5.0
Netherlands	1.0	0.5
France	0.7	0.1
Italy	1.0	-
Sweden	-	0.1
UK	-	0.25
WHO	-	1.0
EU[c]	6	-
EU		1.0[d]

[a] Limit value may not be exceeded and exceeding the guide value should be avoided.

[b] Reducing 1 ng m^{-3} every year from 2005 till 2010 to meet 1 ng m^{-3} in 2010.

[c] To be met in 2010.

[d] Target value for the total content in the PM_{10} fraction.

1.6.5. Secondary Organic Aerosols (SOA)

Organic aerosols comprise of primary organic aerosol (organic compounds emitted directly from sources) and secondary organic aerosol (it can be formed in-situ by condensation of low-volatility hydrocarbon-oxidation products). The capability of volatile organic compound (VOC) to produce secondary organic aerosol depends on three factors (Seinfeld and Pandis, 2006) such as i) the volatility of its oxidation produces, ii) its atmospheric abundance and iii) its chemical reactivity. Organic gases are oxidized by several species mainly O_3, OH and NO_3. Atmospheric oxidation mechanisms of VOC have been studied in detail by Atkinson and Arey (2003). A simplified reaction mechanism for the atmospheric oxidation of a generic VOC has been given in Figure 1.13. According to Seinfeld and Pandis (2006), the formation of SOA follows the three step process.

- Production of SOA compounds from the parent VOC through gas-phase chemical reaction,

- Partitioning of SOA into gas and particle phases (partitioning is influenced by temperature, presence of other organics and humidity),

- Breaking down of SOA to other chemical compound by the particle-phase reaction.
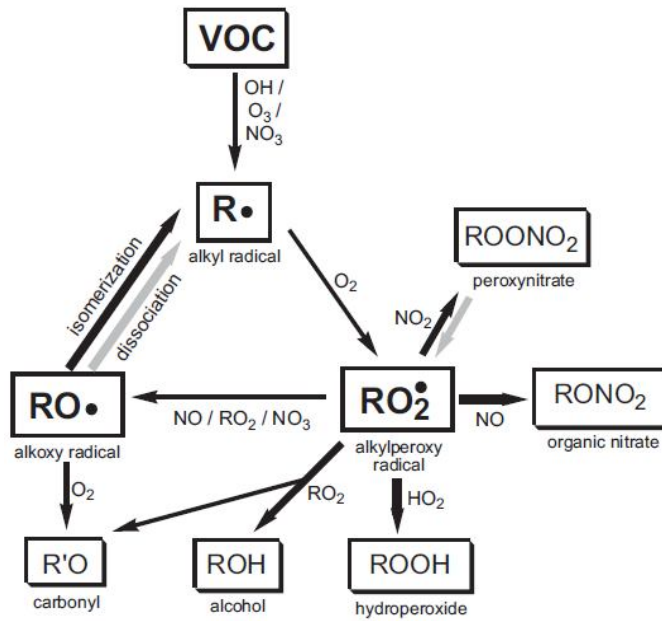
Figure 1.13. Reaction mechanism for the atmospheric oxidation of a generic VOC (Atkinson and Arey, 2003).
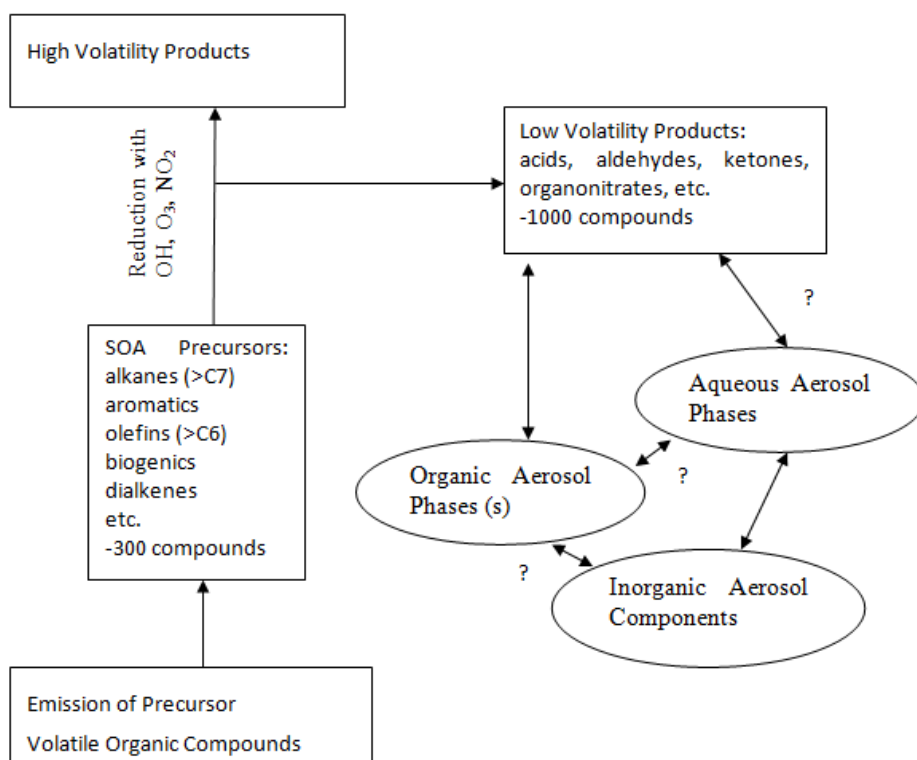
Figure 1.14. Formation of secondary organic aerosol in the atmosphere

A schematic diagram of the formation of SOA in the atmosphere has been given in Figure 1.14. Aromatic hydrocarbons are the most important anthropogenic SOA precursors and principal component of SOA in large urban areas (Pandis et al., 1992) whereas monoterpene, sesquiterpene and isoprene oxidation products are major contributor to SOA in rural forested areas (Odum et al., 1997). Main anthropogenic and natural sources of SOA precursors are combustion of fossil fuels and wood, biomass burning, solvent use, emission by vegetation and oceans (Duce and Mohnen, 1983; Jacobson et al., 2000; Seinfeld and Pandis, 2006). Approximately, 8-40 Tg yr^{-1} of SOA may come from biogenic sources (IPCC) , whilst SOA production may increase up to 50 Tg yr^{-1} due to anthropogenic sources (Kanakidou et al., 2000).

1.6.6. Secondary Inorganic Aerosols (SIA)

Sulphate (SO_4^{2-}), nitrate (NO_3^-) and ammonium (NH_4^+) are the main SIA that are formed from the gas-phase precursors SO_2, NO_x and NH_3.

1.6.6.1.   Sulphate

The formation of $SO_4^=$ from the oxidation of SO_2 follows three different pathways (Figure 1.15): the oxidation of SO_2 by the hydroxyl radical in gas phase, ii) the dissolution of SO_2 in cloud, fog and rain water followed by aqueous-phase oxidation, and iii) the oxidation of SO_2 in reactions in the water of the aerosol particles themselves. H_2SO_4 formed in the above pathways is neutralised by NH_3 to form ammonium sulphate $(NH_4)_2SO_4$ or NH_4HSO_4.
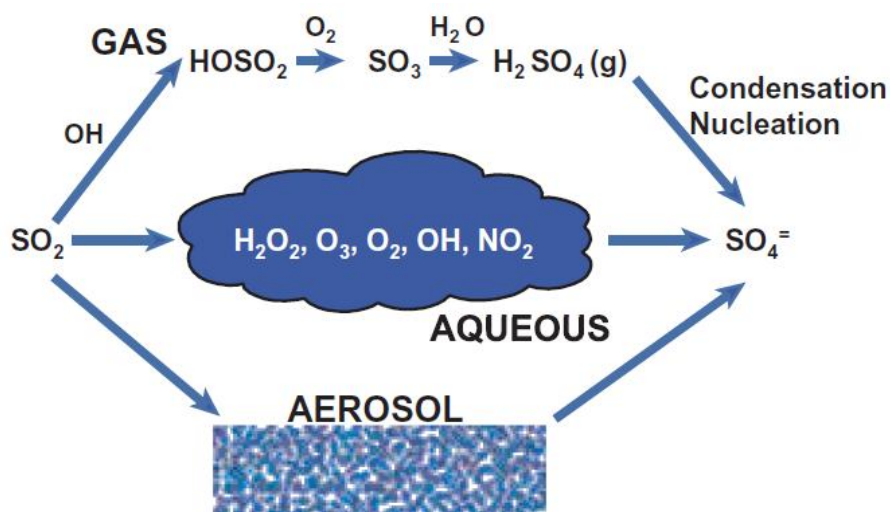
Figure 1.15. Schematic of the three pathways (reaction in the gas, cloud and condense phases) for the formation of SO_4^{2-}, in the atmosphere. (NARSTO, 2004).

1.6.6.2.   Nitrates

Nitrates are formed by the oxidation of NO and NO_2 (NO_x) both in daytime (reaction with OH) and during the night (reaction with ozone and water) (Wayne et al., 1991). Nitric acid is continuously transferred between the gas and the condensed phases (condensation and evaporation) in the atmosphere (Figure 1.16). The formation of aerosol NH_4NO_3 is favoured by availability of NH_3, low temperatures and high relative humidity.
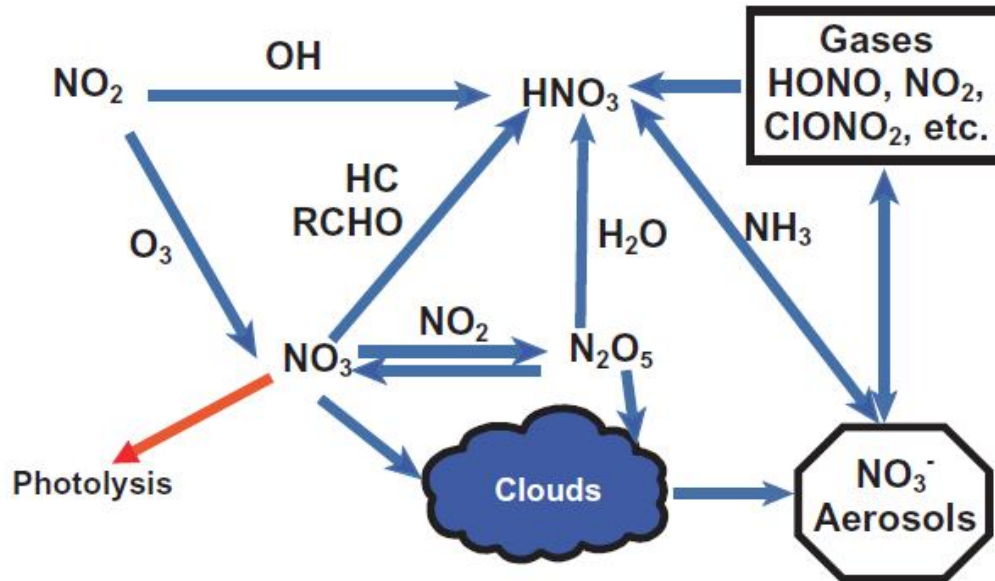
Figure 1.16. Schematic of the formation of HNO_3 and particulate NO_3^- in the atmosphere. Formation of particulate NO_3^- from HNO_3 requires either reaction with NH_3, sea salt or alkaline dust. (NARSTO, 2004)

1.6.7. European limit values for ambient air quality

European Commission directive (2008/50/EC) introduced a range of binding and non-binding objectives for particular matter (Table 1.6). This directives also set limit values for particulate matter for short-term (24-hour) and long-term (annual) exposure.

Table 1.6. Air quality limit and target values for PM_{10} and $PM_{2.5}$ (Adapted from EC, 2008)

Size fraction	Average period	Value	Comments
PM_{10}, limit value	One day	50 µg/m^3	Not to be exceeded on more than 35 days per year. To be met by 1 January 2005
PM_{10}, limit value	Calendar year	40 µg/m^3	To be met by 1 January 2005
$PM_{2.5}$, target value	Calendar year	25 µg/m^3	To be met by 1 January 2010
$PM_{2.5}$, limit value	Calendar year	25 µg/m^3	To be met by 1 January 2015
$PM_{2.5}$, limit value ([a])	Calendar year	20 µg/m^3	To be met by 1 January 2020
$PM_{2.5}$, exposure concentration obligation ([b])		20 µg/m^3	2015
$PM_{2.5}$ exposure reduction target ([b])	0-20% reduction in exposure (depending on the average exposure indicator in the reference year) to be met by 2020		

Note: ([a]) Indicative limit value (Stage 2) to be reviewed by the Commission in 2013 in the light of further information on health and environmental effects, technical feasibility and experience of the target value in Member States.

([b]) Based on a three-year average

1.6.8. **Motivations and outlines of this thesis**

Atmospheric aerosols consist of various organic and inorganic compounds (Alves, 2008). There are different kinds of compounds present in the atmospheric aerosols such as carbonaceous fraction, polycyclic aromatic hydrocarbons, ions, heavy metals, n-alkanes, dicarboxylic acids, water soluble compounds etc. However, high aerosol concentrations can cause a wide range of impacts on human health and also natural ecosystems, agriculture, visibility and tropospheric oxidation capacity. For example, polycyclic aromatic hydrocarbons represent a small part of the particulate matter, but they are ubiquitous organic pollutants, some of which are known as mutagenic and /or carcinogenic (Omar et al., 2006). The elemental carbon (EC) has significant impact on reducing visibility because of its light absorption properties in the atmosphere. In addition, EC is a potential carrier of toxic compounds into human and animal respiratory systems (Japar et al., 1986). On the other hand, researchers are very much concerned about trace metals as some of them are toxic and have hazardous impacts on human health and living organisms (Gracia et al., 2011). Most studies concluded that particulate matter is the main pollutant causing deaths in Europe today. Therefore, scientists all over the world are carrying out researches on atmospheric aerosols because of their great influence on global radiation budget, cloud microphysics, global climate change and human health.

However, various anthropogenic activities are responsible for the emission of aerosol components into the atmosphere. The most important part of the organic compounds includes polycyclic aromatic hydrocarbon which are normally emitted from human activities such as industry, vehicles emissions, incineration of waste and wood burning, domestic heating, oil refining, asphalt production, agricultural burning of biomass, shipping and flying (Ravindra et al., 2008). The main sources of elemental carbon are biomass burning and fossil fuel combustion. In contrast to EC, OC (organic carbon) is not only directly emitted from sources, but also can be produced by atmospheric reactions from gaseous precursors. Humans play a significant role in atmospheric particulate pollution by different ways such as transportation, industrial activities, biomass burning and agricultural activities. However, there are some natural sources which contribute trace elements to the atmosphere such as erosion, surface dusts, volcanic activity, oceans, and forest fires (Karanasiou et al. 2007).

Although several works have been conducted on organic and inorganic components present in atmospheric aerosols in Italy, no extensive investigations have been conducted in Venice. A main limitation of the papers so far published in Italy is that they did not discuss all organic and inorganic pollutants all together and also have collected measurement in a limited number of stations. Moreover, very limited research was conducted about the source apportionment of these compounds which are very important to implement source-related mitigation measures. Furthermore, the recent European Council Directive (2008/50/EC) has given great emphasis to the monitoring of particulate matter (diameter less than 2.5 µm, $PM_{2.5}$) in Europe (EC, 2008). The new annual limit value for $PM_{2.5}$, fixed at 25 µg m^{-3} to be met in 2015, is not achieved yet in several European sites so far. In particular, some studies (Putaud et al., 2010) indicated that particulate matter pollution increases from North to central and Southern Europe. The most adverse situations are reported during the winter season in medium and large cities and, in general, in Benelux and Northern Italy, where high air pollution may cause serious risks for human health (EC, 2004).

This work is the first one conducted in the Veneto region with the collaboration of ARPAV (Agenzia Regionale per la Prevenzione e Protezione Ambientale del Veneto). It includes all important organic (OC/EC and PAHs) and inorganic pollutants (trace elements), which were characterized at regional scale for an extended period of time. Keeping the above points in mind, an investigation has been carried out with the following objectives.

i)   To analyze the chemical composition (EC, OC, PAHs and Trace elements) of $PM_{2.5}$ at regional scale (Veneto)

ii)   To monitor the seasonal trends of the components present in $PM_{2.5}$ at regional scale (Veneto) and their relationship with micro-meteorological parameters.

iii) To quantify source contributions to $PM_{2.5}$ at the Veneto regions using receptor models [Factor Analysis (FA)]

CHAPTER 2

METHODOLOGY

2.1. Study area

2.1.1. The Po Valley

The Po Valley, a vast geographical area located in Northern Italy, included within the basin of the river Po, is bordered to the north and west by the Alps, the Apennines to the south and east by the Adriatic Sea. The territory of the Po Valley covers a very extensive area in different regions of northern Italy such as Piedmont, Lombardy, Veneto and Emilia-Romagna. It is one of the largest plains in Europ, about 47000 km^2 and also one of the most densely populated areas in Italy as well as in Europe (approximately 20 million inhabitants) (Hamed et al., 2007; Larsen et al., 2012; Masiol et al., 2012a; Squizzato et al., 2012a). It is also considered one of the largest industrial, commercial and agricultural zones (Crosier et al., 2007; Koelemeijer et al., 2006; Masiol et al., 2010; Schenone and Lorenzini, 1992).

However, air quality is seriously affected by industrial emissions, urbanization and road traffic (Sogacheva et al., 2007; Stracquadanio et al., 2007). It is also known that the Po Valley represents, for some time, one of the most polluted areas in Europe (Koelemeijer et al., 2006; Masiol et al., 2012b; Putaud et al., 2010; Squizzato et al., 2012a) and struggling with several pollutants especially atmospheric particulate matter, ozone and nitrogen oxides (Belis et al., 2011; Masiol et al., 2012a).

The peculiar topography and unfavorable climatic conditions of this region play a leading role with regard to the high levels of pollution present (Masiol et al., 2010; Sogacheva et al., 2007; Squizzato et al., 2012a). The presence of the Alps in the north and north-west, the Apennines to the south protect the Po valley from cold winds coming from the north-northeast (Crosier et al., 2007; Larsen et al., 2012). These conditions do not allow the dispersion of pollutants, but it favors the accumulation and permanence in air (Hamed et al., 2007; Masiol et al., 2012c; Sogacheva et al., 2007; Squizzato et al., 2012a), making winter the most polluted year period (Larsen et al., 2012).

2.1.2. Veneto Region

The research work was conducted in the Veneto region located in the northeastern part of the Italy. This region has an area of ~18.4×10^3 km^2 which extends 210 km to the North-South direction and 195 km to the West-East direction. Geomorphologically, this region is characterized by northern mountainous areas (29%), intermediate hilly (15%) and plain areas located in the southern part. Such variety, enhanced by the presence of a considerable coastline situated between the lagoon areas and the delta of the Po, makes an appreciable diversified climate that goes from the mountain to the relatively low temperature-zones of the rest of the region (1-3 ^{0}C in January and 23-25 ^{0}C in July). The eastern exposure causes the territory to be crossed by Bora and Scirocco winds that cause abrupt climate change. Annual rainfall peaking at the foothills of the Alps is between 1500 mm to 2000 mm. Rainfall decreases moving towards the alpine areas (less than 1500 mm), hilly areas, plains (1000 mm-1300 mm) and the area of the Po delta (600 mm). Approximately 4,866,324 inhabitants are living at Veneto region with a density of 264 inhabitants/Km ^{2}. The morphological characteristics and climatic conditions have a decisive effect on the distribution of the population concentrated largely in the southern areas of the region. Human activities coupled with peculiar weather conditions which are favorable for accumulation and nucleation of pollutants make polluted this area (EEA, 2013b). There are seven administrative provinces (Venice, Padua, Vicenza, Verona, Treviso, Belluno and Rovigo) and 581 municipalities in the Veneto region. This study included all provincial capitals with the exception of Verona (See Figure 2.1). The features of each station are given at Table 2.1.
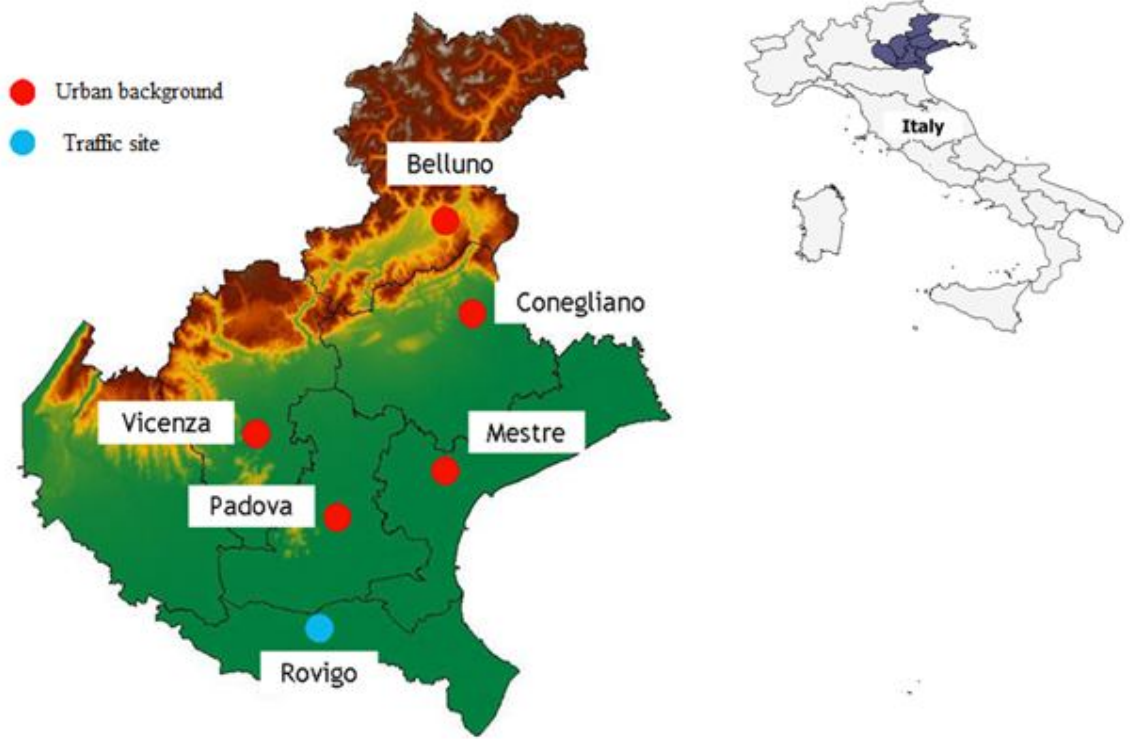
Figure 2.1. The location of the sampling stations.

Table 2.1. The features and meteorological parameters of the measurement sties at Veneto region.

Province	Municipality	Latitude	Longitude	Altitude (m)	Site characteristics	Temperature (^{0}C)	Solar radiation (Wm^{-2})	Wind velocity (ms^{-1})	Humidity (%)	Precipitation (mm)
BL	Belluno	46.143 N	12.218 E	401	Park, residential-commercial	10.9±9.6	147.5	0.7	79.5	0.15
TV	Conegliano	45.890 N	12.307 E	72	Residential area	14.9±9.4	160.1	1.5	62.8	0.12
VI	Vicenza	45.560 N	11.539 E	36	Residential area	13.8±9.9	154.1	0.7	78.5	0.07
PD	Padova	45.371 N	11.841 E	13	Residential area	14.5±9.8	96.1	0.1	71.8	0.08
VE	Venice-Mestre	45.498 N	12.261 E	1	Park, residential	13.0±9.3	147.7	0.7	78.7	0.11
RO	Rovigo	45.074 N	11.782 E	7	Residential-commercial area	13.9±10.2		1.3	76.5	0.05

2.2.   Heating period in the Veneto Region

In this thesis, as mentioned previously, six measurement stations were involved for being representative of the entire region. Each site identifies the specific microenvironments such as:

 The alpine environment: Belluno

- The hilly environment: Conegliano

- The environment of the lagoon: Venice - Mestre

- The environment of the plains: Vicenza, Padua and Rovigo.

The law regulating the periods of switching on and off the heating systems (Law and n.10/91 dpr n.412/93) includes the area of the province of Belluno under F and the provinces of Venice, Padua, Vicenza, Treviso and Rovigo under E. In Zone E, the heating period starts on October 15 and continues until April 15 each year for 14 hours a day. The area F, relative to the location that record lower average temperatures on the national stage, does not provide for any time limitation.

2.3.   Sampling of PM$_{2.5}$

The PM$_{2.5}$ samples were collected by ARPAV (Regional Agency for the Protection of Environment in Veneto) at six major cities located in six provinces of the Veneto region from April 2012 to March 2013 using low-volume samplers (*Low Volume Sampler, LVS*) with a nominal capacity equal to 2.3 m^3 h^{-1}, which draw air continuously for 24 hours starting at midnight (EN 14907:2005). The PM$_{2.5}$ samples were collected on quartz fiber filters (Whatman QMA, GE Healthcare, USA) with a diameter of 47 mm. Sixty samples per sampling site were collected in every alternate month (April, June, August, October, December and February): 10 samples per sampling site in 10 consecutive days of the months selected. The sampler from the company "Zambelli" has been used to collect the samples from Venice (Mestre) whereas the sampler of the company "Tecora" is used for the other five measurement stations. The particles are separated on the basis of a measure of the aerodynamic diameter (D$_{ad}$). The samplers are made by a series of nozzles that allow entering the

particles with a diameter equal to or less than 2.5 micron and preventing the passage of particles with greater diameter.

2.4. Quantification of PM $_{2.5}$

As reported by — EN 14907:2005, PM filters were conditioned before and after being weighted in a climatic chamber provided with a control system for the temperature and humidity (20 $\pm$ 1 ℃ and relative humidity of 50 $\pm$ 5%) (Emerson S05KA Emerson Network Power – Piove di Sacco-Pd). After this, an analytical balance (Sartorius series Genius, mod. SE2, Germany) with a sensitivity of 0.1µg was used to measure the particulate mass collected on the filter surface. Finally, the samples were inserted in the "Petri dishes" and stored in a special freezer at a temperature of -20 ℃. In order to correct the values for particulate matter and evaluate possible contamination of the filter, field blank samples were collected where the filters were placed inside the sampler, but were not exposed to the air flow. Each sampled filter was divided into four sub-samples (16 mm diameter) through the use of a puncher (Figure 2.2) taking the assumption that a punch is the representative of an entire filter, and the particulate matter is homogeneously distributed on the surface.
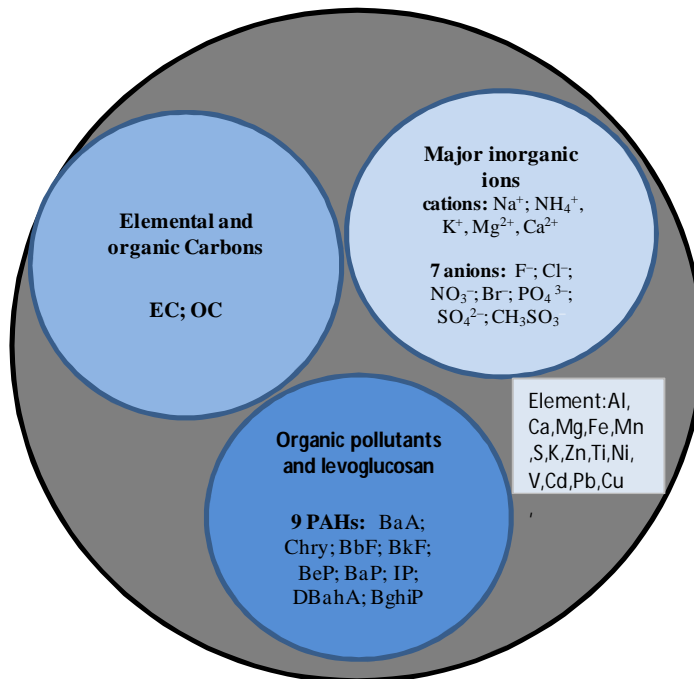
Figure 2.2: Subdivision of the filter into three subsamples

Each sub-sample was treated differently depending on the type of pollutant considered. This thesis project involved the analyses of three of the sub-samples, representative of the organic and inorganic components present in $PM_{2.5}$ such as

- Elemental and organic carbon

- PAHs and

- Trace element.

2.5. Analyses of the carbonaceous fraction

The carbonaceous fraction (Organic and elemental carbon) was quantified with the Sunset Lab OC-EC Aerosol Analyzer (Sunset Laboratory Inc., USA; Figure 2.3), an instrument analyzing the carbonaceous fraction by thermal optical transmission following the NIOSH 5040 protocol.

Fig. 2.3: Sunset Lab OC-EC Aerosol Analyzer

Thermal/optical methods are typically used for the measurements of both organic (OC) and elemental carbon (EC). Three characteristic features of this method are very important. The first one is the optical detection and correction for elemental carbon. Elemental carbon is naturally present in many of these samples from some combustion source such as a diesel exhaust. This black material is a very strong absorber of light, and almost the only absorber in the red light region. In addition to this type of elemental carbon, in the sample more elemental carbon can be formed from some charring of the organic carbon fraction of the sample as it is pyrolyzed during the initial

temperature ramp. This can begin occurring at a temperature as low as 300 ℃ depending on the organic components on the filter. This charring of organic carbon could result in an artificially low measurement of the organic carbon and a higher than actual measurement for the original elemental carbon if no correction is made.
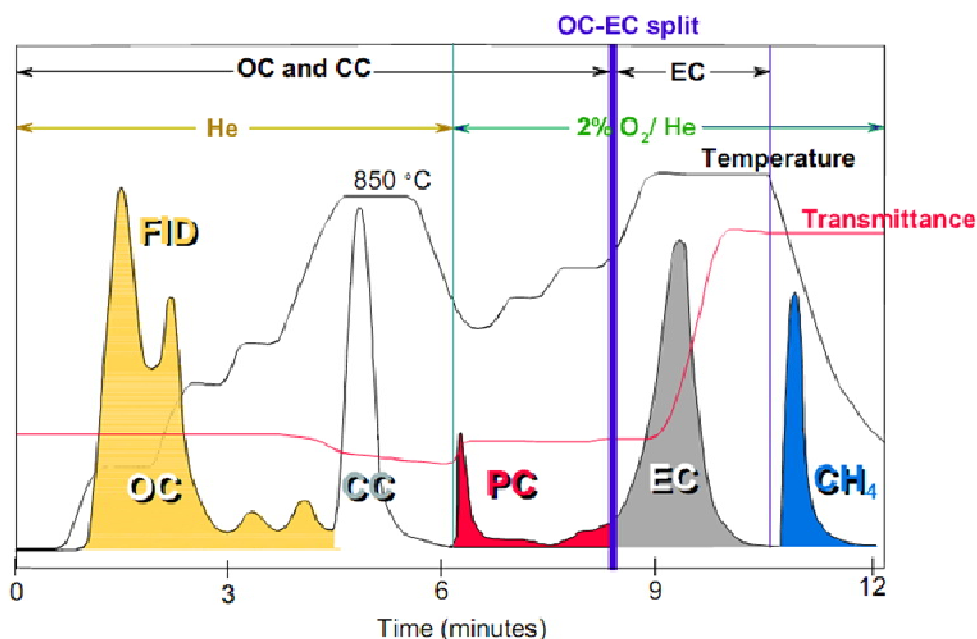
Figure 2.4. Thermogram for filter sample containing organic carbon (OC), carbonate (CC), and elemental carbon (EC). PC is pyrolytically generated carbon or 'char.' Final peak is methane calibration peak.

The determination of organic and elemental carbon by this technique is accomplished through temperature and atmosphere control, considering that EC, as opposed to OC, evolves at temperature higher than 350°C and in oxidant atmosphere. The analysis proceeds essentially in two stages: the first one in helium atmosphere and the second one in oxidant atmosphere, where the temperature is stepped to about 850°C and above 940°C, respectively. However the temperature set points and the residence times at each temperature step change with the thermal evolution protocol used (IMPROVE, NIOSH, EUSAAR). The evolved carbon is catalytically oxidized to CO_2 and then reduced to CH_4, which is quantified by a flame ionization detector (FID). Taking into account the EC light absorbing properties, a He–Ne laser light (passing through the filter) allows continuous monitoring of transmittance in order to correct for pyrolitically generated carbon (PC), which is formed as oxygen enters the oven and determines an

increase in filter transmittance. The point at which the filter transmittance reaches its initial value is defined as the "split" between OC and EC. At the end of each analysis, a known volume of methane is injected into the sample oven allowing the instrument calibration (Figure 2.4).

2.5.1. Calibration

Since it is not available to date an appropriate standard for organic carbon, elemental and carbonates in the aerosol, and as the process of catalytic oxidation-reduction is independent of the type of sample, for calibration of the instrument and to test the efficiency of the thermal-optical method different carbonaceous materials can be used as a standard. In this thesis, the calibration curve was constructed (Figure 2.5) with four standard solutions of sucrose, by plotting the amount(µg) of carbon content in a given volume of solution injected onto the filter (µgC calculated) against those detected by the instrument (µg C instrumental). By calculating the standard deviation of the slope and intercept of the straight regression line and knowing the tabulated value for the variable t -student with a 95% confidence, the slope and the intercept can be considered not significantly different from 1 and 0, respectively.
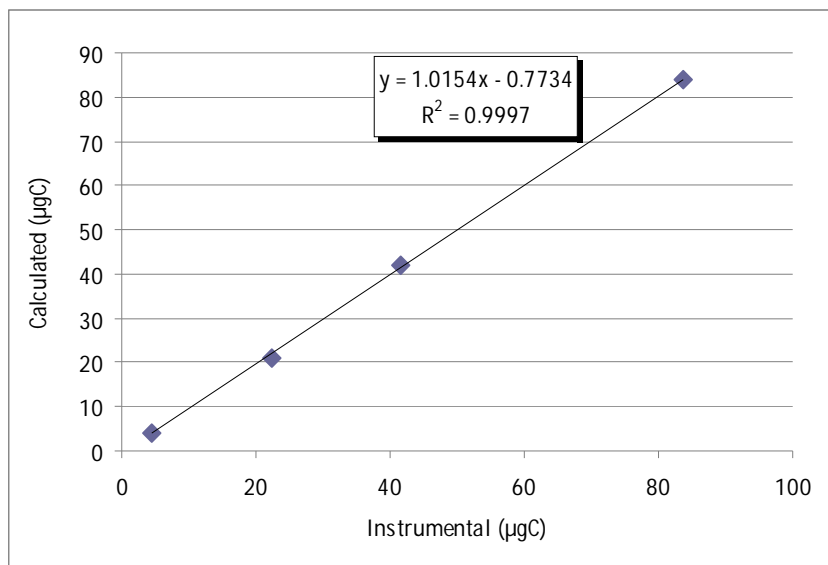
Figure 2.5. Calibration line: plot of µg C calculated against those instrumental for four standard solutions of sucrose.

To assess the Limit Of Detection (LOD) of the thermal - optical method, standard operating procedures and calibration standards were considered in the range of

concentrations from 0.2 to 2 µg C. A calibration curve was prepared by plotting the calculated values in µg of carbon contained in the known volume injected onto the filter against those instrumental.
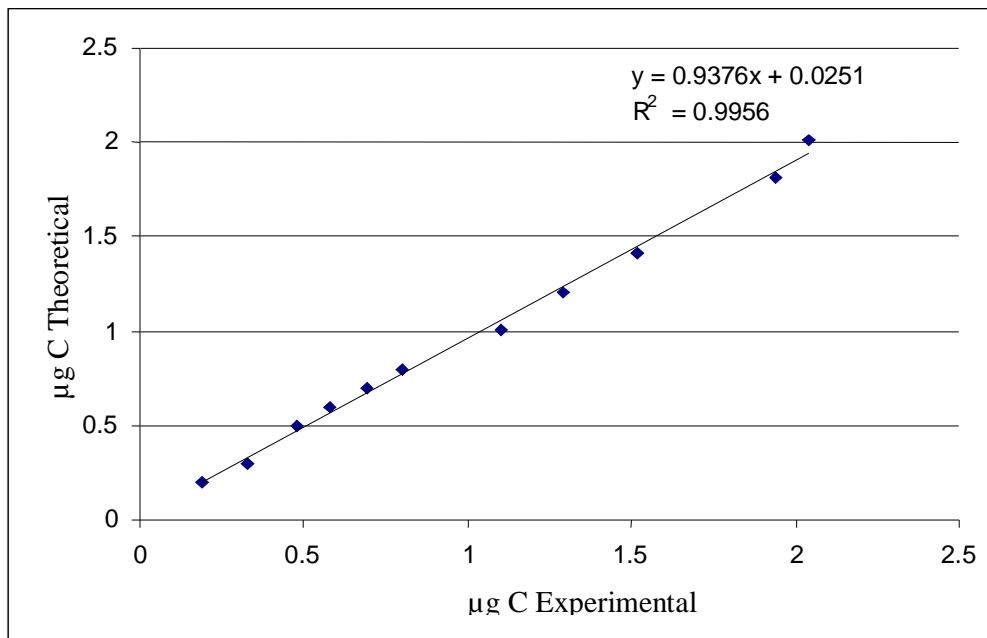
Figure 2.6. Sensitivity plot of µg C calculated against those instrumental for eleven standard solutions of sucrose in a concentration range between 0.2 and 2 µg C.

Finally, LOD was calculated from the linear regression using the following formula:

$$LOD = 3Sy / m$$

Where Sy is the standard deviation of the linear regression and m is the slope of the line. Using this procedure, having obtained a Sy equal to 0.04 and a slope of 0.94, LOD is obtained equal to µg 0.13 of carbon (Figure 2.6). Also in this case we can say that the slope and intercept of the regression line can be considered not significantly different from 1 and 0 respectively at 95% confidence. Organic and elemental carbon analyses were conducted at the laboratory of the Department of Chemistry, University of Bari by following the procedure established by Birch and Cary (1996).

2.6.   Data of pollutants and automatic weather stations

This research also used the meteorological data [rainfall (mm), barometric pressure (mbar), air temperature (^{0}C), solar radiation (Wm^{-2}), relative humidity (%) and wind

speed (ms^{-1})] and gaseous pollutant concentrations (CO, NOx, SO$_2$, and O$_3$) from the continuous monitoring stations of ARPAV and the Meteorological Centre of Teolo for conducting statistical analysis.

2.7. Analysis and quantification of PAHs

One sub-sample has been used for identification and quantification of eight PAHs: benzo [a] anthracene (BaA), chrysene (Chry), benzo [b] fluoranthene (BbF), benzo [k] fluoranthene (BkF), benzo [a] pyrene (BaP), dibenzo [a, h] anthracene (DahA), benzo [ghi] perylene (BghiP) and indeno [1, 2,3-c, d] pyrene (IP).

The analytical procedure was divided into several phases. Each punch (representative part of the sample) of the filter was ultrasonically extracted two times for 25 minutes with 3-5 mL of acetonitrile (CH$_3$CN, HPLC grade, ≥99.9%, Sigma-Aldrich). After completion, the extract was filtered into a vial using PTFE syringe filter with a porosity of 0.2 µm.

For the analysis of the eight congeners a 2695 series Alliance high performance liquid chromatograph (HPLC, Waters, USA), equipped with auto-sampler, quaternary pump, micro-degassercolumn thermostat and interfaced with a 2475 multi λ fluorescence detector, has been used. The mobile phase consisted of a mixture of ultrapure water (Milli-Q) and acetonitrile (CH$_3$CN) (HPLC grade, ≥99.9%, Sigma-Aldrich). HPLC set-up was the following: reversed phase chromatographic column (LC-PAH, 15 cm × 3 mm, 5 mm, Supelco, USA) at a temperature of 25 ^{0}C, injection volume 5 mL, mobile phase system consisting in a varying mixture of ultrapure H$_2$O and acetonitrile at a flow rate of 0.5 mL min^{-1}. Inside the container the water was bubbled with an inert gas, helium, to eliminate any gas dissolved in it. In order to increase the strength of eluent and improve the separations, a gradient elution was carried out. The relationship between the percentage of water and acetonitrile during the run has changed as follows: initial phase: 20% H$_2$O and 80% CH$_3$CN; 100% CH$_3$CN after 13 minutes of running; final phase: 20% H$_2$O and 80% CH$_3$CN). The chromatography column was a reversed phase (*reversed phase*), with a polar stationary phase and polar mobile phase (H$_2$O and CH$_3$CN). The column was maintained at a temperature of 25°C, while the samples were maintained at a temperature of 15 ℃.

The system injects a small aliquot of the sample (5 µL) into the column with a flow rate of 0.5 mL min^{-1}. The eluent is pushed onto the stationary phase due to the applied pressure by a pump to the column head. This system guarantees analysis in a short time and a good resolution. The compounds output from the column are detected with a fluorescence detector, which indicates the presence of the compounds, and generates a signal as a function of time. The fluorimeter measures the energy released in the form of photons to particular classes of fluorescent substances, IPA in our case, when excited with ultraviolet radiation.

The UV light from a lamp (set to a specific wavelength, λ) passes through a flow cell. When the fluorescent sample passes through the cell, absorbs radiation, is excited and emits the fluorescence radiation with higher λ. The intensity of the light emitted is measured by a photomultiplier placed at 90° with respect to the incident beam. The detector used, during each run, makes two changes of wavelength from 270 nm to 290 nm and finally at 300 nm. Each congener emits at a particular wavelength, specific for each compound.

2.7.1. Quality Assurance / Quality Control (QA / QC)

Instrumental response was obtained using five successive dilutions of a certified standard PAH-Mixture PM-613A (Ultra Scientific, USA). The analytical method was systematically validated by measuring the certified reference material ERM-CZ100 PAHs (JRC, Belgium) and recovery efficiencies varied from 75% to 125%. The limit of detection (LOD) for all contenders, calculated using surrogate standards with 0.5 ng mL^{-1} was equal to 0.02 ng m^{-3}. The error was calculated on the intermediate repeatability obtained from the results of the recovery of the reference material. Field blank samples were also collected in order to evaluate the possible contribution of contaminations to PAHs concentrations and every ten samples were placed with a blank (acetonitrile) and two controls.

2.8. Procedure and analytical instrumentation of trace element

2.8.1. Materials and tools used

- Microwave oven (Ethos 1600, Milestone, Italy, Figure 2.7)
- Analytical balance
- Teflon beaker
- Syringe filter (cellulose acetate, diameter 25 mm, porosity 0.45 µm)
- Syringe (50 mL)
- Acetone
- NIST (Standard Reference Material 1648, Urban Particulate Matter)
- Water (Milli-R and Milli-Q)
- Nitric Acid (69%, Fluka-analytical-sigma alrich)
- Hydrogen peroxide (Chem-lab)
- Hydrogen fluoride (Fluka-analytical-sigma Aldrich)
- Inductively coupled plasma optical emission spectrometer (ICP-OES, optima 5300 DV, Perkin-Elmer, USA)
- Inductively coupled plasma mass spectrometer (ICP-MS; Elan 6100, Perkin-Elmer)
- PTFE bottles
- Ceramic scissors
- Tetrafluor methoxi vessels (TFM vessels)

Figure 2.7: Digester ETHOS 1600 Milestone®.

2.8.2. Digestion Procedure

The bottles made of polyethylene (PE) were kept under conditioning with 5% HNO_3 solution for 15 days to avoid the possible contamination of Cd and Zn (possible components of plastics) from the plastic bottle.

I. Before sample digestion, the TMF vessels were filled with acid mixture (4 ml HNO_3: 2 ml H_2O_2: 1 ml HF) and cleaned with three step digestion

II. Filters were placed in TFM vessels

III. Acids were added into the vessel (4 ml HNO_3: 2 mL H_2O_2: 1 mL HF) and the samples were homogenized by gently swirling.

IV. The vessels were closed and set into the rotor segment and finally each cap was tighten by using the torque wrench

V. The segment was inserted into the microwave cavity

VI. The microwave program was run to complete the digestion using the protocol proposed by Karthikeyan et al. (2006) and given in Table 2.2

VII. The rotor was cooled by air until the solution reached the room temperature (time required: allowed 1.5 hrs).

VIII. The digested solution was diluted to 25 mL with ultrapure water, filtered through syringe fitted with a Teflon filter and stored at $4\,^0C$ in PTFE bottles.

IX. After each round of digestion, each vessel was cleaned with acetone to remove any organic residue (especially for winter samples) and, finally, the vessels were filled with the same amounts of chemicals used for sample digestion and cleaned using the same digestion program to be ready for next run.

Table 2.2. Microwave Program

Step	Time	Power (W)
1	5	250
2	5	400
3	2	600

In addition to the samples, the following samples were also treated with the same procedure

- Blank filters
- Blank reagent: solutions containing the same mixture of acids of the samples, useful to verify the quality and the reagents and whether there were phenomena of pollution of the containers during the analysis
- Standard Reference Material (SRM), NIST (National Institute of Standard & Technology): This material was used to evaluate the analytical method adopted to analyse the particulate matter. Approximately 2 g of NIST (Taylor and Kuyatt, 1994) were taken and analyzed according to the similar way as samples (Squizzato, 2011)

Before identification of the elements by ICP-MS and ICP-OES the samples were diluted according to the following way:

- For the ICP -OES:
  - For sample: 5 mL of the sample and 5 mL of Milli-Q water [1:2)]
  - For blank filter: 5 mL of the sample and 5 mL of Milli-Q water [1:2]
  - For blank reagent: 5 mL of the sample and 5 mL of Milli-Q water [1:2]
  - For NIST: two dilutions was prepared; 1 mL sample + 4 mL Milli-Q water [1: 5] and 1 mL sample + 9 mL Milli-Q water [1:10]
- For the ICP-MS, samples were prepared also with the internal standard (Rhenium solution).
  For sample: 1:1 [1.4 mL of Rhenium (100 ppb in the nitric acid solution), 2.1 mL of Milli-Q water and 3.5 mLof sample]
  For NIST: 1: 5 (2 mL solution of Rhenium, 6 mL of Milli-Q water, 2 mL of NIST) to 1:10 (2 mL solution of rhenium, 7 mL of Milli-Q water and 1 mL NIST).

2.8.3. **Inductively coupled plasma optical emission spectrometer**

Figure 2.8: Inductively Coupled Plasma Optical Emission Spectrometry (ICP-OES).

The main advantage of Inductively Coupled Plasma Optical Emission Spectrometry (ICP-OES) (Figure 2.8) instrument is its greater sensitivity and its ability to determine the concentrations of certain elements, at values below the g L^{1} limit. The liquid sample is introduced into plasma as an aerosol suspended in argon gas by a nebulization process. The aerosol samples are desolvated and vaporized and finally undergo an atomization and ionization process in the ICP. Due to high temperature in the plasma (7000-10000 °K), all the elements present in the sample are atomized in argon to achieve a higher energy level than in their ground state. The excited electrons then return to the original state, either directly or by intermediate energy levels, emitting quanta of light energy that generate an emission spectrum at different wavelengths (lines). A layout of a typical ICP-OES instrument is given in Figure 2.9.
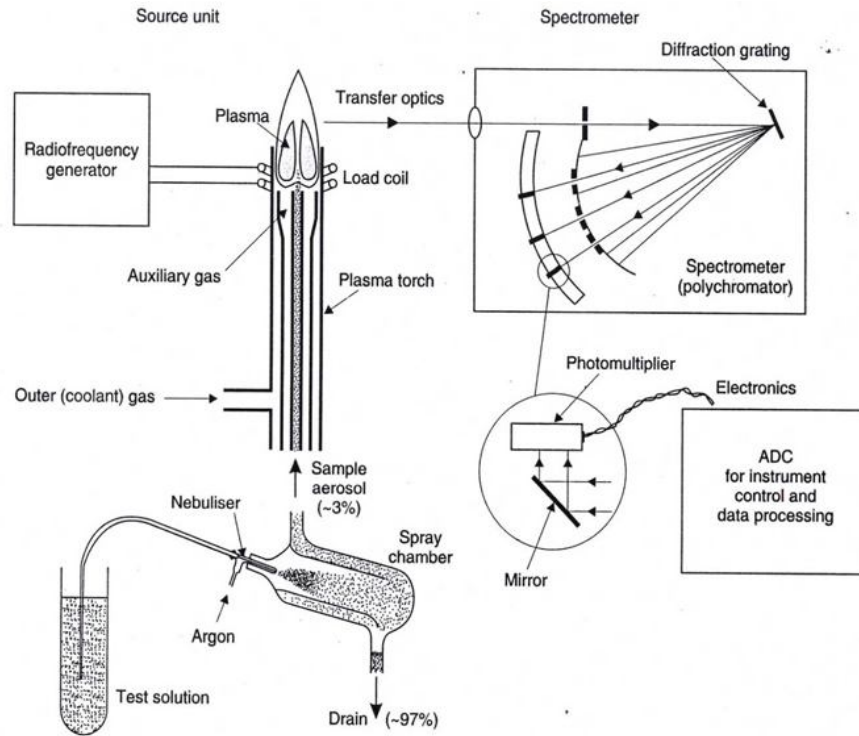
Figure 2.9. A layout of a typical ICP-OES instrument

Since all the atoms in the plasma are excited simultaneously, the light emitted (emission broadband) is a combination of all wavelengths of individual atoms and ions present in the sample and in the plasma gas. The emission of the plasma is polychromatic and this polychromatic light is separated according to individual wavelength by monochromator (measure light at one wavelength at a time) or polychromator (measure light at several different wavelengths at once). Finally the detection of the light is carried out by a photosensitive detection such as photo-multiplier or chare-couple device (CCD) at each designated wavelength. The intensity of the polychromatic light emitted by the sample then passes through an optical system which is selected as a function of wavelength. The concentration of element in the sample is obtained using plot between emission intensities of the signals and the sample compared to reference solutions of known concentration.

The model used (OptimaTM 5300 DV Perkin-Elmer) is characterized by a dual detector system: the UV detector operates at a wavelength of between 165 and 403 nm, while the VIS detector between 404 and 782 nm, so as to cover a high range of wavelengths. The intensity of each wavelength is then converted into electrical signals

by a detector CDD (Charge Coupled Detector Device). Elements determined by ICP-OES and ICP-MS have been listed in Table 2.3.

2.8.4. Inductively coupled plasma mass spectrometer

The principle of operation of the first part of the instrument is very similar with ICP-OES. The Inductively Coupled Plasma Mass Spectrometer (ICP-MS) is an analytical tool that allows the determination of some elements, also present below the single part per trillion (ppt) level (Fig. 2.10). It combines two components: a source for the inductively coupled plasma to produce the ionization and a quadrupole mass spectrometer for the separation and detection of the ions produced (Fig. 2.11). A liquid sample is introduced by a peristaltic pump into a nebulizer and converted to fine droplets in the presence of a stream of argon that acts as a carrier, and pass through a spray chamber before entering the ICP torch.

In the ICP, the torch generates the plasma which creates very hot zone (The plasma thus produced can also reach temperatures of 6000-10000 °K) which lead to the complete ionization of the elements present in the sample. The plasma is generated by passing through a series of concentric quartz tubes (ICP torch) that are covered at one end by a radio frequency (RF) coil. A radio frequency generator supplies current to the coils, with a frequency of 40 MHz, to induce a magnetic field coupled with the argon. Due to the high thermal energy, the liquid sample goes through a series of transformations (desolvation, evaporation and vaporization of the liquid phase, atomization of the solids present, ionization) leading to the production of the ionic species to be sent to the mass spectrometer.

Figure 2.10: Inductively Coupled Plasma Mass Spectrometer (ICP-MS).
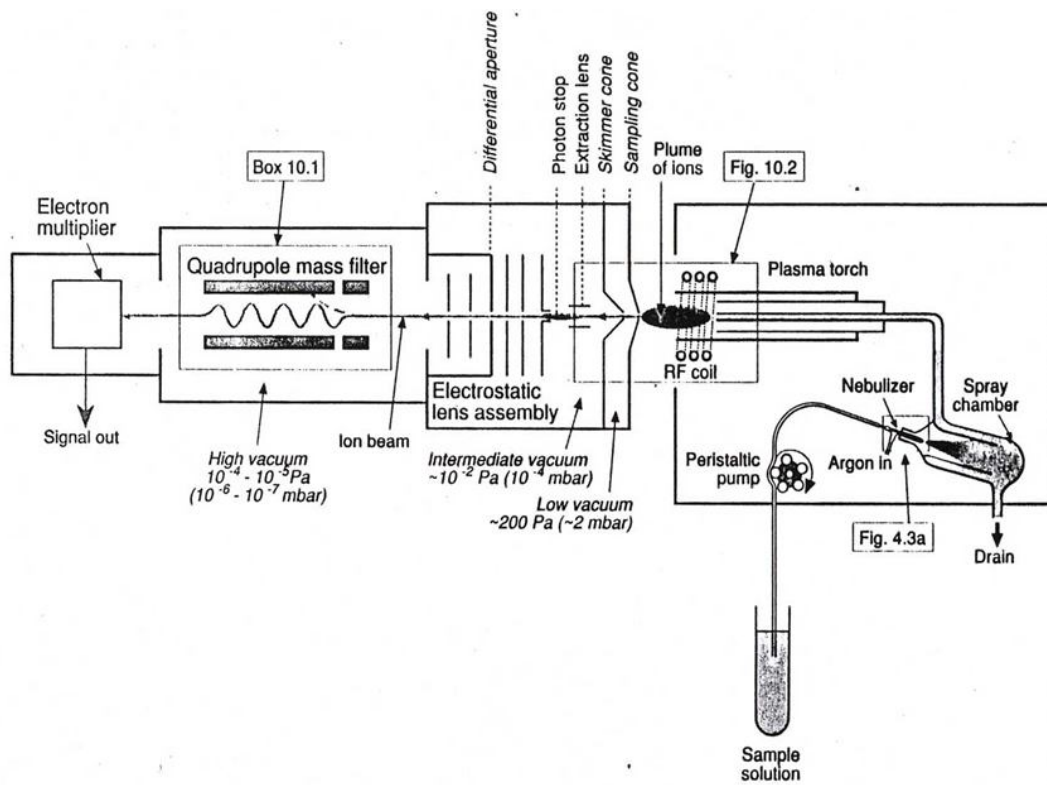
Figure 2.11 Schematic of ICP-MS instrument

As the atoms continue their travel through the plasma, they absorb more energy and eventually release one electron to form singly charged ions. The singly charged ions exit the plasma and enter the interface region. The area of the interface is the connection between the system of generation of the plasma and the mass spectrometer and consists of two coaxial cones: the first has a hole of about 1.1 mm and is said "sampler". The ions produced by the plasma pass through said hole forming a supersonic jet, then through the second cone called "skimmer" with a hole of about 0.9 mm. The beam finally reaches the ion lens that focuses and directs it to the quadrupole. They have the function to reduce the pressure between the plasma generation system, which operates at ambient pressure and temperatures of 7500 °C, and the mass spectrometer, working in conditions of high vacuum (10^{-5} torr) and low temperature.

In the quadrupole, the ions are separated by a magnetic field, according to the speed with which they move, which strictly depends on the mass / charge ratio (m / z) of the ion. Therefore appropriate voltages are applied to the bars, thus creating the conditions so that only specific ratios mass / charge can walk the path through the bars to the detector. The ions leaving the quadrupole are finally captured by a detector that functions as a counter and produces electrical signals proportional to the ion flux transmitted by the analyzer of the mass.

Table 2.3. List of elements analyzed by ICP-OES and ICP-MS

ICP-OES			ICP-MS		
Element	Wavelength (λ, nm)	LOD (ng m^{-3})	Element	Mass number	LOD (ng m^{-3})
S	180.669	146.51	V	51	0.13
Zn	206.200	9.77	Co	59	0.09
Fe	239.562	27.46	Ni	60	2.86
Mn	257.610	1.67	Cu	63	1.80
Mg	285.213	616.97	As	75	0.0
Ca	317.933	1090.34	Cd	111	0.09
Ti	336.121	3.22	Sb	121	0.43
Al	394.401	499.07	Pb	208	0.99
Ba	493.375	9.42			
K	766.490	240.61			

2.8.5. Methodological aspects and quality control and quality assurance

Filter blanks and field blanks (filter kept inside the sampler but not used for air filtering) were prepared and analyzed together with the samples, following the same procedures and the values obtained were routinely subtracted from those of the samples. For ICP-OES, the calibration technique is based on the use of external standards. This type of calibration, which precedes the reading of samples, is the measurement of the signal intensity of the elements of interest in a blank and in one or more known concentrations of standards and whose range values must cover the range of concentrations of the elements to be analyzed in the samples. These standards, after being corrected of the blank, serve to draw calibration curves for each element correlating the intensity of the signal and the known concentration of the element. Single- and multi-ionic standard for IC and ICP (Fluka – Riedel-de Haën) were used to test the linearity and calibrate the instrument response. With regard to the ICP-MS, calibration method is based on the use of internal standards and the internal standard, that is, usually an isotope having a mass which does not interfere with the analytes present in the matrix and added to each sample at a known concentration to correct any variation in the intensity of their signal to the known concentration. In the present work, it was decided to use the Rhenium (100 ppb), which meets these requirements. It can therefore normalize signal intensity of all analytes compared to those of the isotope used as a standard. As mentioned before, in addition to the samples, filed blanks were also analyzed, necessary for the calculation of the limit of detection (LOD). The limit of detection (LODs) was calculated for each ion and element as the three times the standard deviation of the blank values for each analyzed period. It is defined as "the concentration that gives a signal equal to three times that of the noise". The average LODs are reported in Table 2.3. The quality and accuracy of quantitative analysis were routinely checked analyzing the NIST SRM 1648 standard for air particulate. The recoveries of ions and elements were in the range of 80-110%.

2.9. Source apportionment

Various statistical tools such as diagnostic ratios, conditional probability function and factor analysis have been used to identify possible sources of particulate matter $PM_{2.5}$.

2.10. Data processing

2.10.1. Wind roses

Wind roses were built in order to assess the influence of local conditions on air quality and the program used for the construction of wind roses is the WRPLOT View of Lakes Environmental. The wind rose depicts the frequency of winds for each specified direction and speed classes for a given location and time period. The matrices loaded into the program contain the following information: year, month, day, hour, wind direction, wind speed and rainfall for each sampling site. In addition to this information, it is necessary to specify the sampling station and the corresponding values of latitude and longitude.

2.10.2. Back trajectories

The trajectories were simulated using the program HYSPLIT version 4.9 of the NOAA /ARL (National Oceanic and Atmospheric Amministration / Air Resources Laboratory) (Draxler and Rolph, 2011). The GDAS files are loaded into the program downloaded from the archive of the Air Resources Laboratory (NOAA, USA). Each trajectory was calculated by setting a total run time equal to -96 hours, the latitude and longitude of the stations considered, a basic quota of 20 m, ie within the mixing layer height and the same model 10000 m. For each day, 4 different trajectories were determined related to six hours (03:00, 09:00, 15:00, and 21:00 UTC). Overall, 240 trajectories were calculated for each sampling site. As accuracy in back trajectory calculation descreases with distance and time because of model assumptions and spatial-temporal resolution of the meteorological data, 4 back-trajectories per day seem to be the most suitable option. Subsequently, cluster analysis was performed on the back- trajectories obtained in order to reduce errors associated to single trajectory (Stohl, 1998) and to join the masses of air with similar characteristics.

2.10.3. Statistical analysis

The data have been processed by using various statistical softwares such as "R", Origin, STATISTICA, WRPLOT View™ and Hysplit.

CHAPTER 3

CHARACTERIZATION OF METEOROLOGICAL PARAMETERS

3.1. Local Contribution

3.1.1. Wind Roses

In order to interpret the data on the basis of local atmospheric circulation nine wind roses were built for each station (one for each month, summer, winter and annual). The comparison between the summer and winter is useful in order to assess whether and how much the wind speed affects the observed concentrations. The wind is divided into six classes and the % of calm refers to winds with speeds less than 0.5 ms^{-1}. The monthly wind roses for all stations are given in Appendix 3.1.

3.1.1.1. Belluno

From the observation of the wind roses (Figure 3.1) we notice that wind prevails in Belluno from South / South-West. The annual wind speed is 0.8 ms^{-1} whereas the wind speed was 0.9 ms^{-1} and 0.6 ms^{-1} during summer and winter, respectively. The percentages of calm reach 26.8%, 33.5% and 35.8% during summer, winter and annually, respectively.
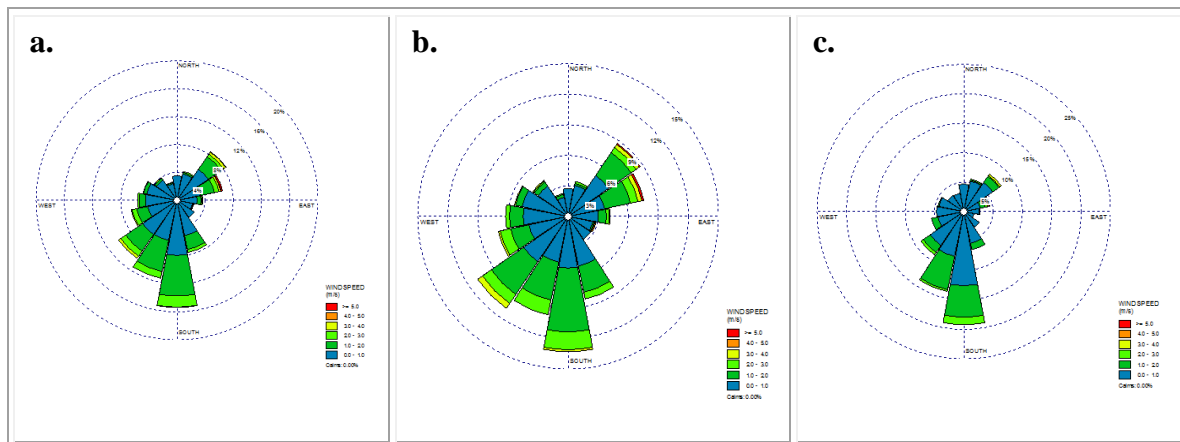
Figure 3.1. Wind-rose at Belluno [a. annual, b. summer, c. winter]

3.1.1.2. Treviso

In the station of Conegliano the wind has come from the North-West, Southeast and Northeast while North-west is the dominant during both winter and summer (Figure 3.2). Annually, average wind speed is 1.56 ms^{-1} while the wind speed is 1.65 ms^{-1} and 1.41 ms^{-1} during summer and winter, respectively. Treviso is characterized by stronger winds than in Belluno, which is affected by much lower proportions of calm (11.8%).
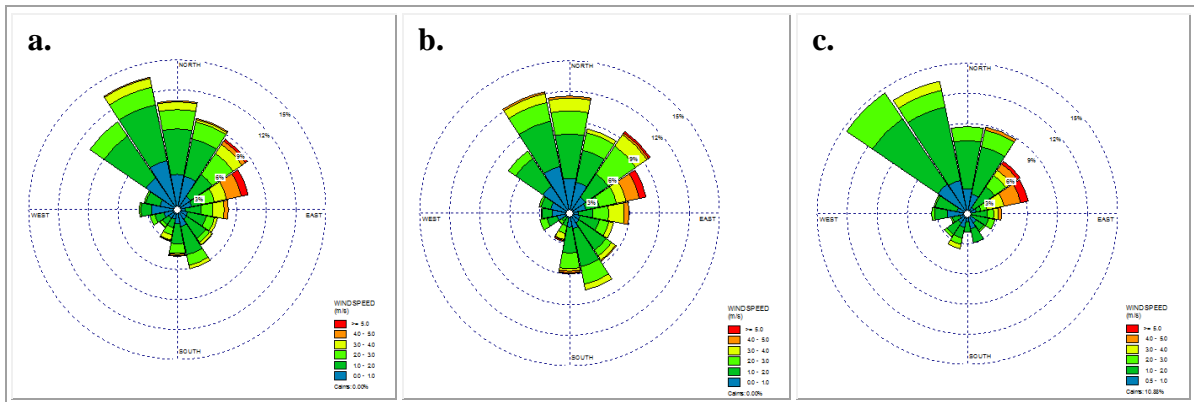
Figure 3.2. Wind-rose at Treviso [a. annual, b. summer, c. winter]

3.1.1.3. Vicenza

The station of Vicenza is characterized by an average calm (29.8%) and an average speed of 0.9 ms^{-1} with prevalence from East and South-West (Figure 3.3). In summer, however the wind speed reaches 1.1 ms^{-1} with prevalence from East. The calm is equal to 20.5%. On the contrary, South and South-East direction is prominent during winter (wind speed 0.6 ms^{-1}).
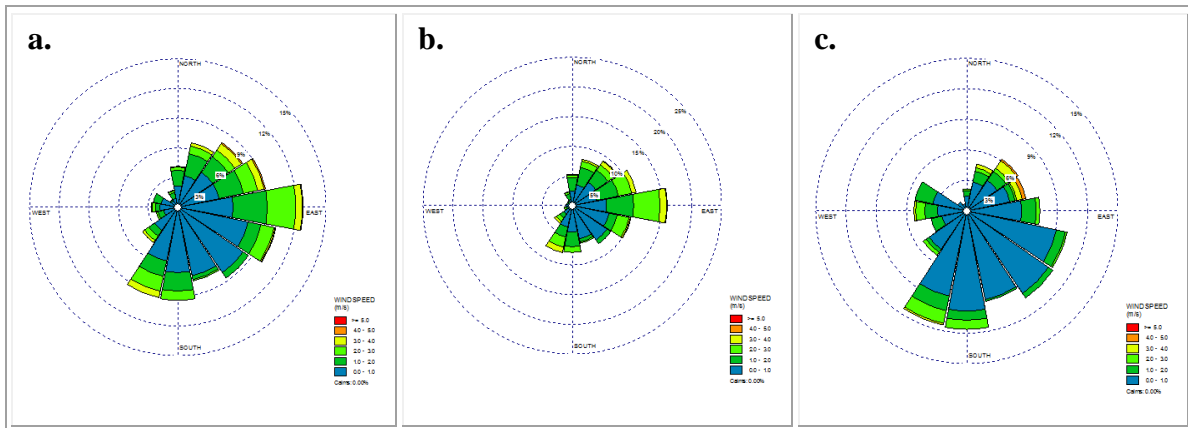
Figure 3.3. Wind-rose at Vicenza [a. annual, b. summer, c. winter]

3.1.1.4. Padova

Padua is characterized by very weak winds (0.2 ms^{-1}) from the north-eastern quadrant with calm of 20% (Figure 3.4).
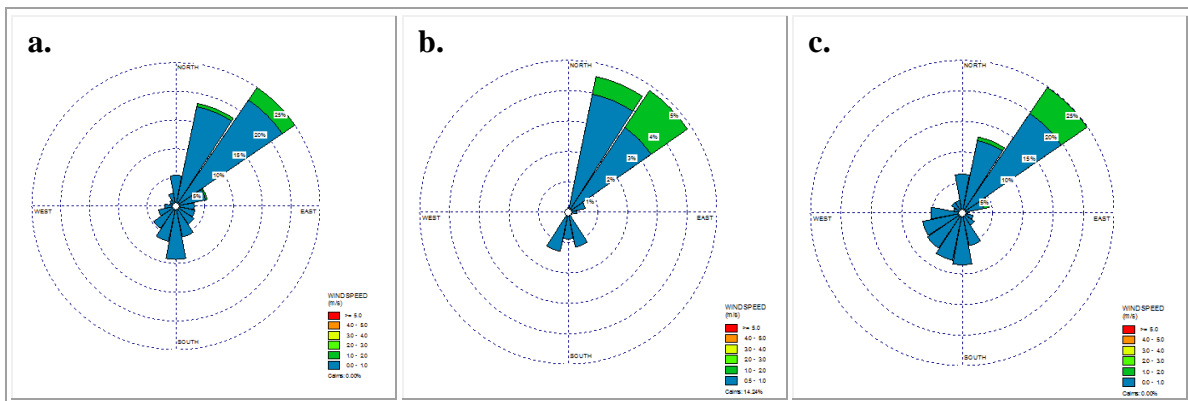
Figure 3.4. Wind-rose at Padova [a. annual, b. summer, c. winter]

3.1.1.5. Venice

In the station of Mestre both the seasons are characterized by weak winds (0.9 ms^{-1} and 0.4 ms^{-1} in summer and winter, respectively) that blow predominantly from North, South-East and West. Summer has a percentage of calm equal to 20.9%, while winter has a value equal to 21.3% (Figure 3.5).
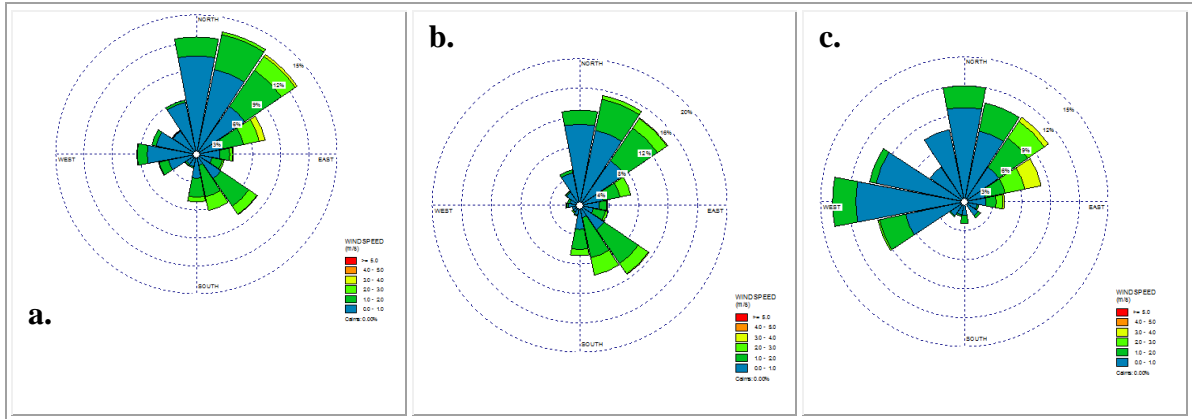
Figure 3.5. Wind-rose at Venice [a. annual, b. summer, c. winter]

3.1.1.6. Rovigo

The Rovigo Station recorded a very low percentage of calm (0.8%). The average speed is higher than the most of the stations, and falls into the second class (1.4 ms^{-1}). The winds blow from the north- East and South-West (Figure 3.6). The wind rose for the month of December and February was not built due to lack of data.
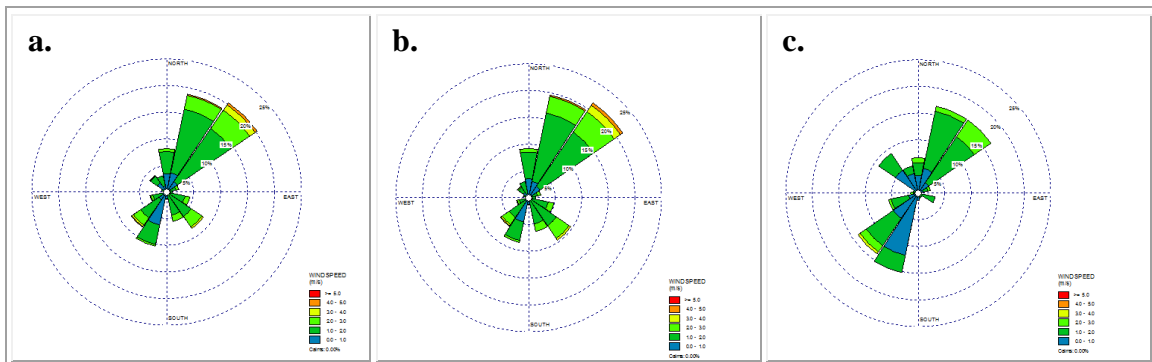
Figure 3.6. Wind-rose at Rovigo [a. annual, b. summer, c. October]

3.1.1.7. Wind Roses at Veneto Region

In general the winds are low to medium intensity in all six stations (in particular in the station of Padua) (Figure 3.7). Rovigo and Padua can be distinguished from other stations: the first one is characterized by very low percentages of calm during the whole period considered and Padua is characterized by very weak winds. The presence of very weak winds favors the accumulation of pollutants and consequently high concentrations in the air. However, from the observation of wind roses, it is not possible to identify a clear relationship between the concentration of pollutants and the speed of the wind.
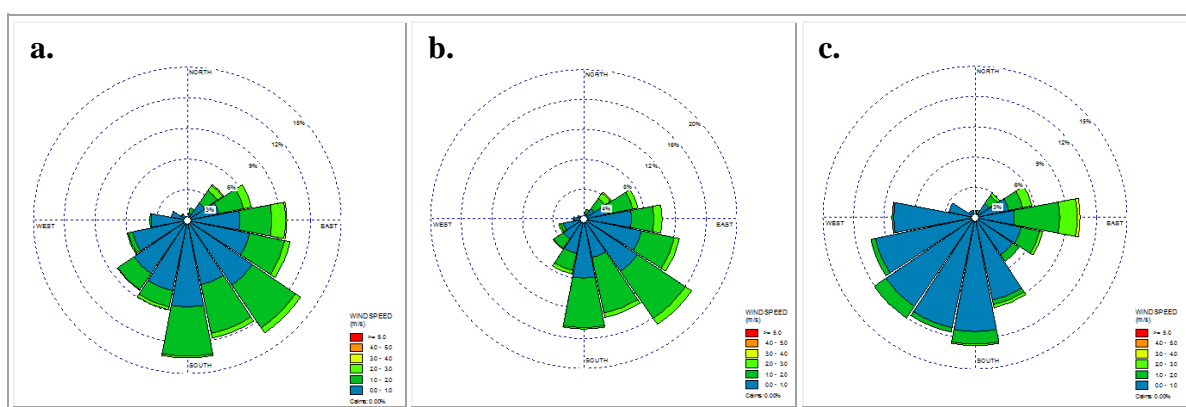
Figure 3.7 Wind-rose at Veneto region (a. annual, b. summer, c. winter)

3.2. Long-distance transport

The calculation of *back-trajectories* through the use of meteorological data stored is potentially useful for identifying the source areas of pollutants (Baker 2010). They describe the path traveled by a particle in a given period of time and then allow it to tell which locations it comes (Abdalmogith and Harrison, 2005). The potential influence of long-range transports on the chemical composition of aerosol in Veneto was estimated by a cluster analysis on the back-trajectories. Back-trajectories were computed by using the HYSPLIT model (Draxler and Rolph, 2013; Rolph, 2013). The setup was: 96 h backward; starting height at 20 m a.s.l.; 4 trajectories per day at 3, 9, 15 and 21 UTC calculated separately for all the sites. For a single trajectory is associated with a high rate of uncertainty, which depends on the accuracy of the meteorological data used and the level of approximation of the model. The problem can be overcome by calculating a large

number of trajectories, which are subsequently grouped through an analysis of the cluster (Baker, 2010). This multivariate analysis technique groups the data into several groups *(clusters),* according to their similarity. In this study, 4 *back-trajectories* were calculated for each sampling day considered. For each station total 240 trajectories were obtained. A clustering algorithm using the Euclidean distance measure (Carslaw, 2014) was further applied to group back-trajectories into clusters depending on their potential origin. From the observation of the figures, 7 areas of air masses origin have been identified (Table 3.1) such as (1) Mediterranean (2) Local (3) Western Europe (4) North-Western Europe (5) North Europe (6) North Eastern Europe and (7) Adriatic. In all the stations, it is noticed that highest air masses are originated from local (Table 3.1).

Table 3.1. Percentage of origin of air masses in the six stations

	Mediterranean	Local	Western Europe	North-western	North	North-Eastern	Adriatic
Belluno	7	59	4	21	9		
Treviso	11	54	7		11	18	
Vicenza	7	42		19	3	30	
Padova	9	35	4		11	41	
Mestre	12	31			13	24	20
Rovigo	12	33	4			28	23
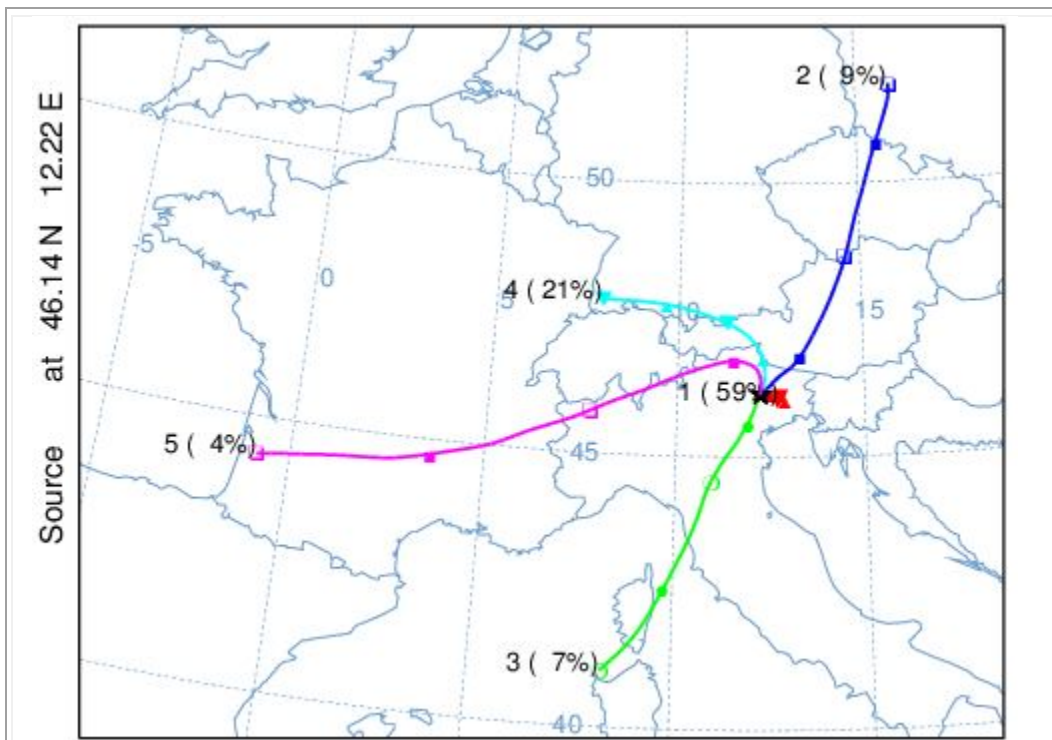
Figure 3.8. Results of the back-trajectory cluster analysis for Belluno station
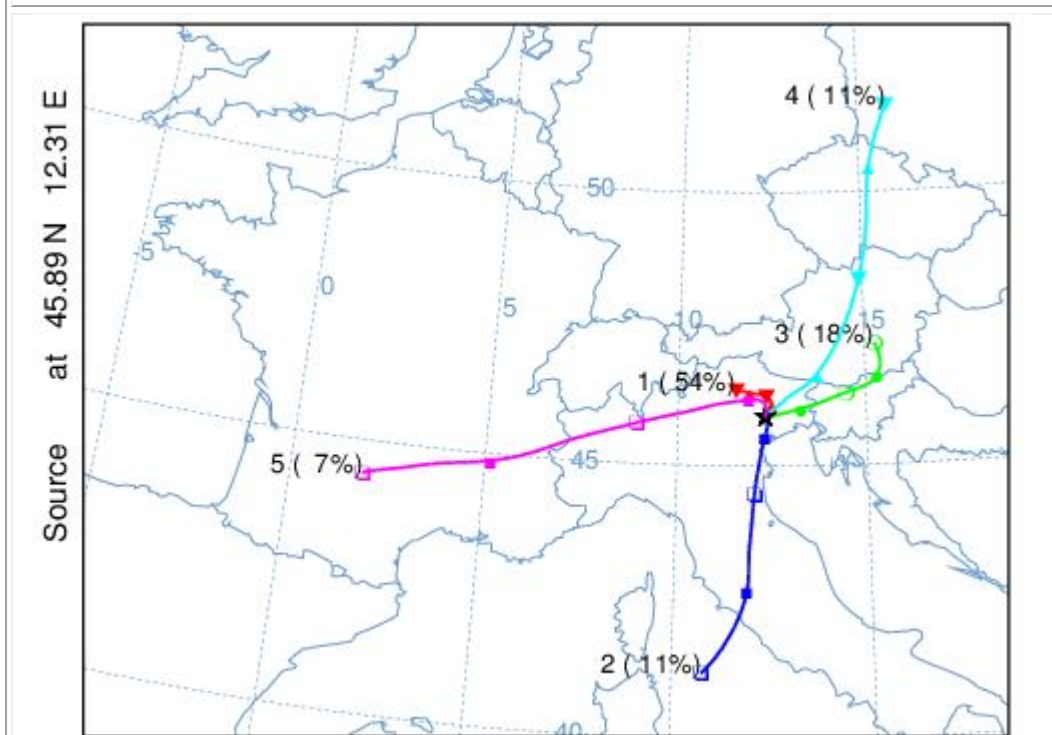
Figure 3.9. Results of the back-trajectory cluster analysis for Treviso station
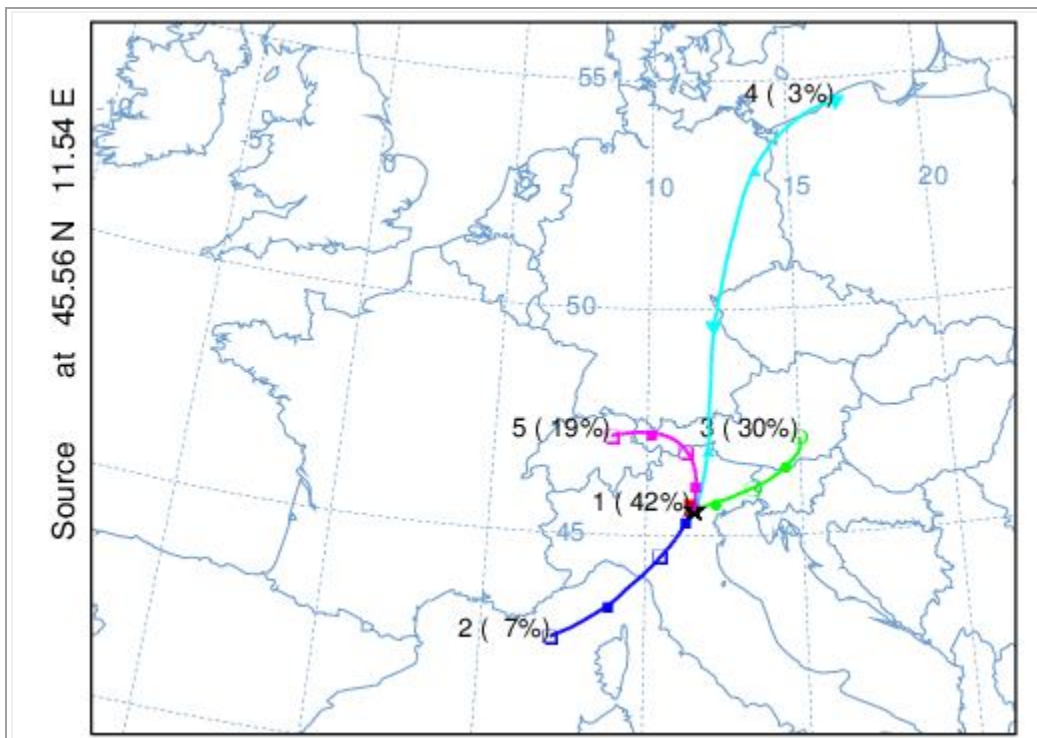
Figure 3.10. Results of the back-trajectory cluster analysis for Vicenza station
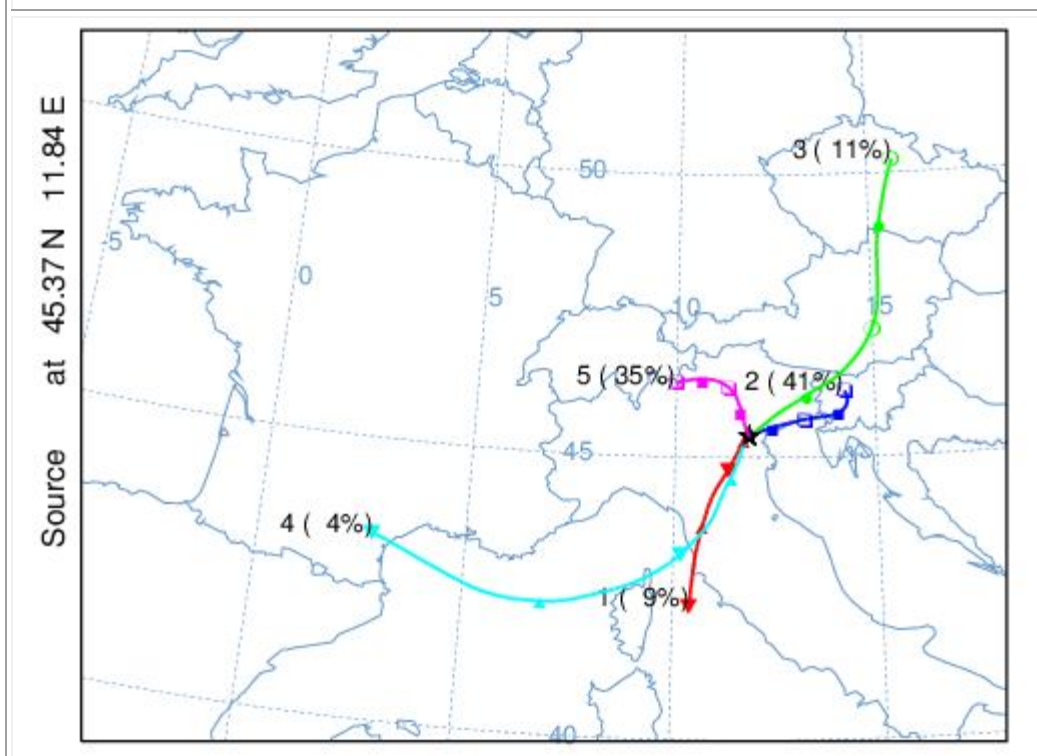
Figure 3.11. Results of the back-trajectory cluster analysis for Padova station

70
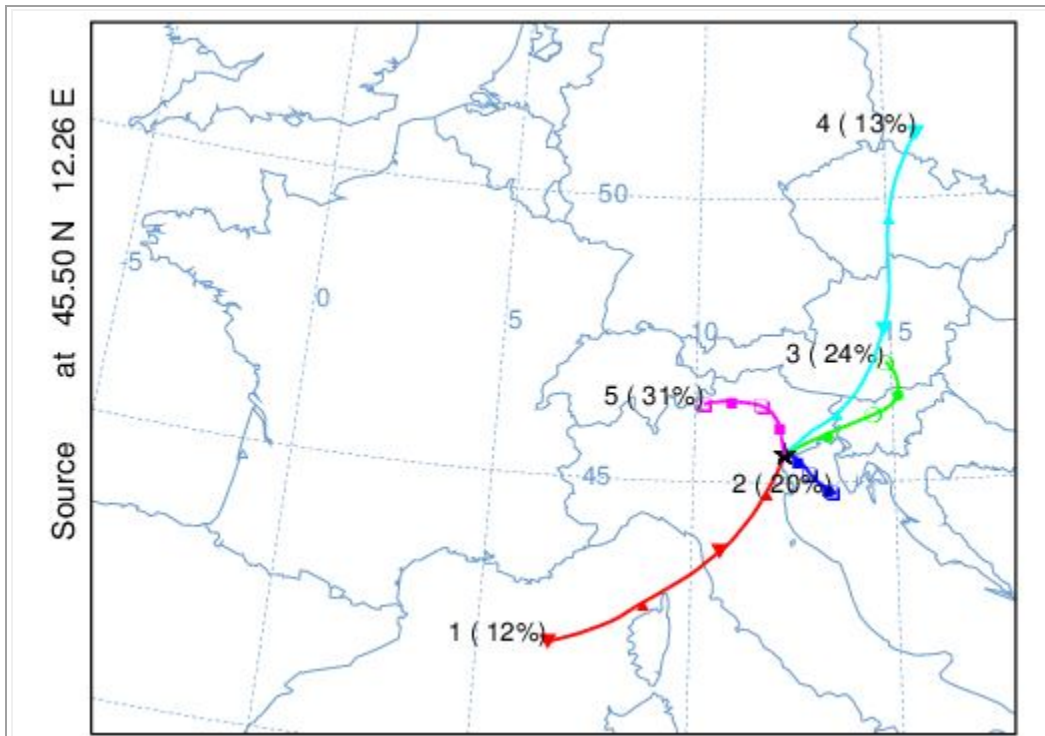
Figure 3.12. Results of the back-trajectory cluster analysis for Venice station
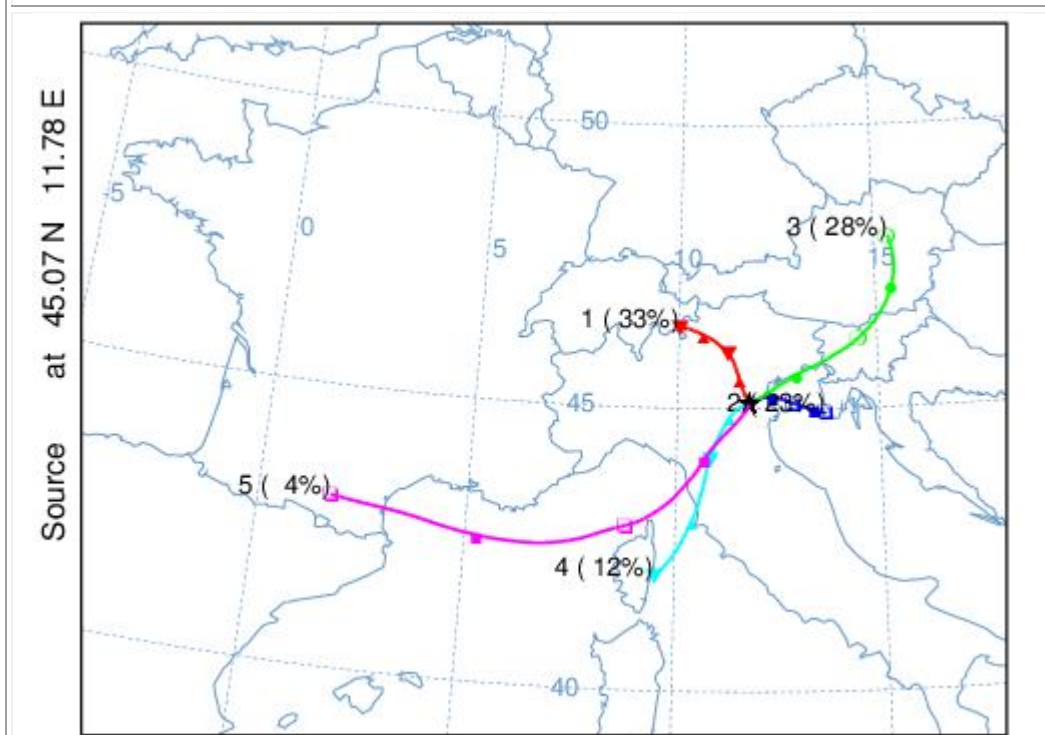
Figure 3.13. Results of the back-trajectory cluster analysis for Rovigo station

CHAPTER 4

CARBONACEOUS AEROSOLS

4. CARBONACEOUS AEROSOLS

4.1. Introduction

Carbonaceous compounds account for an important fraction of atmospheric particulate matter (PM), generally contributing between 30 and 50% of PM with aerodynamic diameter < 2.5 μm ($PM_{2.5}$) in many European urban areas (Putaud et al., 2004). In the recent years, the scientific community has paid much attention to the carbonaceous fraction of PM, since it may affect the global radiation budget, cloud microphysics (Seinfeld and Pandis, 1998; Lyamani et al., 2006) and has effects on the global climate change (Hitzenberger et al., 1999; Dan et al., 2004). In addition, increased levels of urban carbonaceous PM are significantly associated with cardiovascular mortality and morbidity (Na et al., 2004; Ito et al., 2011) and several organic compounds of known or suspected carcinogenic and/or mutagenic potential are commonly found in PM, e.g., polycyclic aromatic hydrocarbons (PAHs) and polychlorinated biphenyls (PCBs) (WHO, 2000).

The carbonaceous PM is composed of a refractory component, commonly called elemental carbon (EC) and an organic fraction (OC). EC is a primary pollutant being mainly released in particle-phase from the incomplete combustion of carbon-containing fuels. On the contrary, OC includes thousands of different organic compounds (e.g., aliphatic, aromatic hydrocarbons, carboxylic acids and carboxylic compounds with polar substituent, etc.) with widely varying chemical and physical properties, such as molecular weights, level of oxidations and gas-particulate partitioning. OC can be directly emitted as a primary OC from many sources including combustions, industrial emissions, geological and natural sources. It can also form in the atmosphere as secondary OC, when some volatile and semi-volatile organic compounds (VOC and SVOCS) are chemically transformed and the products undergo condensation or nucleation.

Although many recent researches have studied the carbonaceous fraction of PM, its chemical characterization is not comprehensively accomplished yet and some formation mechanisms are still unclear (Jacobson et al., 2000). In addition, the quantification of primary and secondary OC is a very challenging task due to several reasons, such as the breaking down process of OC into primary and secondary organic carbon, potential

sampling and analytical artefacts, effects of meteorological conditions during the sampling, etc. However, an estimation is possible through several indirect methods. Among others, the EC-tracer method is a widely accepted technique (Turpin and Huntzicker, 1995; Castro et al., 1999, Lim and Turpin 2002; Cabada et al., 2004; Harrison and Yin, 2008) and uses EC as a tracer of primary organic carbon (POC).

Several studies have been conducted across Italy on the carbonaceous PM (e.g., Lonati et al., 2005, 2007: Milan; Perrone et al., 2011: Milan; Larsen et al., 2012: Po Plain Italy; Cuccia et al., 2013: Milan; Malaguti et al. 2013: Trisaia ENEA Research Centre) and a recent review of available data was also recently published (Sandrini et al., 2014). However, data available for the Veneto Region, NE Italy, are quite limited so far. This is a serious gap, as Veneto is one of the most industrialized areas of Italy and is located in the Eastern part of the Po Valley, which is a well-known European hot-spot for many air pollutants, including PM_{10}, $PM_{2.5}$ and PM_{10}-bound PAHs (Masiol et al., 2013). The presence of high mountain ranges, i.e. the Alps to the North and NW and the Apennines to the South, protects the Po Valley from cold winds coming from the NE (Larsen et al., 2012). In addition, the occurrence of frequent and prolonged wind calm periods, atmospheric stability conditions, persistent thermal inversions and lower planetary boundary layer heights during the night-time may favour the accumulation of locally-emitted pollutants especially during the coldest months (Masiol et al., 2014).

This chapter mainly discussed (i) quantification of the seasonal and spatial trends of carbonaceous aerosols in the Veneto Region; (ii) effects of meteorological factors on the carbonaceous PM, and (iii) estimation of the contribution of secondary organic carbon (SOC) formation to the frequent exceeding of air quality standards for $PM_{2.5}$.

4.2. Methodology

4.2.1. Conditional Probability Function (CPF) and Conditional Biovariate Probability Function (CBPF)

Conditional probability function is an important tool for the identification of local point sources (Kim et al., 2003; Kim et al., 2005) and it estimates the probability that a source is

located within a particular wind direction sector, Δθ (Ashbaugh et al., 1985; Begum et al., 2010). CPF is defined as:

$$CPF_{\Delta\theta} = \frac{m_{\Delta\theta}\,|_{C>x}}{n_{\Delta\theta}}$$ .... (4.1)

Where $m_{\Delta\theta}$ is the number of samples from the wind direction θ having concentration C is higher than or equal to a threshold value x and $n_{\Delta\theta}$ is the total number of samples of the same wind sector Δθ. Here, x represents a high percentile concentration (75th or 90th). Recently a new technique is developed by Uria-Tellaetxe and Carslaw (2014) combining conditional probability function with bivariate polar plots to detect and characterize the source of pollutants. Bivariate polar plots show how a concentration of a species varies jointly with wind speed and wind direction in polar coordinates and give directional information on sources as well as wind speed dependence of concentrations. The conditional bivariate probability function (CBPF) includes wind speed with CPF and allocates the observed pollutant concentration to cell defined by ranges of wind direction and wind speed which is defined as:

$$CBPF_{\Delta\theta,\Delta u} = \frac{m_{\Delta\theta,\Delta u}\,|_{C>x}}{n_{\Delta\theta,\Delta u}}$$ ....(4.2)

Where $m_{\Delta\theta,\Delta u}$ is the number of samples from the wind direction $\Delta\theta$ with wind speed interval Δu having concentration C higher than or equal to a threshold value x and $n_{\Delta\theta,\Delta u}$ is the total number of samples in that wind direction-speed interval. Details of the CPF and CBPF methods will be found elsewhere (Uria-Tellaetxe and Carslaw, 2014). For wind direction data, daily weighted circular mean was calculated from hourly wind direction data and used for CPF and CBPF.

4.2.2. Back-trajectory analysis

A cluster analysis on the back-trajectories was performed to investigate the potential effects of long-range transports on the levels of EC, OC and TC. Back-trajectories were computed by using the HYSPLIT model (Draxler and Rolph, 2013; Rolph, 2013). The setup was: 96 h backward; starting height at 20 m a.s.l.; 4 trajectories per day at 3, 9, 15 and 21 UTC calculated separately for all the sites. A clustering algorithm using the

Euclidean distance measure (Carslaw, 2014) was further applied to group back-trajectories into clusters depending on their potential origin.

4.3. Results and discussions

4.3.1. Overview on results

Summary statistics of the atmospheric concentration of $PM_{2.5}$, Total Carbon (TC) and Total Carbonaceous Aerosols (TCA) at the six provinces of Veneto region are presented in Table 4.1. $PM_{2.5}$ concentrations varied from 3 µg m^{-3} to 83 µg m^{-3} with mean [mean±standard deviation (SD)] of 24±17 µg m^{-3}. The concentration of $PM_{2.5}$ showed an increasing trend from warmer months (June, 12 µg m^{-3}, August, 17 µg m^{-3}) to colder months (December, 41 µg m^{-3}, February, 38 µg m^{-3}). The higher mean annual concentration was found in Padova (29 µg m^{-3}), followed by Vicenza (28 µg m^{-3}), Rovigo (27 µg m^{-3}) and Venice (25 µg m^{-3}), whereas comparatively lower mean concentrations were observed in Belluno (17 µg m^{-3}) and Treviso (18 µg m^{-3}). These PM levels are comparable to the concentrations normally observed in Milan (Lonati et al., 2005; 33 µg m^{-3}) (Lonati et al., 2007; winter, 58 µg m^{-3} and summer, 25 µg m^{-3}) and Florence (Giannoni et al., 2012; annual mean value 19±10 µg m^{-3}). The higher values recorded during the colder months were substantially due to the atmospheric stability and lower mixing layers resulting in pollutant accumulation at ground level. On the contrary, atmospheric dispersion due to increased wind speeds and wide mixing layer heights was responsible for the lower PM concentrations in warmer months (Ferrero et al., 2010). It is noted that vertical mixing is the key factor to disperse the pollutants originated from primary pollution. The PBL (planetary boundary layer) height is 450 m (Bigi et al., 2012) in winter, whereas it increases during summer (1500-2000 m) due thermal convective activity (Di Giuseppe et al., 2012).

Among the six measurement cities, $PM_{2.5}$ concentrations in four cities exceeded the annual mean concentration limit set by the 2008/50/EC directive: annual mean value 25 µg m^{-3} which will be met by 2015 (EC, 2008) (Table 4.1).

The total organic mass associated with OC (here designated as organic matter, OM) was calculated by multiplying the measured OC by a factor of 1.4, as suggested by Lonati et al., (2005). TCA is calculated as sum of OM and EC. The average annual contribution of TCA to $PM_{2.5}$ is 39% ranging from 19% to 89%. The mean OC concentration was 5.5±4.0 µg m^{-3} (mean±SD) accounting for 22% to the total $PM_{2.5}$ and 79% to the TC. On the contrary, EC varied from 0.2 to 11.9 µg m^{-3} with a mean value of 1.3 µg m^{-3} and contributing to 5% of the total $PM_{2.5}$ and 21% of the TC. A similar value was found by Lonati et al. (2007) in Milan, where the OC value ranged from 0.4 to 35.8 µg m^{-3} with a mean annual value of 9±7 µg m^{-3} and EC value ranged from 0.4 to 5 µg m^{-3} with mean annual value of 1.3 µg m^{-3}. The concentrations of OC and EC reported in various European cities are given in Table 4.2.

Table 4.1. Summary statistics for $PM_{2.5}$ and total carbon in $PM_{2.5}$ (µm^{-3}) (Veneto region).

Sampling site	$PM_{2.5}$ (µm^{-3})	TC (µm^{-3})	TCA (ug m^{-3})	TCA/$PM_{2.5}$ (%)
Belluno	17.4±12	6.2	8.6	50.0
Treviso	19.7±13	5.6	7.9	39.0
Vicenza	28.1±18	7.0	9.9	34.0
Padova	28.7±19	8.2	11.6	39.0
Venice	25.3±17	6.8	9.6	37.0
Rovigo	27.2±19	6.9	9.5	36.0
Mean (Veneto reion)	24.4	6.8	9.53	39.0
Median	18.4	4.3	6.1	37.6
SD	16.7	5.1	7.3	11.1
Range	3.0-82.7	1.2-24.5	1.7-35.6	19.2-88.8

Table 4.2. Organic and elemental carbon concentrations in various European cities.

City	OC	EC	Authors
Helsinki	3	1.2	Viidanoja et al., 2002
Budapest	6.8	3.3	Salma et al., 2004
Amsterdam	3.9-6.7	1.7-1.9	Viana et al., 2007
Barcelona	3.6-6.9	1.5-2.6	Viana et al., 2007
Birmingham			Harrison and Yin, 2008
winter	3.7	1.2	
spring	2.8	0.6	
Oslo	1.7	1	Jedynska et al., 2014
Athens	3.5	1.6	Jedynska et al., 2014
Paris	2.2	1.8	Jedynska et al., 2014
London/Oxford	1.4	1.3	Jedynska et al., 2014
Rome	3.7	2.3	Jedynska et al., 2014
Munich	2.7	0.5	Jedynska et al., 2014

4.3.2. OC/EC Ratio

The OC/EC ratios ranged from 0.7 to 15.4 with an annual mean value of 4.5 (Table 4.3). A similar result was observed in Milan (annual mean value 6.5) by Lonati et al. (2007) and at urban background (from 2.1 to 8.4) and urban traffic (from 2.9 to 8.3) sites in Tuscany (Giannoni et al., 2012). These values, which are similar to the values observed in most of the urban background sites in the Po Valley (summer: from 5 to 7; winter: from 3 to 10) and also comparable to the rural sites of the Po Valley, suggest a regional influence of SOA coming from anthropogenic and biogenic sources in summer and the extensive wood burning utilization for residential heating in winter (Larsen et al., 2012). Condensations of gas phase semi-volatile organic species due to lower temperature combined with frequent events of air stagnation are responsible for increased OC/EC ratios in the Po Valley (Gilardoni et al., 2011; Larsen et al., 2012; Sandrini et al., 2014). However, the mean OC/EC ratios in this study were generally found above the values observed in most European cities. The OC/EC ratios in summer and winter in Amsterdam, Barcelona, and

Ghent were 2.8-4.7, 2.6-3.1 and 3.5-4.4, respectively. The higher OC/EC ratios were referred to the formation of secondary organic carbon in addition to primary organic carbon (Kim et al., 2000; Na et al., 2004).

4.3.3. Spatial and seasonal trends

Monthly variations of OC and EC concentrations are shown in Figure 4.1. Generally the higher concentrations were found during colder months, while lower concentrations were found in the warmer ones. The highest OC level was observed in December (11.4 µg m^{-3}), the lowest in April (2.2 µg m^{-3}). The monthly organic carbon concentration gradually increased from April to December. Both the OC and EC concentrations were higher in February (9.1 µg m^{-3}), than in other months except December. Although the monthly mean of EC concentration does not exhibit larger variability, it follows the same pattern as OC with maxima during the colder months and minima in the warmer ones. Data categorized according to province, reveal the highest mean annual OC concentration in PD (6.8 µg m^{-3}) while the lowest mean value in TV (4.5 µg m^{-3}). OC concentrations varied slightly among the provinces and differences were not statistically significant as confirmed by Kruskal–Wallis one-way analysis of variance (p-value 0.08). However, variations for EC values among the provinces were statistically significant (Kruskal–Wallis one-way analysis of variance test, p-value 0.00).

The combined effect of the lower air temperature favouring the particle-phase partitioning of semi-volatile organics and the additional emission sources in the form of biomass burning or household heating systems are possibly the main factors for higher OC concentrations in winter months (e.g., Viana et al., 2007; Schwarz et al., 2008). Moreover, the daily variability of OC concentrations is higher in winter than in summer probably because of significant local contributions with remarkable daily variability, whereas homogenous contributions from regional-scale secondary organic aerosols are the reason behind lower variability of OC concentrations in summer months (Viana et al., 2007). The origin of carbonaceous aerosols can be evaluated from the relationship between OC and EC (Turpin and Huntzicker, 1995). A strong relationship between OC and EC is the indication of dominant primary sources (e.g. vehicle emissions, cooking, various

combustion processes). In this study, a statistically significant positive correlation (r=0.76) between OC and EC was observed for all data in absence of any categorization. Before statistical analysis, normality of the data was tested and data of OC and EC were not normally distributed. This was confirmed by observing histogram, boxplot and finally by applying the Shapiro-Walk tests (assumption, $p < 0.05$ was not met). LogOC and logEC have been used instead of OC and EC during statistical analysis as the normality assumption was not met and correlation analysis was performed using robust procedure.

By sorting the data into months, positive correlations between elemental and organic carbon were observed in all the months except December (Table 4.3). However, the correlation is comparatively higher in the warmer months than in the colder ones. This weaker correlation and higher OC/EC ratio during the winter months is probably due to the influence of SOC (Secondary Organic Carbon) formation or other significant primary organic sources (Na et al., 2004). This result is similar to the one obtained by Kim et al. (2000), who suggest that the EC and OC may not be emitted from a single dominant primary source (Na et al., 2004). The relationship between organic and elemental carbon of each provinces was also determined (Table 4.3).

An effort was given to provide a comparison of carbonaceous particulate matter between weekdays and weekend (Figure 4.2). Generally weekdays showed higher TC concentrations as compared to weekend. All the measurement sites follow the same pattern and showed the highest TC concentration in Wednesday whereas the lowest concentration was observed in Sunday, indicates nonappearance of pollution from commuting and other professional activities (Martellini et al., 2012). This is also pointed out that the highest OC concentration was also observed during Wednesday whereas the highest EC concentration was observed in Thursday. Moreover, both OC and EC concentrations showed higher concentrations during Saturday than Monday may be due the fact that most of the business operations are functioned during Saturday in Italy.

Table 4.3 Monthly and province averaged values of OC, EC and OC/EC ratios in PM$_{2.5}$ (μm^{-3}) and Correlation of logOC and logEC

Month **Province**

Month	OC ($\mu g\ m^{-3}$)	EC ($\mu g\ m^{-3}$)	OC/EC	Robust correlation coefficient	Classical correlation coefficient	Province	OC $\mu g\ m^{-3}$	EC $\mu g\ m^{-3}$	OC/EC	Robust correlation coefficient	Classical correlation coefficient
February	9.1	1.5	6.8	0.74	0.57	Belluno	4.9	1.3	4.4	0.76	0.75
April	2.2	0.8	3.0	0.47	0.43	Treviso	4.5	1.1	4.5	0.81	0.79
June	2.6	0.6	4.4	0.70	0.69	Vicenza	5.8	1.3	4.6	0.74	0.73
August	3.2	0.8	4.5	0.72	0.70	Padova	6.8	1.5	4.7	0.76	0.68
October	4.4	1.3	3.5	0.33	0.23	Venice	5.7	1.1	5.4	0.82	0.81
December	11.4	2.9	5.1	-0.06	0.01	RO	5.2	1.7	3.7	0.58	0.57
Annual	5.5	1.3	4.5			provinces	5.5	1.3	4.5		
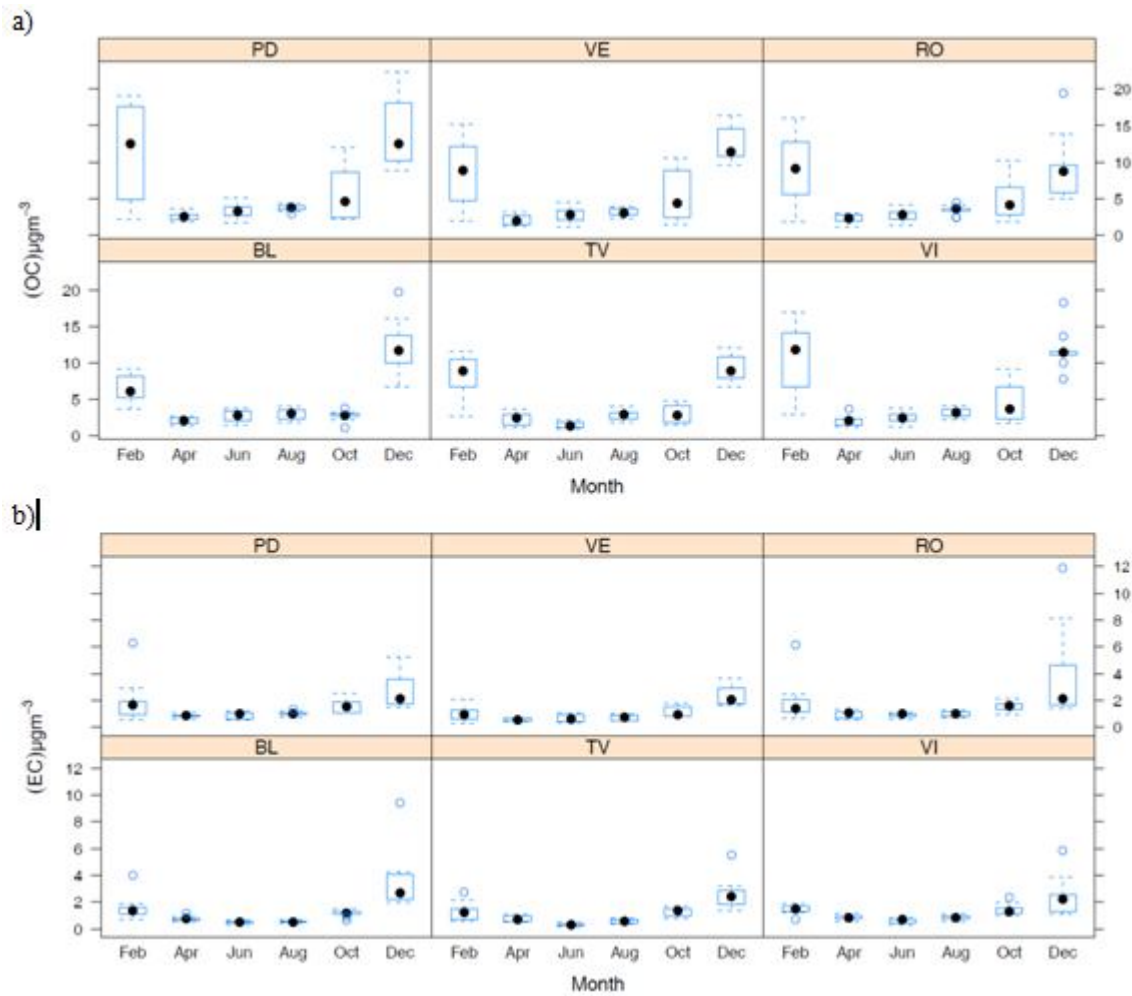
Figure 4.1. Boxplots of OC (a) and EC (b) conditional per Month and Provinces of Veneto.

Table 4.4. A correlation matrix between carbonaceous particulate matter and meteorological parameters.

	logOC	logEC	Temperature	Solar radiation	Wind velocity	Relative humidity
a. Annual						
logOC	1					
logEC	**0.76**	1				
Temperature	**-0.62**	**-0.66**	1			
Solar radiation	**-0.58**	**-0.72**	**0.77**	1		
Wind velocity	**-0.44**	**-0.52**	**0.20**	**0.41**	1	
Relative humidity	**0.32**	**0.47**	**-0.62**	**-0.70**	**-0.34**	1
b. Summer						
logOC	1					
logEC	**0.49**	1				
Temperature	**0.43**	**-0.19**	1			
Solar radiation	-0.05	**-0.54**	**0.63**	1		
Wind velocity	**-0.52**	**-0.59**	-0.03	**0.35**	1	
Relative humidity	-0.20	**0.26**	**-0.83**	**-0.69**	-0.08	1
c. Winter						
logOC	1					
logEC	**0.41**	1				
Temperature	**-0.60**	**-0.39**	1			
Solar radiation	**-0.41**	**-0.48**	**0.34**	1		
Wind velocity	**-0.28**	**-0.31**	-0.03	0.38	1	
Relative humidity	-0.03	**0.16**	0.02	**-0.40**	**-0.50**	1

*values with bold mark showed statistically significant
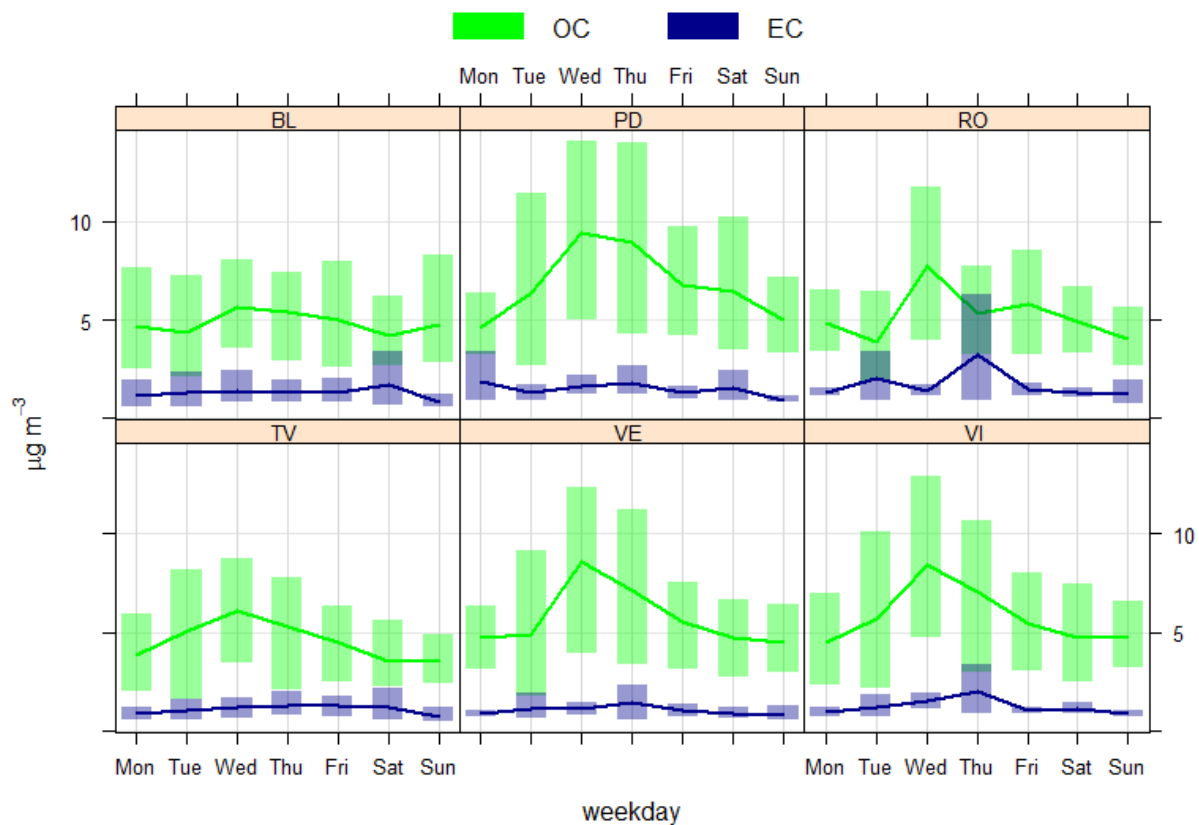
Figure 4.2. Plot showing weekly OC and EC concentrations (mean with 95% confidence interval) at Veneto region

4.3.4. Factors affecting organic and elemental carbon levels

A correlation analysis between some weather parameters with organic and elemental carbon data was performed following a robust procedure in order to identify the factors affecting carbonaceous compounds variations (Table 4.4). EC and OC had a statistically significant negative relationship with temperature and solar radiation. This result suggests an increased emission during the winter months and it is similar to the findings of Li et al. (2012). Organic and elemental carbon also showed a negative relationship with wind velocity. This is probably due to the clearing function of wind (Pindado et al., 2009). Similar results were also reported for PAHs measured across the Veneto region (Masiol et al., 2013). A weak positive correlation was observed both for OC and EC concentrations with relative humidity. The absorption of pollutants may increase with the rises of humidity (Elbayoumi et al., 2013). For illustration purpose, data have been categorized into two groups to be consistent with the dates in which domestic heating is switched off (15 April) and on (15 October) according to the national legislation: warm period (from April to October 14) and cold period (from October 15 to March). The correlation of OC with temperature was positive in the warm period, negative in the cold one. A positive correlation between OC with temperature during the warm period may be due to the contribution of the secondary organic carbon (Grivas et al., 2004), whereas a negative correlation between OC and temperature may be related to the increased household heating during the cold period. An additional explanation for this negative correlation can also be found in the presence of lower pollutant dispersions with stable atmospheric condition during winter (Vardoulakis and Kassomenos, 2008). A negative correlation between wind velocity and organic and elemental carbon was observed in both the seasons.

Finally, statistically significant weather factors controlling OC and EC were investigated by fitting linear models using a robust procedure based on weighted likelihood (Markatou et al., 1998). Robust techniques enable to overcome small deviations from normality and the presence of few outliers. A robust model selection procedure based on a weighted Akaike Information Criterion (Agostinelli, 2001) was also used, to choose the best model. This turned out to be the model including only temperature and wind. An additional confirmation was also provided by the robust t-test based on the full model in which

temperature, humidity, wind velocity and solar radiation were considered as meteorological variables.

The selected model expression is the following:

$$\log(OC) = \alpha_1 \log(EC) + \alpha_2 Temperature + \alpha_3 Wind + \sum_{i=1}^{6} \beta_i I(Month_i) + \varepsilon \;\dots\dots\; (1)$$

A robust R^2 of the selected model is 0.79. The *p-value* and level of significance of the model parameters and other related information is provided as Appendix 4 (Table A-4.1). This procedure identifies three outliers, namely PD 39, 40 and VE 39 (see, Appendix 4). After checking those observations, we found that comparatively higher relative humidity values were observed in these days and sampling sites (in PD, RH>91% and VE, RH>95%). This may be one of the reasons.

4.3.5. Secondary organic Aerosol estimation

The quantification of primary and secondary organic carbon is quite difficult since no direct analytical methods are available. Several indirect methods have been used to estimate the secondary organic carbon. Among them, the EC tracer method is a widely accepted one: EC is used as a tracer of Primary Organic Carbon (POC) (Turpin and Huntzicker, 1995; Cabada et al., 2004). SOC is calculated by the following equation:

$$SOC_{sec} = OC_{tot} - EC \, (OC/EC)_{pri}$$

Where SOC_{sec} is the secondary OC and OC_{tot} is the measured total OC. Primary organic carbon (POC) is calculated from the EC $(OC/EC)_{pri}$. However, without conducting a complete profile of the organic carbon and emission source, it is difficult to define the contribution of the primary source. Several authors have recommended to substitute the primary OC/EC by the minimum OC/EC ratio (Castro et al., 1999):

$$SOC_{sec} = OC_{tot} - EC \, (OC/EC)_{min}$$

Based on this technique, the minimum OC/EC ratio of this study is 1.29, which is the mean of 5% lowest OC/EC ratio. The mean annual primary and secondary organic carbon concentrations are 1.7 µg m^{-3} and 3.8 µg m^{-3}, respectively (Table 4.5). In the cold period comparatively higher secondary organic carbon values were found than in the warm one. For illustration purpose, all data have been divided into two periods; warm period (April to October 14) and cold period (October 15 to March). Cold period mean SOC concentration is 6.8 µg m^{-3}, contributing for 76% of the cold period TOC (Total Organic Carbon), while the warm period SOC (1.4 µg m^{-3}), contributes, on average, for 52% to the warm period TOC.

To overcome the limitations of the EC/OC minimum ratio method (the EC tracer method does not account for the variability of primary sources and does not consider non-combustion OC associated with EC, which is mainly of biogenic origin) a regression approach has been suggested (Turpin and Huntzicker, 1995):

SOC=OC-POC=OC-[aEC+b]

where *a* is the primary combustion ratio and *b* is the non-combustion primary OC. Based on this approach, the annual mean of the SOC is 3.8 µg m^{-3}, contributing for 69% of the total organic carbon; the warm period SOC is 1.3 µg m^{-3}, contributing 49% of the warm period OC and the cold period SOC is 6.4 µg m^{-3}, contributing to 72% of the cold period OC (Table 4.5). It is interesting to observe that SOC is higher in the cold period than in the warm one, differently from the expected pattern of higher concentration in the warm period as a consequence of favourable meteorological conditions and the occurrence of photochemical reactions. However, the seasonal variation of SOC follows the same trend of total OC with higher concentrations during the household heating season, when higher emission of organic precursors occur. Moreover, a lower mixing layer height in winter favours SOC precursor stagnation and SOC formation (Dan et al., 2004; Duan et al., 2005).

Table 4.5. Primary and secondary organic carbon (Veneto region) estimated from both minimum OC/EC ratio and regression approach.

Locations	Period	Minimum OC/EC ratio			Regression Approach			
		POC	SOC	% SOC to TOC	Slop	POC	SOC	% SOC to TOC
This study	Feb	2±1	7±4	78	1.01	3.1	6.0	66
	Apr	1.3±0.4	0.9±0.6	43	1.49	1.3	0.9	42
	Jun	1.3±0.6	1.3±0.8	49	3.54	0.9	1.7	66
	Aug	2.3±0.7	1.0±0.5	30	3.60	2.2	1.1	33
	Oct	1.7±0.5	3±3	61	0.08	2.8	1.6	36
	Dec	3±2	9±4	77	0.47	4.7	6.8	59
	Summer	1.27	1.39	52	1.45	1.4	1.3	49
	Winter	2.16	6.76	76	0.85	2.5	6.4	72
	Annual	1.69	3.79	69	0.82	1.7	3.8	69
Birmingham	Summer	1.4	0.6	70				
(PM$_{10}$)[a]	Winter	1.7	1.2	59				
Milan, Italy[b]			4.36	84				
Beijing urban[c]	Summer		5.30	48				
	Winter		23.10	59				

[a] Harrison and Yin, 2008; [b] Lonati et al., 2007; [c] Dan et al. 2004
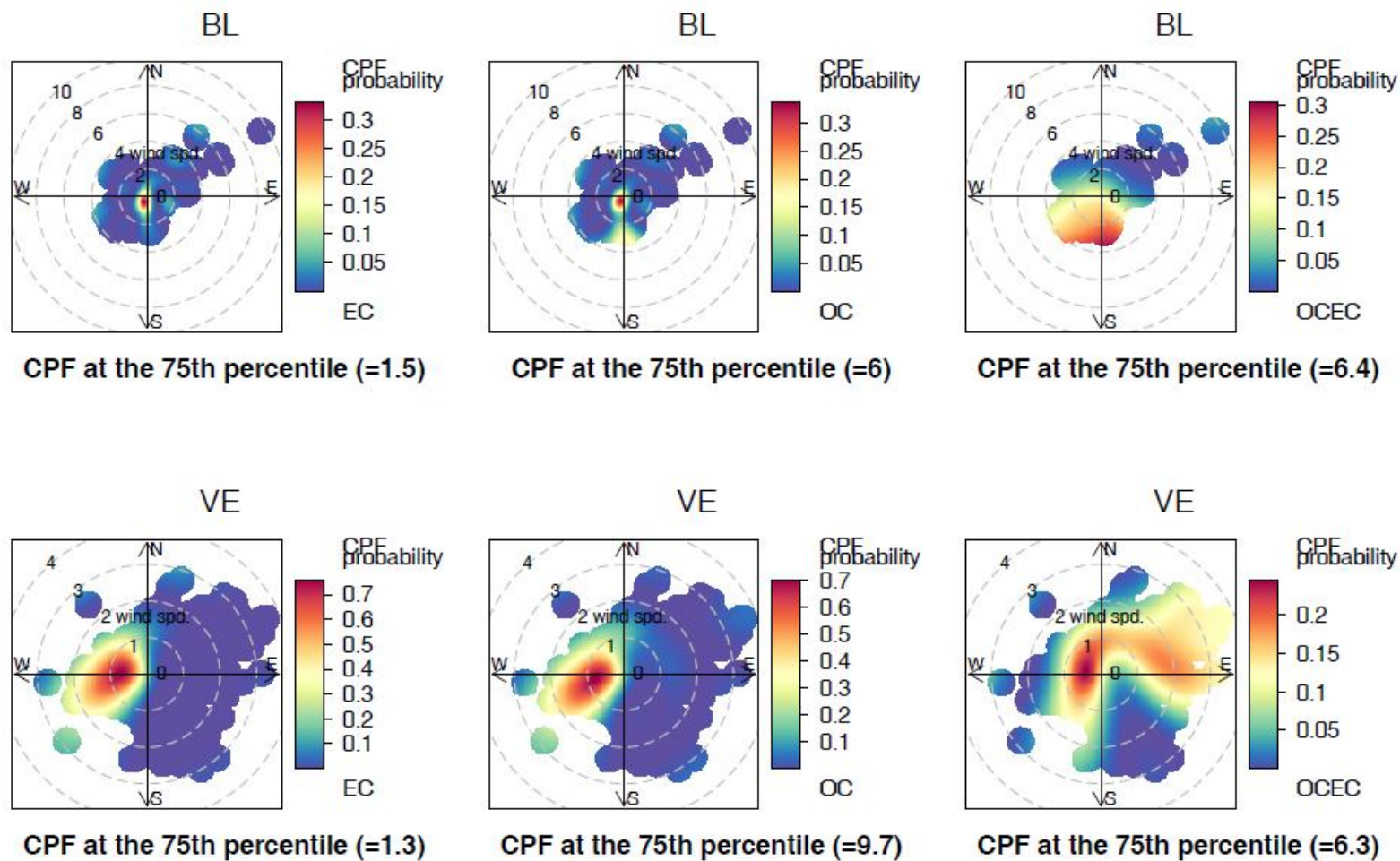
Figure 4.3. CBPF plots for EC, OC concentrations and OC/EC ratios in BL and VE

4.3.6. Conditional Probability Function (CPF) and Conditional Bivariate Probability Function (CBPF)

Among the six measurement sites, BL and VE have been selected to investigate the potential local sources of carbonaceous PM. BL is an interesting case of study for a number of reasons: (i) it is located in an alpine valley surrounded by high mountains, mostly peaking at ~800-2000 m; (ii) the atmospheric circulation is strongly affected by the arrangement of mountains; (iii) the sampling site is located in a public park in the middle of the city; (iv) both hardwood (from local trees) and softwood (mostly from conifers) are widely burned for domestic heating in stoves, most of which are dated, i.e. built with old technologies and without any system for emission mitigation; (v) road traffic is moderate; (vi) the site is located ~500 m East from a railway station, where trains are all diesel-powered; (vii) there are no large industries. On the contrary, VE has opposed characteristics: (i) it is located in a completely flat area; (ii) the wind regimes are affected by sea/land breezes in the warm seasons; (iii) the sampling site is located in the NE part of the city; (iv) methane is commonly used for domestic heating, but there has been a recent increase in the use of wood (i.e. logs, briquettes, chips and pellets) in modern stoves; (v) road traffic is intense with frequent congestion of the main roads in rush hours; (vi) a railway station is located ~2.6 km SSE (mostly electric-powered trains) and an international airport at ~6 km E; (vii) a large industrial area is hosted in the southern part of the city, including a main thermoelectrical power plant, oil refineries, incineration facilities, chemical and steel plants. City maps with highlighted sources are reported as Figure A-4.4.

CPF plots for EC, OC concentrations and OC/EC ratios in BL and VE are provided in Figure A-4.5, whereas CBPF plots are shown in Figure 4.3. The plots for BL emphasize sectors, where the concentration is >75th percentile, equal to 1.5 and 6 µg m^{-3} for EC and OC, respectively. While CPF evidences that higher probabilities of high concentration may originate from all the directions, CBPF plots clearly show that the higher concentrations of EC and OC occur under wind calm conditions and for very low winds blowing from S (toward the historic city center). This wind regime corresponds to the prevailing wind

direction in colder months, especially in December and February (Figure A-4.6) and indicates that domestic heating is the main source of both OC and EC. This result is also confirmed by analyzing the plot for OC/EC ratio. Both emission studies (e.g., Hildemann et al., 1991; Watson et al., 2001; Schauer et al., 2001; 2002) and monitoring campaigns at urban and rural sites (e.g, Schwartz et al., 2008; Harrison and Yin, 2008; de la Campa et al., 2009; Pirovano et al., 2015) reported larger proportion of OC emitted by biomass burning and domestic heating with respect to mobile sources. In particular, OC/EC ratios ranging from 1 to 4 have been reported for diesel- and gasoline-powered vehicles (Schauer et al., 2002), while OC/EC varying from 17 to 40 for wood combustion (Schauer et al., 2001). In BL, high probabilities of OC/EC >6.4 are evidenced toward the city centre, confirming the relative dominance of OC derived from biomass and wood burning. In the opposite way, despite mobile sources seem not to be the main sources of carbonaceous $PM_{2.5}$, their role as strong EC sources cannot be disregarded: the CBPF clearly shows that lower probabilities of high OC/EC ratios are measured to NE, i.e. toward a main traffic road often congested during weekends (most malls, shops and stores are to NE) and to WNW, i.e. toward main roads and the railway (diesel-powered trains only) and bus station.

CPF plots for VE indicate high probability of both EC and OC >75th percentile (i.e., 1.3 and 9.7 µg m^{-3}, respectively) for winds blowing from WSW and NW, while CBPF plots (Figure 4.3) show high probabilities mainly for winds blowing from WSW, i.e. toward the main urban area of Mestre, which also hosts some main roads affected by heavy traffic and an orbital road (Figure A-4.4). Wind rose showing the monthly wind speed and direction frequencies at Venice are provided in Figure A-4.7. Some insights seem to point out that vehicular traffic is the main source of carbonaceous $PM_{2.5}$ in VE:

- The results are consistent with NO_2 data collected during 2000-2013 in the same site (Masiol et al., 2014). NO_2 is largely emitted by road traffic in urban environments and a recent increase in NO_2 levels in Europe has been related to the growing proportion of diesel-powered vehicles, which are known to have higher primary (direct) emissions of NO_2 (Carslaw et al., 2007);
- CBPF clearly shows that probabilities of high OC/EC ratios (>6.3) are measured mainly toward W and also spreading over the 1st and 2nd quadrant, i.e. toward the

suburbs and semirural areas surrounding the city, where the use of alternative fuels to methane for domestic heating is increasing.

Finally it could be concluded that both biomass & wood burning and vehicular traffic are probably the main local sources of carbonaceous particulate matter in Veneto region.
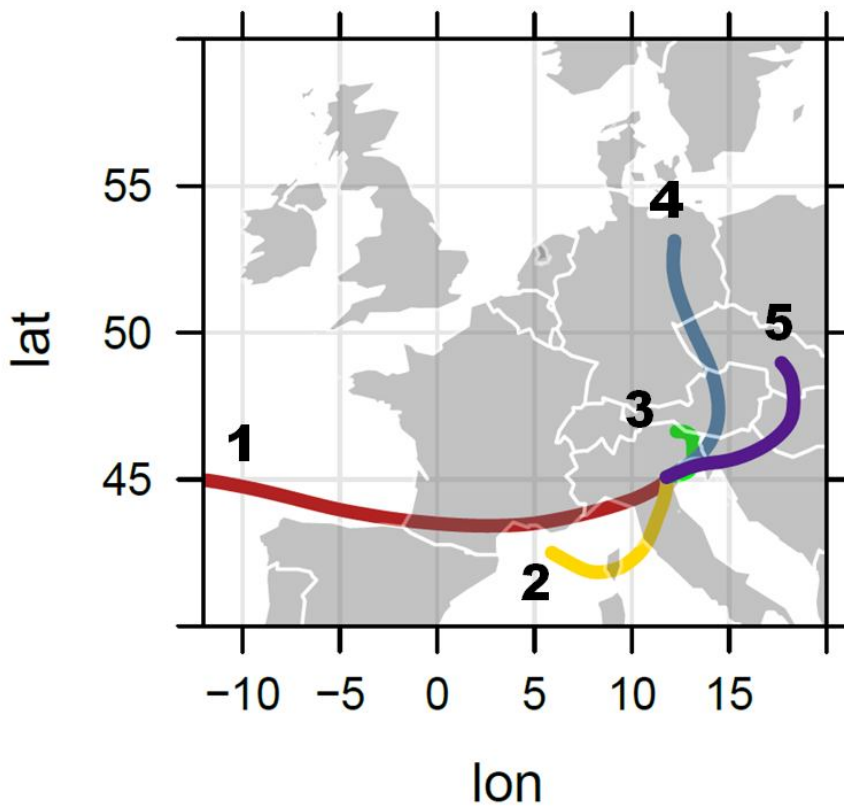
Figure 4.4. Results of the back-trajectory cluster analysis for RO station.

Table 4.6 . Results of the cluster analysis on the back-trajectories. Data are reported as average±standard deviation.

Back-trajectory clusters	VI			PD		
	OC	EC	TC	OC	EC	TC
	$(\mu g\ m^{-3})$	$(\mu g\ m^{-3})$	$(\mu g\ m^{-3})$	$(\mu g\ m^{-3})$	$(\mu g\ m^{-3})$	$(\mu g\ m^{-3})$
(Cluster 1) Local	5±4	1.2±0.9	6±4	7±6	2±1	8±7
(Cluster 2) Northern	5±6	1.3±0.8	6±6	9±6	2±1	10±7
(Cluster 3) Eastern	4±4	1±0.4	5±4	6±5	1.3±1	7±5
(Cluster 4) Mediterranean	4±3	1±0.4	5±3	5±4	1.1±0.4	6±4
(Cluster 5) Western Europe	8±6	1.7±1	10±7	2±0.2	1±0.4	3±0.4

Back-trajectory clusters	VE			RO		
	OC	EC	TC	OC	EC	TC
	$(\mu g\ m^{-3})$	$(\mu g\ m^{-3})$	$(\mu g\ m^{-3})$	$(\mu g\ m^{-3})$	$(\mu g\ m^{-3})$	$(\mu g\ m^{-3})$
(Cluster 1) Local	8±5	1.4±0.9	10±5	7±5	2±2	10±5
(Cluster 2) Adriatic	4±3	1.0±0.3	4±3	5±4	1.4±1	6±5
(Cluster 3) Eastern	4±3	1.0±0.4	5±4	5±4	1.3±1	6±5
(Cluster 4) Mediterranean	4±4	1.0±0.2	4±4	4±3	1±0.4	6±3
(Cluster 5) North(VE)/ Western Europe(RO)	7±5	1.0±0.5	8±6	3±1	1.±0.6	4±2

4.3.7. Potential effects of long-range transports

In this study, four back-trajectories were simulated for each day and site in the flat areas of the region (VI, VE, PD, RO) as the topography of the territory may have effects on the reconstructions of back-trajectories for BL and TV, which are in and close to the Alps, respectively. The optimum number of clusters was then established by analyzing the change in the total spatial variance: all sites exhibited five main clusters with similar origins. Clusters (Figure 4.4) were then identified according to their provenance as: (1) Western Europe, (2) Mediterranean, (3) local, (4) Northern Europe and (5) Eastern Europe. The daily OC, EC and TC concentrations have been subsequently assigned to each of the clustered trajectories. Statistics for chemical composition data in each cluster are presented in Table 4.6.

Generally, OC, EC and TC show similar results at all the sites, with concentrations slightly higher for clusters 1, 4 and 5 and the inter-cluster comparison shows only small differences. In particular, the site RO can be roughly selected as the most reliable one for analysing the long-range transports, as it is located far away from the mountain chains and the city has fewer local industrial emissions and traffic. In RO, the highest levels of OC are associated with air masses blowing from Northern (6.7 $\mu g\ m^{-3}$) and Eastern (5.7 $\mu g\ m^{-3}$) Europe, while results for the remaining origins are quite constant (4-5 $\mu g\ m^{-3}$). In summary, results indicate that trans-boundary transports have only a limited influence on the levels of OC and EC in the Veneto region.

4.4 CONCLUSIONS

In this work, for the first time, EC and OC concentrations were investigated in $PM_{2.5}$ in the Veneto region for an extended period of time. The mean organic carbon concentration was 5.48 $\mu g\ m^{-3}$, contributing for almost 22% of the total $PM_{2.5}$ and 79% of the total carbon, while EC average value was 1.31 $\mu g\ m^{-3}$, contributing for 5% of the total $PM_{2.5}$ and 21% to the total carbon. The monthly OC concentration gradually increased from April to December. The EC did not vary in accordance with OC, but the highest values were recorded in the colder months, as well. The OC/EC ratios ranged from 0.71 to 15.38 with a mean value of 4.54, which is higher than the values observed in most of the other

European cities. In this study, a positive statistically significant relationship (r=0.76) between elemental and organic carbon was observed without any categorization of the data. However, the correlation is comparatively better in the warmer months than in the colder ones. In this study, a weak correlation coefficient between elemental and organic carbon during colder months suggests that the EC and OC may not be emitted from a single dominant primary source. Statistically significant micro-meteorological factors controlling organic and elemental carbon were investigated by fitting linear models using a robust procedure based on weighted likelihood. Temperature and wind velocity turned out to be significantly related to the carbon fractions with a multiple R^2 value of 0.79. The secondary organic carbon contributed for 69% of the total organic carbon during the study period as confirmed by both the approaches of OC/EC minimum ratio and regression. It is interesting to observe that SOC is higher in the cold period than the warm one (in contrast with the expected pattern of higher concentration in summer), as a consequence of lower temperature and stable atmospheric conditions favouring accumulation of pollutants and hastening the condensation or nucleation of volatile organic compounds. The local contribution to OC and EC was investigated by both CPF and CBPF plots indicate that both domestic heating from biomass burning and natural gas as well as road transport emissions are the main local sources of carbonaceous particulate matter. The potential effects of long-range transports on the OC and EC levels were analysed by clustering the back-trajectories in the sites located in the flat areas of the region. Results revealed no significant differences in the levels of both OC and EC, when air masses had passed across different European regions, indicating that trans-boundary transports have a limited effect on the carbonaceous PM variations in the Veneto region.

CHAPTER 5

POLYCYCLIC AROMATIC HYDROCARBONS (PAHs)

5. Polycyclic Aromatic Hydrocarbons (PAHs)

5.1. Aims

This chapter mainly deals with i) seasonal and spatial trends of atmospheric PAHs in the Veneto Region (ii) the effects of micro- meteorological factors on particulate PAHs and (iii) Sources of PAHs

5.2. Results and Discussions

5.2.1. Overview of PAHs

Among the 16 PAHs listed in the carcinogenic category by USEPA, eight particulate PAHs [benz(a)anthracene (BaA), chrysene (Chy), benzo(b)fluoranthene (BbF), benzo(k)fluoranthene (BkF), benzo(a)pyrene (BaP), indeno(123-cd)Pyrene (IP), dibenzo(ah)anthracene (DahA), and benzo(ghi)perylene (BghiP)] were identified and the annual mean level of analyzed congeners ($\sum_8$PAHs) was 12 ± 14 ng m^{-3} and fluctuated from 0.2 ng m^{-3} to 70.4 ng m^{-3} (Table 5.1). Total concentrations of all carcinogenic congeners ($\sum_8$PAHs) were calculated and BaF contribution was the highest (17.6%), followed by BaP (16.8%), IP (16.8%), BghiP (16%), Chry (14.3%), BaA (8.4%) and DBahA (1.7%), respectively. The observed BaP concentration in Veneto has been compared with other studies around the world because BaP is the most important carcinogenic PAH and often it is used to represent the concentration of total PAH (Fertmann et al., 2002; Brown and Brown, 2012). The annual mean value of BaP is 2 ± 3 ng m^{-3}, fluctuating from 0.01 to 14.02 ng m^{-3}. The mean BaP concentration is higher during winter season 4 ± 4 ng m^{-3}) as compared to summer (0.5 ± 1.0 ng m^{-3}). This annual mean BaP value is comparatively higher than those reported in Spain (Zaragoza), UK (London, West Greece (Kozani), Germany (Gothenburg, Dettenhausen) and lower than that observed in Poland (Gdańsk) and China (Nanjing) (Table 5.2). The observed BaP value is similar to the concentration measured in Croatia (Zagreb), Czech (Prague) and East of France (Table 5.2). In this study, the highest values of BaP especially in winter may be due to the biomass burning for household heating and cooking (Belis et al., 2011; Masiol et al., 2013). The annual mean BaP value is two-times higher than the recommended value of BaP (1 ng m^3) set by EU directives (2004/107/EC directives) (EC, 2004).

Table 5.1. Summary statistics for PM$_{2.5}$ (µg m^{-3}) and $\sum_8$PAHs (ng m^{-3}) levels

	BL (ng m^{-3})	TV (ng m^{-3})	VI (ng m^{-3})	PD (ng m^{-3})	VE (ng m^{-3})	RO (ng m^{-3})	Annual (ng m^{-3}) (Mean±SD)
PM$_{2.5}$							
Mean±SD	18±12	20±13	28±18	29±19	25±17	27±19	24±17
Median	14.6	14.7	20.9	20.6	18.2	19.5	18.4
Min	3.0	3.1	5.9	7.8	4.9	4.7	3.0
Max	52.6	56.9	82.7	77.2	73.5	75.1	82.7
PAHs							
BaA	1.7	1.2	0.8	1.1	0.8	0.6	1.0±1.4
Chry	2.8	2.1	1.3	1.8	1.3	1.2	1.7±2.3
BbF	3.4	2.4	1.6	1.9	1.8	1.3	2.1±2.3
BkF	1.7	1.1	0.7	0.9	0.8	0.6	1.0±1.1
BaP	3.4	2.2	1.4	1.9	1.7	1.1	2.0±2.5
IP	3.7	2.4	1.5	1.7	1.7	1.2	2.0±1.5
DBahA	0.3	0.3	0.1	0.1	0.2	0.1	0.2±0.2
BghiP	3.3	2.1	1.5	1.7	1.6	1.2	1.9±1.1
Mean±SD	20±19	13.3±15	9±10	11±13	10±11	7.0±	12±14
Median	16.0	8.2	4.2	4.9	4.9	3.7	5.2
Min-Max	0.4-66.2	0.3-49.1	0.2-41.5	0.4-70.4	0.3-41.5	0.2-37.6	0.2-70.4

Table 5. 2. Comparison of BaP concentration (ng m^{-3}) with previous studies

Country	City	Monitoring site	Particle size	Mean BaP (ng m^{-3})	References
Italy	Veneto	Residential area	PM$_{2.5}$	2.0 [annual] 3.68 [winter] 0.53 [summer]	
	Venice	Urban and rural	PM$_{2.5}$	1.2	Masiol et al., 2012b
	Florence	Urban Traffic	PM$_{2.5}$	0.49	Martellini et al., 2012
Spain	Valencia	Urban	PM$_{2.5}$	0.27	Viana eta l., 2008b
	Gipuzkoa	Urban	PM$_{2.5}$	0.15	Villar-Vidal et al., 2014
	Zaragoza	Rural	PM$_{10}$	0.09	Callen et al., 2003
Greece	Kozani	Urban	PM$_{2.5}$	0.09	Evagelopoulos et al. (2010)
Sweden	Stockholm	Urban-traffic	PM$_{2.5}$	1-2 [range]	Bostrom et al., 2002
Finland	Kurkimäki,	Residential	PM$_{10}$	1.3	Hellen et al. 2008
UK	London	Urban-Traffic	PM$_{10}$	0.77	Brown et al., 2012
UK	West Midlands	Urban	PM$_{2.5}$	0.15	Harrison and Yin, 2010
Germany	Gothenburg	Urban background	PM$_{2.5}$	0.39	Bari et al., 2010
	Dettenhausen	Rural	PM$_{10}$	1.6	Bari et al., 2010
Netherlands	Amsterdam	Urban background	PM$_{2.5}$	0.33	Saarnio et al., 2008
France	East of France (Alsace, Franche-Comté and Lorraine)	Urban	PM$_{10}$	2.1	Delhomme and Millet (2012)
Poland	Gdańsk	Urban background	PM$_{2.5}$	9.67 [winter]	Rogula-Kozłowska et al., 2014
		Urban background	PM$_{2.5}$	0.14 [summer]	
	Diabla Góra	Rural background	PM$_{2.5}$	2.43 [winter]	
		Rural background	PM$_{2.5}$	0.05 [summer]	
Croatia	Zagreb		PM$_{2.5}$	3.18 [winter]	Šišović et al., 2005
Czech	Prague	Urban background	PM$_{2.5}$	3.03 [Nov-Jan]	Saarnio et al., 2008
USA	Atlanta[Oct-Dec]	Urban	PM$_{2.5}$	0.27	Li et al., 2009
Malaysia	Kuala Lumpur	Semi-urban	PM$_{2.5}$	0.30	Khan M.F., 2015
China	Nanjing	Urban	PM$_{2.5}$	3.56	He et a., 2014

5.2.2. Seasonal trends and spatial variations of PAHs

Monthly concentrations of $\sum_8$PAHs for all measurement sites are given in Figure 5.1. Generally, the higher concentrations were found during colder months, whereas comparatively lower concentrations were observed during warmer months. The highest $\sum_8$PAHs level was observed in December (33.9 µg m^{-3}) followed by February (17.2 µg m^{-3}), April (9.2 µg m^{-3}), October (7.3 µg m^{-3}), June (0.8 µg m^{-3}) and August (0.7 µg m^{-3}). These reported variations in different months are statistically significant as confirmed by Kruskal-Wallis one-way analysis of variance (*p-value, 0.000*). The average value (mean±standard deviation) of $\sum_8$PAHs during winter was 21±14 ng m^{-3}, whereas during summer the mean concentration was 4 ±7 ng m^{-3}; more than five-times lower than the winter season mean concentration. The $\sum_8$PAHs difference between the levels of two seasons showed statistically significant variation in Wilcoxon-Mann-Whitney t-test (*p value=0.000*). The seasonal trend of PAHs coincided with observed PM$_{2.5}$, with higher values in the cold period and lower values in warm period. This is due to the pollutant accumulation in the atmosphere due to stable atmosphere and lower mixing layer and also to atmospheric photochemistry. PAHs concentrations may be influenced by photo-chemical oxidation driven by solar radiation and several atmospheric oxidants such as ozone and radicals (hydroxyl, NO, NO$_2$) (Arey and Alkinson, 2003; Esteve et al., 2006; Ringuet et al., 2012, Masiol et al., 2013) especially during summer. Volatile PAHs absorption on particle due to lower atmospheric temperature may also be another reason for increasing concentration in winter (Ravindra et al., 2006; Galarneau, 2008).

Between two seasons, only cold period data were used to observe the spatial variations of PAHs in Veneto region because from the monthly distribution of the data (Figure 5.1), it is obvious that the concentrations of PAHs levels are minimum and quite similar in all the measurement stations during summer months, probably because of the influence of oxidation and volatilization processes (Masiol et al., 2013). As the normality assumption (p>0.05) was not met by Shapiro-Wilk test, a non-parametric Kruskal-Wallis one way analysis of variance was performed to test the significance of variations among measurement sites. Finally, a pair-wise comparison was observed using Wilcoxon rank sum test with Bonferroni correction and the result shows that PAHs levels of BL are

significantly different from the values of VE, RO and VI (Table A-5.1). An inter-site relationship (Table A-5.1) was evaluated using Spearman's rank correlation technique and a significant positive relationship (p<0.01) was found in all the sites suggesting the occurrence of simultaneous changes of values over the study areas (Masiol et al., 2013).
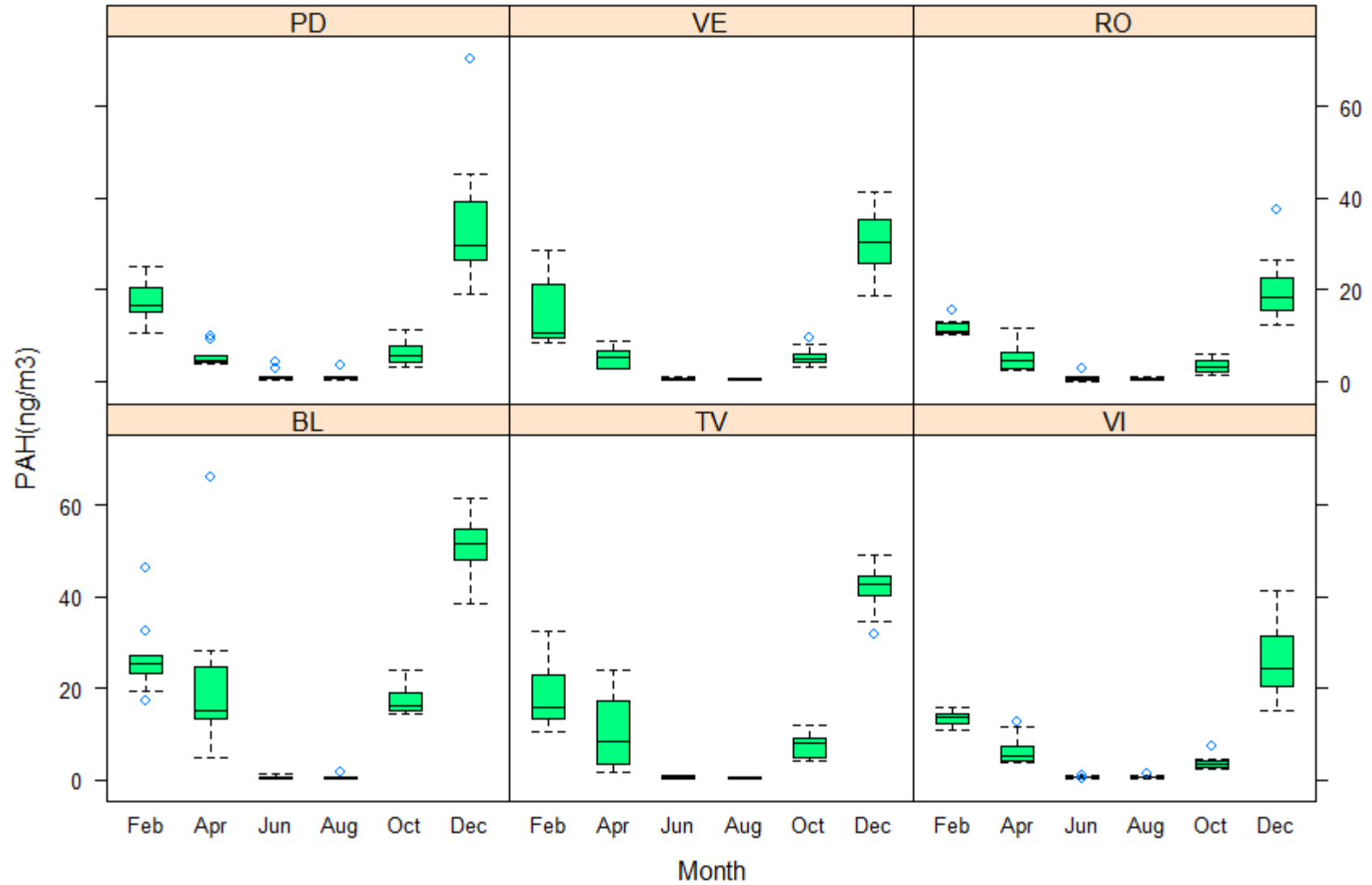
Figure 5.1. Seasonal values of the sum of the analyzed congeners ($\sum_8$PAHs) in the Veneto region
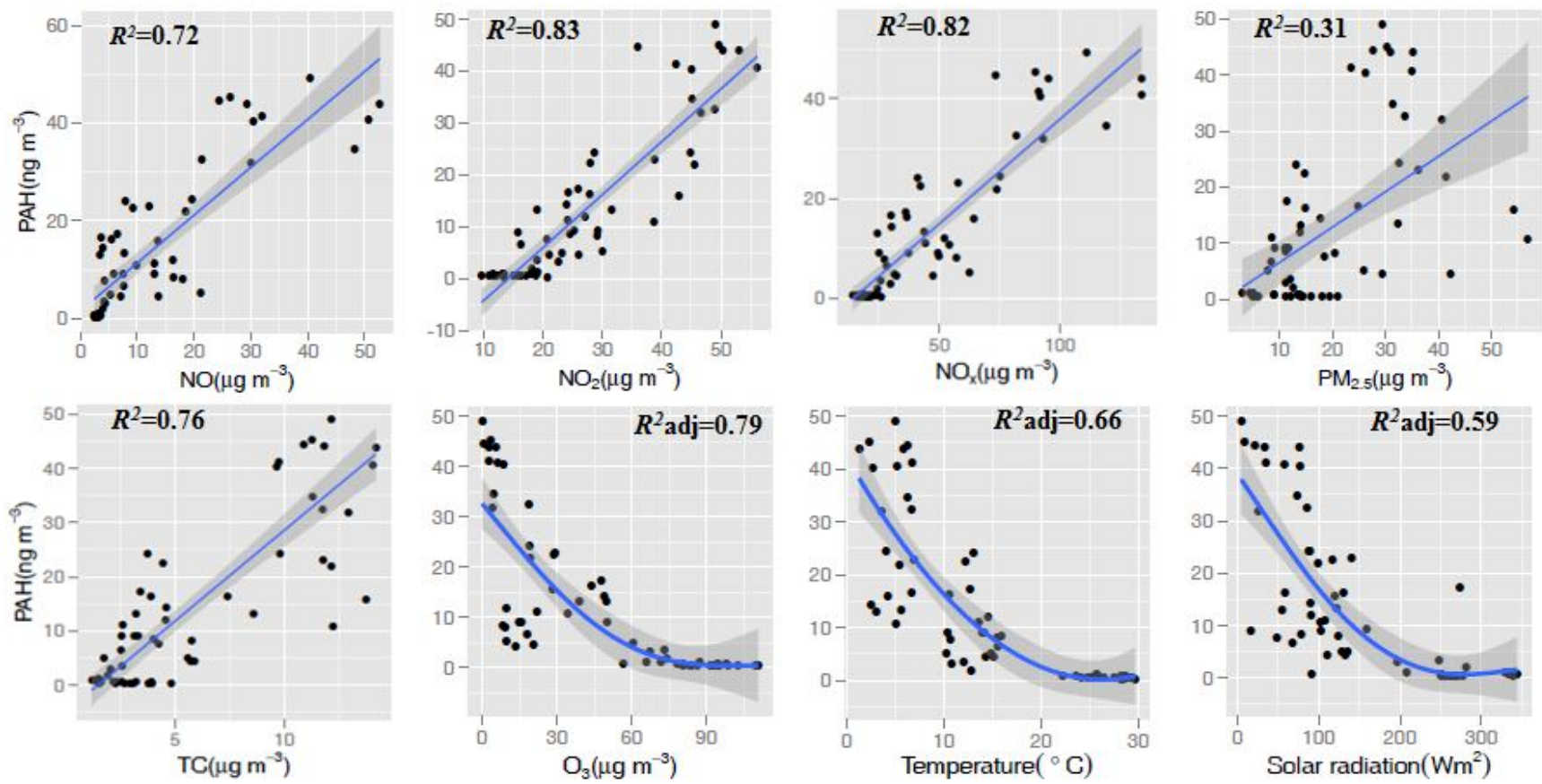
Figure 5.2. Scatterplots of $\sum_8$PAHs versus atmospheric pollutants and micrometeorological parameters in Veneto region.

5.2.3. Meteorological factors affecting PAHs levels

The results of the correlation analysis of the $\sum_8$PAHs with meteorological parameters and other atmospheric pollutants are reported in Table 5.3. The relationship was computed using a Spearman's correlation analysis as the normality assumption was not met. Atmospheric temperature showed statistically significant negative ($p<0.05$) correlation with $\sum_8$PAHs ($r = -0.89$). This suggests that temperature increase favours the evaporation of particulate PAHs from particle to gas phase, whereas condensation of gas phase PAHs onto particles increases at a lower atmospheric temperature. This observation is similar to the findings of other researchers (Kitazawa et al., 2006, Tham et al., 2008, Masiol et al., 2013, He et al., 2014). Solar radiation which also follows the same diurnal pattern of atmospheric temperature showed a negative correlation with PAHs ($r = -0.76$). Photochemical transformation of particulate PAHs (photo-degradation) under intense sunlight might be the reason for negative correlation between particulate PAHs and solar radiation (Chetwittayachan et al., 2002). A significant negative correlation was observed between wind speed and PAHs concentrations ($r = -0.264$). The observed significant positive relationship between humidity and PAHs ($r = 0.51$) suggests the depositional effect of gas phase PAHs on the particulate PAHs (Mastral et al., 2003; Ravindra et al., 2008; Agudelo-Castaneda and Teixeira, 2014). The correlation between PAHs and rainfall is not statistically significant and does not follow any special pattern.

On the contrary, significant positive correlations which were observed with most of the air pollutants ($PM_{2.5}$, TC, NO, NO_2, NO_x and SO_2) suggest that these pollutants are strongly linked to each other and share same emission sources and transformation pattern. A negative relationship of Ozone with PAHs suggests that photo-degradation of the particulate PAH is occurred during the reaction with O_3. This result is identical to the one obtained by Park et al. (2002) and Tsapakis and Stephanou (2005). The regression analysis has been done to find whether the relationships among $\sum_8$PAHs with measured air pollutants and micro-meteorological parameters are linear or not. The PAHs levels exhibit linear relation with NO, NO_2, NO_x, OC, EC, and $PM_{2.5}$ whereas it shows exponential behavior with ozone, temperature and solar radiation (Figure 5.2).

Table 5.3. Spearman's correlations of $\sum_8$PAHs with meteorological parameters and air pollutants at Veneto region. Significant correlations at *p<0.05* are marked.

	Veneto region	BL	TV	VI	PD	VE	RO
Pm$_{2.5}$	**0.43**	**0.37**	**0.57**	**0.52**	**0.55**	**0.48**	**0.44**
TC	**0.56**	**0.55**	**0.72**	**0.57**	**0.59**	**0.60**	**0.52**
NO	**0.77**	**0.87**	**0.88**	**0.87**	**0.88**	**0.67**	**0.84**
NO$_2$	**0.67**	**0.84**	**0.88**	**0.74**	**0.81**	**0.60**	**0.76**
NO$_x$	**0.74**	**0.86**	**0.89**	**0.81**	**0.87**	**0.64**	**0.81**
SO$_2$	0.07	0.12	0.57	-	0.58	-0.28	0.46
O$_3$	**-0.78**	**-0.76**	**-0.87**	**-0.85**	**-0.83**	**-0.83**	**-0.81**
Temperature	**-0.89**	**-0.88**	**-0.89**	**-0.94**	**-0.93**	**-0.92**	**-0.91**
Radiation	**-0.76**	**-0.73**	**-0.80**	**-0.76**	**-0.77**	**-0.79**	-
Humidity	**0.51**	**0.62**	**0.37**	**0.67**	**0.63**	**0.52**	**0.66**
Wind	**-0.24**	**-0.56**	-0.22	-0.36	-0.18	-0.20	-
Precipitation	0.15	0.02	0.07	0.28	0.20	0.06	0.16

Table 5.4. BaP$_{TEQ}$ and BaP$_{MEQ}$ for all the congeners

	BL		TV		VI		PD		VE		RO		Annual	
	TEQ	MEQ	TEQ	MEQ	TEQ	MEQ	TEQ	MEQ	TEQ	MEQ	TEQ	MEQ	TEQ	MEQ
BaA	0.2	0.1	0.1	0.1	0.1	0.1	0.1	0.1	0.1	0.1	0.1	0.1	0.10	0.08
Chry	0.0	0.1	0.0	0.0	0.0	0.0	0.0	0.0	0.0	0.0	0.0	0.0	0.02	0.3
BbF	0.3	0.9	0.2	0.6	0.2	0.4	0.2	0.5	0.2	0.4	0.1	0.3	0.20	0.51
BkF	0.2	0.2	0.1	0.1	0.1	0.1	0.1	0.1	0.1	0.1	0.1	0.1	0.10	0.11
BaP	3.4	3.4	2.2	2.2	1.4	1.4	1.9	1.9	1.7	1.7	1.1	1.1	1.95	1.95
DBaA	0.3	0.1	0.2	0.1	0.1	0.0	0.1	0.0	0.2	0.0	0.1	0.0	0.16	0.05
BghiP	0.0	0.6	0.0	0.4	0.0	0.3	0.0	0.3	0.0	0.3	0.0	0.2	0.02	0.36
IP	0.3	1.0	0.2	0.6	0.1	0.4	0.2	0.5	0.1	0.5	0.1	0.3	0.17	0.54
Total	5+5	6+6	3+4	4+5	2+2	3+3	3+3	4+4	3+3	3+4	2+2	2+2	3+3	4+4

5.2.4. Health Risks Assessment

BaP has been recognized as the most important carcinogenic PAH and used as an indicator to potential carcinogenicity to human. However, the only BaP indicator is not sufficient enough to assess the risk of PAH as it is a reactive substance. Moreover, every congener has its own toxicity. In order to estimate the carcinogenic risk of total PAH to human, Toxic Equivalency Factor (TEF) method has been widely applied.

BaP-toxic equivalent (BaP_{TEQ}) has been calculated from the following formula:

$$BaP_{TEQ} = \sum (PAH_i \times TEF_i) \ldots\ldots\ldots\ldots\ldots.. (5.1)$$

Here, PAH_i is the concentration of an individual PAH and TEF_i is the corresponding toxic equivalence factor. TEFs were used from Nisbet and LaGoy (1992) (Appendix, Table A-5.2). Similarly, Mutagenic Equivalency Factor (MEF) has been assessed from the above equation just with replacement of TEF with MEF following the values proposed by Durant et al. (1996).

The calculated BaP equivalent values (both BaP_{TEQ} and BaP_{MEQ}) are given in Table 5.4. Regional BaP_{TEQ} values fluctuated from 0.02 to 18.2 ng m^{-3} with an annual value (mean±standard deviation) of 3±3 ng m^{-3}, similar to the value found in Dettenhausen, Germany (2.7 ng m^{-3}: Bari et al., 2010). The highest contribution to the total carcinogenic potential of the PAH mixture has come from BaP (72%), followed by BbF (8%), IP (6±6%), DBahA (6%), BaA (4%), BkF (4%), Chry (1%) and BghiP (1%). This calculated BaP_{TEQ} is higher than the reported value in Florence (Italy, 0.79 ng m^{-3}: Martellini et al., 2012), Athens (Greece: Marino et al., 2000), Mexico City (Mexico, 2.17, but lower than those reported in Zabrze (Poland, 7.94 ng m^{-3}: Ćwiklak et al., 2009), 2008), Shanghai (China, 5.95 ng m^{-3}: Cheng et al., 2007).

The regional average BaP_{MEQ} value (mean ± standard deviation) was 4±4 ng m^{-3}, ranging from 0.03 to 23.20 ng m^{-3} (Table 5.4). The most contributing congener to BaP_{MEQ} was BaP (54%), followed by IP (15%), BbF (14%) and BghiP (10%).

Both BaP related carcinogenicity (BaP_{TEQ}) and mutagenecity (BaP_{MEQ}) values are higher in Veneto region as compared to most of the urban environment in Europe. Finally, the life time lung cancer risk (LCR) from inhalation was estimated using the following equation.

$$LCR = BaP_{TEQ} \times UR_{BaP} \ldots\ldots\ldots\ldots\ldots (5.2)$$

The unit risk (UR_{BaP}) is defined as the number of people at risk of lung cancer with BaP 1 ng m^{-3} over lifetime of 70 years and the suggested unit risk (UR) is 8.7×10^{-5} (ng m^{-3}) (WHO, 1987; 2000). The calculated LCR values are 2.4×10^{-4}, 4.4×10^{-4} and 7.0×10^{-5} for annual, winter and summer, respectively. The annual and winter time health risk values exceeded the health-based guideline of 10^{-5} (Boström et al., 2002) and acceptable risk level of European Union (10^{-6} to 10^{-4} per year: EC, 2001).

5.2.5. Comparison of particulate phase $\sum_8 PAHs$ (P) with total PAH (G+P)

As the gas-phase concentration of PAHs was not measured in this study, an attempt was given to predict gas-phase PAHs (P) concentrations, calculated following the similar approach of Xie et al. (2013) based on the theory developed by Pankow (1994a,b). However, mean concentration of total PAH (G+P) is 11.57 ng m^{-3} which is little bit higher than the particle phase (P) data sets (11.53 ng m^{-3}). Similarly, both carcinogenic equivalent concentrations (BaP_{TEQ}) and mutagenic equivalent concentrations (BaP_{MEQ}) exhibited little difference between P-phase (3 ± 3 and 4 ± 4ng m^{-3}, respectively) and G+P data sets (3 ± 3 ng m^{-3} and 4 ± 4 ng m^{-3}, respectively). The calculated LCR value for G+P data set was 2.3×10^{-4}. From the above results (mean concentration, BaP_{TEQ}, BaP_{MEQ} and LCR), it could be concluded that the difference is very little between P data and G+P data set in Veneto region.

5.2.6. Source apportionment

5.2.6.1. Diagnostic ratio

Diagnostic ratio method compares of pairs of PAHs and considered as introductory method to identify sources effectively. However, ratios should be used cautiously because ratio can be altered due to reactivity and degradation of some PAH congeners in the atmosphere (Robinson et al., 2006a, 2006b; Tsapakis and Stephanou, 2003). Six diagnostic ratios [IP/(IP+BghiP), BaP/(BaP+Chry), BbF/BkF, BaP/BghiP, IP/BghiP and BaA/(BaA+Chry)] were used to identify potential sources (Table 5.5). As the ratio [IP/(IP+BghiP)] is a good indicator of diesel (0.35-70), wood (0.62) and coal burning (0.56); the ratio of [IP/(IP+BghiP)] (0.51) found in this research indicates a strong contribution both from biomass burning and vehicular emission from diesel engine. The [BaP/(BaP+Chry)] ratio was found to be a good source indicator of vehicular emissions, the ratios 0.5 and 0.75 for diesel and gasoline emission, respectively. The ratio in this study was 0.5, suggests vehicular emissions from diesel engines. The ratio of [BbF/BkF] obtained in this study (2.15) is comparative to the value (>0.5) reported by Park et al. (2002), suggests prevalence of emissions from diesel. For indicator [BaP/BghiP], a ratio of 0.5-0.6 indicates traffic emission while ratios ranged from 0.92-6.0 suggest coal combustion. According to Caricchia et al. (1999), ratio of [IP/BghiP] provides information about vehicular emissions. A ratio of <0.4 is indicative of gasoline while a ratio equal to 1 is indicative of diesel emission. The IP/BghiP ratio is 1.05 closest to the ratios appropriate for diesel emission. The [BaP/BaP+Chry] ratio in this study is 0.37, similar to the values reported by Soclio et al. (2002), suggests combustion is the dominant source of PAHs in this region. From the diagnostic ratio, it is apparent that biomass burning and vehicular emissions from diesel engines are the main sources of PAHs emissions.

Table 5.5 Diagnostic ratio

	BL	TV	VI	PD	VE	RO	**Veneto**	**Reference source emission**
IP/(IP+BghiP)[a,b,c]	0.53	0.53	0.49	0.49	0.52	0.51	**0.51**	0.56 (coal) 0.60 (wood burning) 0.35-0.70 (Diesel emission)
BaP/(BaP+Chry)[d,e]	0.55	0.52	0.52	0.52	0.56	0.48	**0.53**	0.5 (Diesel)
BbF/BkF[f,g]	2.00	2.13	2.23	2.17	2.19	2.26	**2.15**	>0.5 (Diesel)
BaP/(BghiP)[f,g]	1.02	1.03	0.94	1.11	1.05	0.95	**1.03**	0.5-0.6 (Traffic emission) 0.9-6.6 (coal combustion)
IP/BghiP[h]	1.12	1.12	0.96	0.97	1.06	1.03	**1.05**	<0.4 (gasoline) ~ 1 (Diesel)
BaA/(BaA+Chry)[i]	0.38	0.37	0.37	0.38	0.38	0.35	**0.37**	>0.35 (combustion)

[a]Grimmer et al. (1983), [b]Ravindra et al. (2006), [c]Kavouras et al. (2001), [d]Khalili et al. (1995), [e]Guo et al. (2003), [f]Pandey et al. (1999), [g]Park et al. (2002), [h]Caricchia et al. (1999), [i]Soclo et al. (2002)
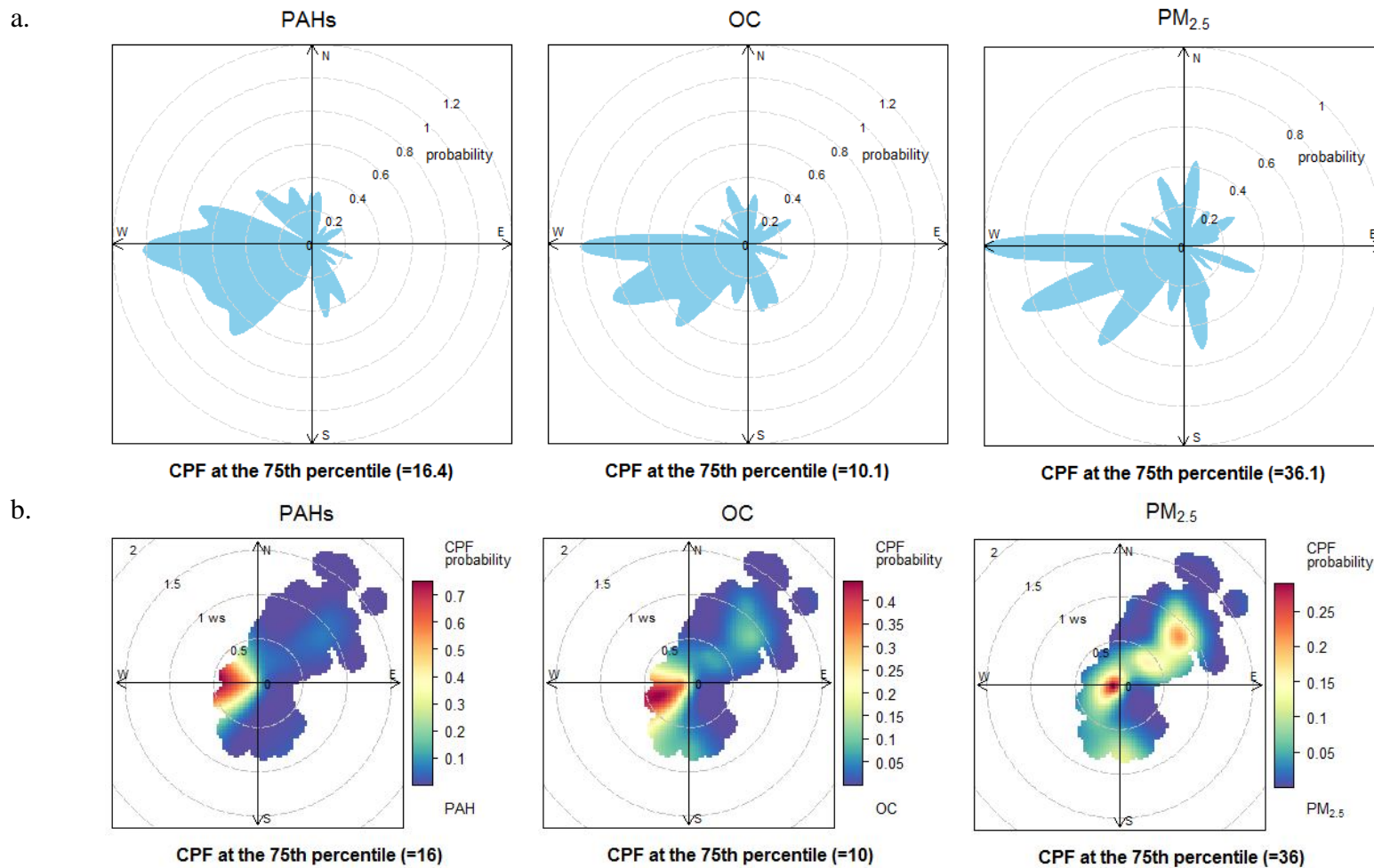
Figure 5.3. CPF (a) and CBPF (b) plots PAHs, OC and PM₂.₅ for PD

5.2.6.2. Local sources

The CPF (Conditional Probability Function) and CBPF (Conditional Bivariate Probability Function) have been calculated according to the procedure described by Uria-Tellaetxe and Carslaw (2014). The measurement site Padova (PD, flat area) has been selected to explain the local sources of PAHs and $PM_{2.5}$. The CPF plots and CBPF plots for PAHs, OC and $PM_{2.5}$ have been given in Figure 5.3. The conventional CPF plots highlight sources where the concentration is >75th percentile PAHs, OC and $PM_{2.5}$ concentration, equal to the concentration of, 16.6 ng m^{-3} PAHs; 10.3 ug m^{-3} OC and 42.2 µg m^{-3} $PM_{2.5}$.

In PD, CPF plots indicate the probability of sources of both PAHs and $PM_{2.5}$ from all the direction except east, corresponding to the direction of wind in winter months especially December (Figure A-5.1). CBPF plots show that the maximum concentrations of PAHs and $PM_{2.5}$ occur under very low wind speed conditions from NW directions, suggests, domestic heating from biomass burning is the main local sources. In addition, there is possibility of coming PAHs and $PM_{2.5}$ from NE direction, corresponding to the direction where most of the urban areas of Padova are located, suggests vehicular traffic also play significant role.

Therefore it could be concluded that both domestic heating from biomass burning and natural gas as well as road transport emissions are the main local sources of PAHs in Veneto region same as carbonaceous particulate matter.

5.3. CONCLUSION

The concentrations of PAHs at Veneto ranged between 0.2 to 70.4 ng m^{-3} with a mean value of 11.5 ng m^{-3}. The average BaP concentration was 2.0 ng m^{-3}, contributing 17.4% to the total PAHs which is two times higher than the recommended value set by the European Union Air Quality Directives. Concerning temporal trends of PAH, the highest concentration was recorded during the colder months as compared to the warmer months may be due to the biomass burning for household heating and cooking. Moreover, Volatile PAHs absorption on particle due to lower atmospheric temperature and atmospheric stability may also be another reason for increasing concentration in cold period. Among the six measurement cities, the highest concentration of PAHs was observed at Belluno whereas the lowest concentration was detected at Rovigo. In this study an inverse correlation was observed between PAHs with temperature, solar radiation, wind speed and ozone.

BaP is the contributor of 75% of the BaP$_{TEQ}$ and LCR value suggests that carcinogenic risk associated to PAHs is higher than health-based guideline of 10^{-5} and acceptable risk level of European Commission (10^{-6} to 10^{-4} per year). Almost all the sampling days in cold period, PM$_{2.5}$ and BaP levels exceeded the limit set by EC. From the diagnostic ratio, it is apparent that biomass burning and vehicular emissions from diesel engines are the main sources of PAHs emissions.

CHAPTER 6

TRACE ELEMENTS

6.1. Aims

This chapter deals with spatial and temporal variability of trace element in urban particulate matter and also to investigate the possible sources of trace element in $PM_{2.5}$.

6.2. Seasonal and spatial variations

The mean concentrations of 18 measured trace elements have been given in Table 6.1 whereas monthly concentrations of trace elements for all measurement sites have been given in Figure 6.1. Among 18 elements the most abundant elements are Fe, Ca, Al, S, K, Mg and Zn. Most of the elements showed the highest concentration in VI as compared to others. The mean concentration of Fe, which is mainly originated from non-exhaust traffic elements and crustal is 185 ng m^{-3}, fluctuated from 13.7-10175 ng m^{-3} and found higher concentrations in winter months. The highest mean concentration of Fe was observed in PD while the lowest mean concentration was found in BL and TV. The highest concentrations of Ca and Al were observed in warmer months. The mean annual concentration of Ca and Al are 961 and 590 ng m^{-3}, respectively and varied from 545.2-5625 and 250-2328 ng m^{-3}, respectively. Ca and Al both showed the highest concentration in BL and the lowest mean concentration was observed in VE and TV, respectively.

The annual mean concentration of S is 730 ng m^{-3}, ranged from 73.3-2327 ng m^{-3}. The highest mean concentration was observed in February and the highest concentration was found in RO. Potassium (K), a tracer of biomass burning (Puxbaum et al., 2007; Saarnio et al., 2010) showed the highest concentration in winter months. The mean annual concentration of K is 410 ng m^{-3} and fluctuated from 120-1246 ng m^{-3} and the highest mean concentration was observed in VI. Both Mg and Ti showed higher concentration in summer months. The mean concentration of Mg is 415 ng m^{-3} whereas the mean concentration of Ti is 5.6 ng m^{-3}, mostly found in mineral dust. The concentration of Mn ranged from 0.83-293 ng m^{-3} with a mean value of 8.3 ng m^{-3} whereas the annual mean value of Zn is 40.3 ng m^{-3} and ranged from 4.9-313 ng m^{-3}. The highest concentrations of Mn and Zn are observed in winter months and supposed to be originated from vehicular emissions and road dust suspension. The concentration of Mn showed significantly higher concentration in VI than other measurement station. Barium (Ba) also showed the highest

mean annual concentration in winter months, having a mean concentration of 12.3 ng m^{-3} and ranged from 4.7-283 ng m^{-3}. The concentration of arsenic (As) varied from 0-7.5 ng m^{-3} with an annual mean value of 0.79 ng m^{-3}. Arsenic is mainly originated from coal burning showed the highest concentration in winter months. The mean concentration of Cd is 0.19, fluctuated from 0.05 to 15.9 ng m^{-3}. The nickel (Ni) concentration ranged from 1.4-1007.8 ng m^{-3} with an annual mean value of 11.2 ng m^{-3}. The mean concentration of vanadium (V) is 0.88 ng m^{-3} and varied from 0.07-9.5 ng m^{-3}. The highest mean concentration of Ni was observed in April whereas the V showed the highest mean concentration in August and both the metals are good tracers of oil combustion. The highest concentration of Ni was observed in VI whereas the highest concentration was found in PD. The concentration of antimony (Sb) varied from 0.22-9.1 ng m^{-3}, with an annual mean value of 1.5 ng m^{-3}. The mean concentration of Cu is 4.2 ng m^{-3} and varied from 0.9-70 ng m^{-3}. Both Sb and Cu showed higher concentrations in winter months.

6.3. Weekly concentration variations of trace elements

A comparison of the levels of trace metals in particulate matter between weekdays and weekend for all the stations has been provided in Figure 6.2 and Figure 6.3 whereas a comparison over Vento region is given in Figure A-6.1. Generally weekdays showed higher total $\sum_{18}$ trace element concentrations as compared to weekend. However this differences between weekdays and weekend for $\sum_{18}$ trace element were not statistically significant as confirmed by Mann-Whitney U test (*p value* = 0.71). All the measurement sites follow the same pattern and showed the highest $\sum_{18}$ trace element concentration on Wednesday, whereas the lowest one was observed on Thursday. Individually, the elements such as Fe, Mn, Ba, Sb showed statistically significant higher concentrations during weekday than weekend. The concentration differences between weekday-weekend may be due to the number concentration variations of PM particles, which showed strong correlations with vehicular traffics particularly with diesel combustion (Hussein et al., 2004).

Table 6.1. Summary statistics of trace element levels in $PM_{2.5}$ ($\mu g\ m^{-3}$)

	BL	TV	VI	PD	VE	RO	Annual	Ranges
Fe	57±20	74±65	552±1609	155±84	135±63	138±62	185±676	14-10175
Ca	904±505	638±562	1500±946	959±614	608±306	1158±1497	961±883	545-5625
Al	438±316	376±261	1519±451	427±326	294±152	488±438	590±539	250-2328
S	457±266	544±477	870±564	751±429	742±507	1015±573	730±513	73-2327
K	403±255	343±234	548±225	423±311	339±293	4042±292	410±277	120-1246
Mg	314±43	331±177	728±129	406±193	309±00	400±277	415±219	308-1676
Ti	5±3	2±2	9±3	4±3	6±3	7±3	6±4	2-18
Mn	2±1	2±2	25±45	7±5	7±6	7±5	8±20	1-293
Zn	16±12	29±46	56±41	56±54	39±31	46±30	40±40	5-313
Ba	11±10	10±36	18±25	12±14	10±9	13±9	12±20	5-283
As	0.4±0.3	0.4±0.3	1±0.7	0.5±0.3	1.6±1.5	0.9±0.4	0.8±0.8	0-8
Cd	0.1±0.0	0.1±0.0	0.1±0.1	0.2±0.3	0.6±2.1	0.1±0.3	0.2±0.9	0.1-16
Ni	2±3	2±2	51±159	7±6	3±2	2±1	11±1	1-1008
Pb	3±1.6	3.4±3.1	8±9	9±6	6±5	7±5	6±6	0.5-41
Sb	0.8±0.7	0.5±0.4	2±1.4	2.4±1.5	2.3±1.8	1.4±1.2	1.5±1.4	0.2-9
V	0.3±0.6	0.2±0.4	1±1.6	1.2±1.5	1.6±2.3	1±1.6	1.0±1.5	0.1-10
Co	0.1±0.0	0.1±0.0	0.5±1.8	0.1±0.1	0.1±0.0	0.1±0.0	0.1±0.8	0.1-12
Cu	2.40±1.50	1.1±0.7	8±12	8±5	3±2	2.7±2	4±6	0.9-70
Mean	2616±821	2356±1206	5896±2487	3228±1326	2505±907	3690±2277	3382	
Median	2411	2130	5324	3180	2408	3021	2824	
Min-Max	1350-5430	1326-9199	2890-17205	1445-6252	1372-5850	1482-10207	1326-17205	
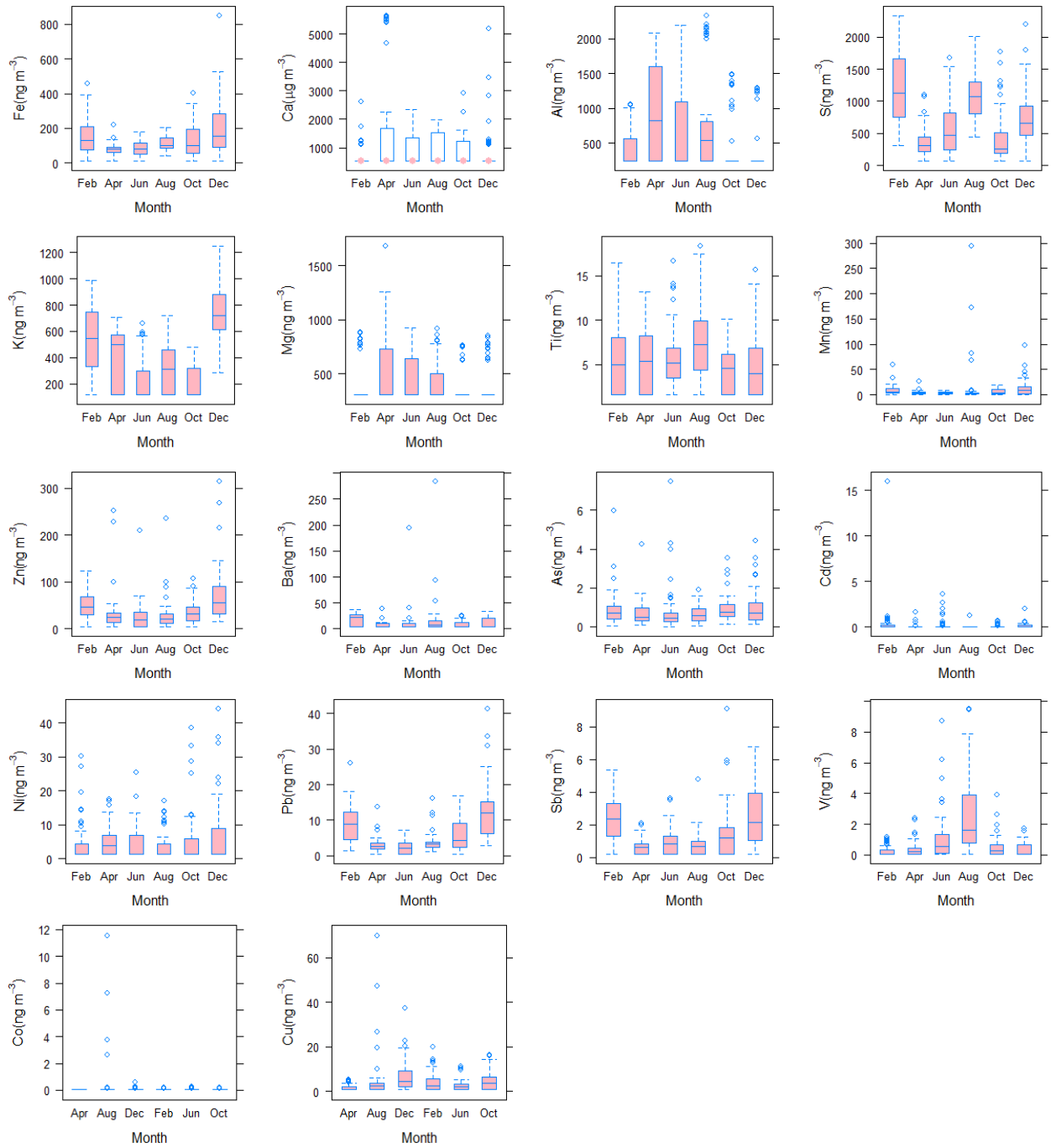
Figure 6.1. Monthly variations of trace element concentrations over the Veneto region

Table 6.2. Comparison of the trace elements concentrations with other countries.

	Italy	Italy	Bangladesh	Spain	Turkey	Portugal	UK	China	Korea	Greece
	This study	Venezia (Via Lissa)	Gonoa	Dhaka	Barcelona	Zonguldak	Lisbon	Castlemorton	Zhengzhou	Incheon	Thessaloniki
PM		2009	2011 $PM_{2.5}$	2006	2001	2004-05 $PM_{2.5}$	2001	1999	2010 $PM_{2.5}$	2009-10 $PM_{2.5}$	2011-12 $PM_{2.5}$
Fonte		(Squizzato, 2011)	Bove et al., 2014	(Salam et al., 2008)	Moreno et al., 2007	Tecer et al., 2012)	(Almeida et al., 2005)	(Allen et al., 2001)	Geng et al., 2013	Choi et al., 2013	Tolis et al., 2015
Fe	185±676	294	120±55	433		130	120	78	1248.8±1026	710.7	0.86±0.6
Ca	961±883	951	88±55			197±312	230		753.1±596	287.6	1.92±1.5
Al	590±539	503	40±49			94±258	77		579.6±509	177.5	0.74±0.97
S	730±513	1232	1266±753								
K	410±277	563	95±55			208±169	120		750.8±440		0.42±0.38
Mg	415±219	347	39±21			66			305±267	154.3	0.38±0.38
Ti	5.6±3.6	16.1	7±4		26.3	12±15	8.5			17.9	0.003±0.002
Mn	8.3±20.1	7.9	4±3		9.6	8±6	2.3	1.7	112.5±49.2	35.8	0.09±0.06
Zn	40.3±40.3	45	16±12	381	55.5	58±44	18	11	444.1±295	248.7	0.20±0.57
Ba	12.3±20	12.3			9.3			1.0	36.9±23		
As	0.79±0.8	1.9		6.28	1.1		0.31		21.2±8	100.1	
Cd	0.19±0.9	3.6		13.2	0.6			0.14	12±13	2.1	
Ni	11.2±0.8	3.8	7±4		5.2	3.0±1.2	2.6	1.3	3.3±2	18.8	0.03±0.04
Pb	6.0±5.7	15.4	5±3	204	40.3	11.9±7.4	8.6	7.9	124±48	57.6	0.05±0.03
Sb	1.5±1.4	3.6			4.3		1.5				
V	0.88±1.5	4.6	15±11		9.5		6.7		3.7±2	73.9	0.011±0.01
Co	0.13±0.8	7.2					0.087	0.06	0.8±0.6	0.8	
Cu	4.2±6.2	12.7	6±5	95	31.7	61±20	5.4	1.1	24.1±10.3	83.5	0.17±0.38
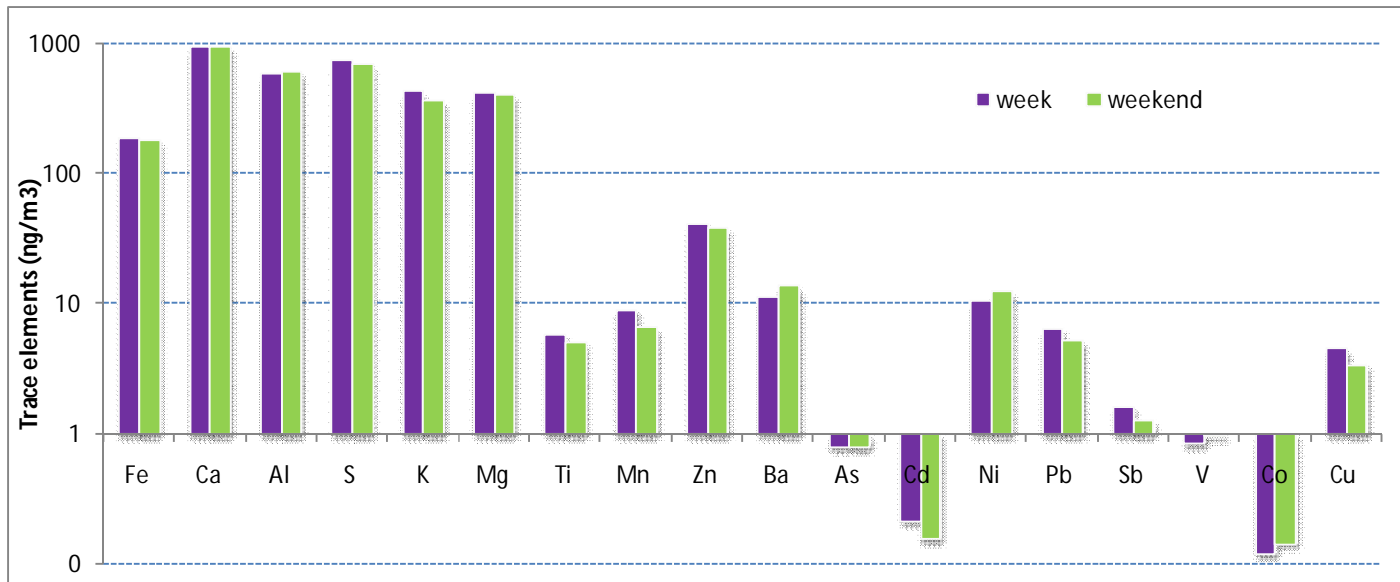
Figure. 6.2 Comparison of the concentrations of trace elements between weekdays and weekend.
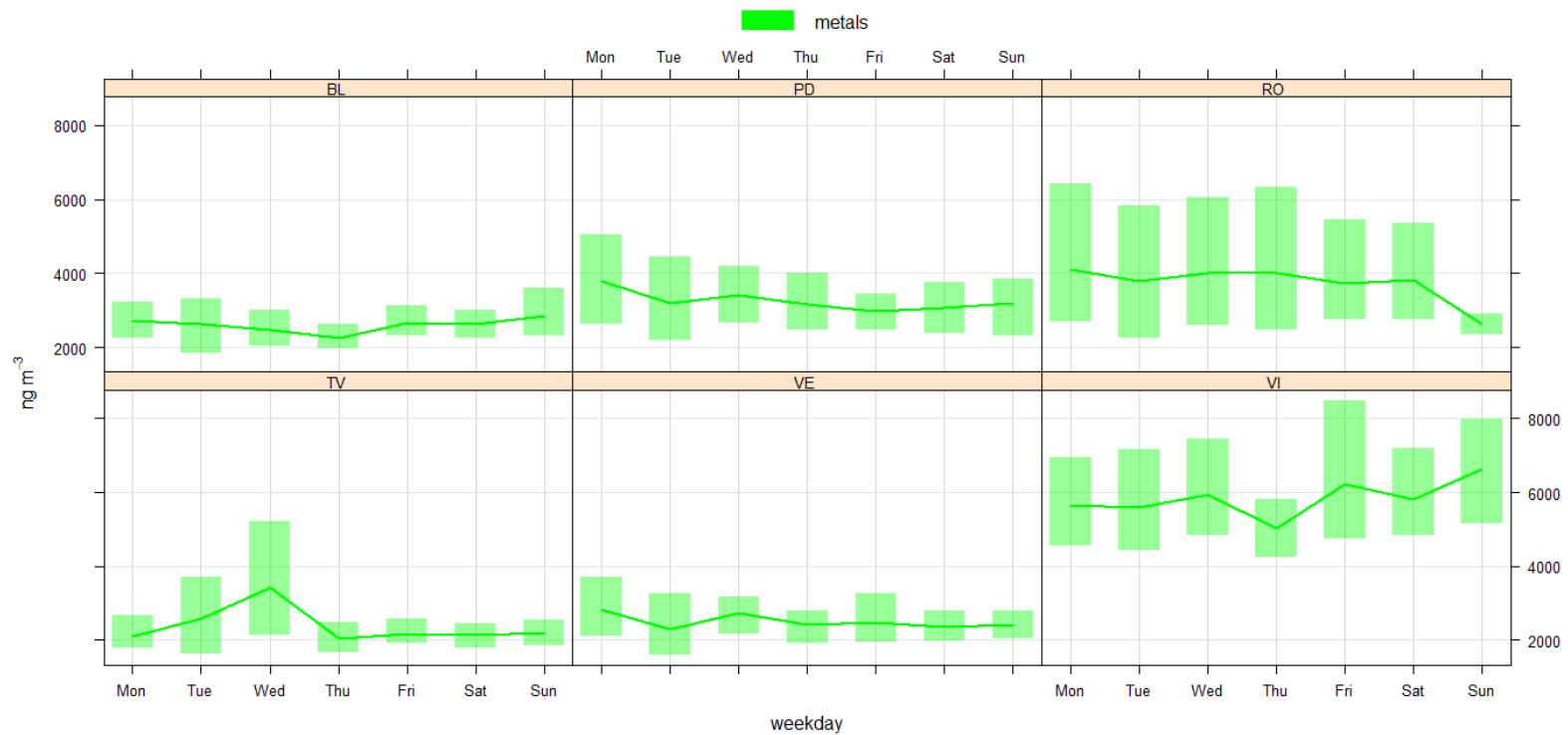
Figure 6.3. The concentrations of total metal ($\sum_{18}$ metal) between weekdays and weekend in all the station

6.4. Comparison with other Italian and international studies

The concentration of trace elements determined in this study was compared with other countries. From the concentrations values of the elements in Veneto region, it is apparent that the concentrations of some elements such as Ca, Al, Ni, K and Mg are much higher than other studies except Zhengzhou, China. Although Fe concentration is comparatively higher in Portugal (Lisbon), UK (Castlemorton) and Greece (Thessaloniki) but lower than Bangladesh (Dhaka) and China. The concentration of Fe, As, Zn and Pb are much higher in our study than in Dhaka, Bangladesh. However, Cd, V, As and Cu showed comparatively lower concentrations than other studies (Table 6.2). The results of this study are quite similar with the research conducted by Sqizzato (2011) probably because of their geographical proximity, although a significant difference is found for several elements such as cobalt, sulfur and titanium.

6.5. Enrichment Factor (EF)

The concept "enrichment factor" was first introduced by Rahn 1971 (Lee et al., 1994) and is used to identify the sources of elements present in atmospheric aerosols and it assesses the influences of crustal sources on trace element composition in PM. EF has been calculated using the following equation.

$$EF = \frac{\left(\frac{X}{Y}\right) aerosol}{\left(\frac{X}{Y}\right) crust} \qquad (Eq\ 6.1)$$

(X/Y) aerosol = is the ratio between the concentrations of target/measured element and reference element in aerosol;

(X/Y) crust= is the ratio between the concentrations of target/measured elements and reference elements in Earth's crust

Usually Al, Fe, Si and Ti have been given priorities as reference materials because of lacking of predominant anthropogenic sources. In this study Fe is selected as reference material (Alves et al., 2015) because Al and Si are supposed to be main components in the

fly ash of the thermal power plants (Petaloti et al., 2006). The composition of crustal elements and then the concentrations of each element in the earth's crust used in the equation were chosen to calculate EF on the basis different scientific articles (Taylor, 1964; Cox, 1989; Wedepohl, 1995). The mean concentration of the elements present in the earth crust used (Table 6.3) may actually differ from the actual composition of the soil of the study area, which depends on the geochemical properties and its potential contamination from anthropogenic sources. In addition, the reference element chosen (Fe) may also be issued from other sources as well as from the crust. For this reason, an average value is used in the Table 6.3 which, however, could not always be significant for some elements of crustal origin.

An elements is considered to be crustal origin if EF<1, while the element is supposed to be non-crustal origin for EF value greater than 5 (Gao et al., 2002). The most enriched (EF>100) elements are S, Zn, As, Cd, Pb, and Sb, suggested that these elements are mainly coming to the atmosphere from the emissions of various anthropogenic activities. Low EF values are found for (<5) Fe, Al, Ti, Mn, Mg, V and Co, supposed to be originated from soil or road dust resuspension.

Table 6.3. Average concentration of the elements in the earth's crust and calculation of the enrichment factor

Element	Concentration (Reference element)	Estimated Earth Crust						
		Site						
		BL	TV	VI	PD	VE	RO	Veneto
Fe	57060[b]	1.0	1.0	1.0	1.0	1.0	1.0	1
Ca	48600[b]	18.7	10.2	3.2	7.3	5.3	9.9	6.1
Al	82000[c]	5.4	3.6	1.9	1.9	1.5	2.5	2.2
S	408[b]	1127.9	1032.9	220.4	678.5	771.1	1029.9	552
K	15000[c]	27.1	17.7	3.8	10.4	9.6	11.2	8.4
Mg	29000[c]	10.9	8.9	2.6	5.2	4.5	5.7	4.4
Ti	5700[a]	0.8	0.3	0.2	0.2	0.5	0.5	0.30
Mn	950[a]	2.1	1.8	2.7	2.6	3.1	2.9	2.7
Zn	79[b]	206.4	280.7	73.8	261.9	207.3	240.6	157.4
Ba	425[a]	25.8	18.6	4.3	10.7	10.4	12.4	9.0
As	1.8[a]	218.0	168.0	55.1	106.6	370.0	213.9	136.2
Cd	0.15[c]	402.5	258.4	75.8	541.0	1697.0	331.3	398
Ni	90[c]	32.4	17.4	58.5	28.6	12.2	8.4	38.5
Pb	12.5[b]	241.5	212.1	66.8	252.6	215.5	220.3	148.3
Sb	0.2[c]	4176.3	2054.5	754.7	4333.9	4942.4	2960.7	2298.4
V	149[b]	2.0	1.0	0.7	3.1	4.4	2.8	1.83
Co	30[c]	1.7	1.3	1.7	1.0	0.7	0.7	1.32
Cu	55[a]	43.9	15.4	15.5	51.8	21.5	20.3	23.3

[a]Taylor, 1964; [b]Cox, 1989; [c]Wedepohl, 1995

6.6. Correlations among trace elements

To find the relationships among trace elements, only VI and PD were selected. As data were not normally distributed, a non-parametric test "Spearman" correlation was performed to find significant relationship among trace elements. Strong correlation was observed among crustal elements especially Ca, Al and Ti, revealed that these elements are coming from soil dust. On the contrary, elements related to vehicular traffic such as Fe, Mn, Zn, Pb, Sb, Cu and V showed strong correlations in both sites (Table 6.4). However, strong correlations among Mn, Fe, Pb and Zn, sometimes may be also considered as tracers of emissions of steel industries, such as that present in the territory. The dust emitted from a steel mill are primarily derived from the processes of melting and refining steel and are characterized by a much higher content of some metals (especially iron, manganese, chromium, nickel and zinc) than the dust emitted from traffic and heating. Moreover, arsenic (As) also showed strong relationship with S and Mn. The strong correlation of Cu with Mn, Cd, Ni, Sb and V suggested that these elements are known as traffic markers (Sernbeck et al., 2002; Iigima et al., 2009; Duan et al., 2012) and primarily originated from traffic-oriented sources such as exhaust brake wear, tires, fossil fuel combustion, road line paintings and the galvanized security barriers (Gao et al., 2014).

Relationship among trace element and meteorological factors such as wind, temperature, solar radiation, humidity and precipitation were also determined (Table 6.5) and it revealed that these relationships follow the same pattern like OC-EC and PAHs. Most of the elements showed negative relationship with temperature and wind velocity may be due to the presence of lower pollutant dispersions with stable atmospheric condition during winter (Vardoulakis and Kassomenos, 2008).

Table 6.4. Relationships among elements of all the measurement sites. Only significant values are given (p <0.05)

VI	Fe	Ca	Al	S	K	Ti	Mn	Zn	Ba	As	Cd	Ni	Pb	Sb	V	Cu
Fe																
Ca																
Al		0.52														
S	0.49															
K	0.45			0.59												
Ti	0.54		0.27	0.53	0.47											
Mn	0.90			0.40	0.46	0.47										
Zn	0.48		-0.40	0.45	0.56	0.28	0.51									
Ba	0.33		-0.27	0.54	0.33	0.50	0.28	0.53								
As	0.77		-0.31	0.71	0.54	0.44	0.76	0.62	0.42							
Cd	0.27			0.29	0.38		0.31	0.51		0.38						
Ni	0.71			0.28	0.36	0.30	0.69			0.41						
Pb	0.68		-0.46	0.63	0.60	0.36	0.69	0.81	0.51	0.85	0.42	0.36				
Sb	0.38	-0.30	-0.71	0.33	0.32	0.00	0.46	0.75	0.44	0.56	0.49		0.78			
V	0.69			0.70	0.49	0.69	0.57	0.30	0.35	0.69	0.29	0.44	0.47			
Cu	0.86	-0.04	-0.34	0.49	0.44	0.41	0.87	0.58	0.38	0.85	0.31	0.62	0.77	0.57	0.56	

PD	Fe	Ca	Al	S	K	Ti	Mn	Zn	Ba	As	Cd	Ni	Pb	Sb	V	Cu
Fe																
Ca																
Al		0.84														
S	0.41															
K	0.65			0.45												
Ti		0.60	0.59	0.36												
Mn	0.83				0.62											
Zn	0.37				0.31		0.49									
As	0.60	-0.50	-0.46				0.67	0.38								
Cd	0.61				0.67		0.59	0.29		0.35						
Ni	0.50	0.38	0.34		0.56	0.44	0.47	0.29			0.32					
Pb	0.78		-0.30	0.41	0.58		0.89	0.49		0.70	0.58	0.34				
Sb	0.75			0.44	0.66		0.71	0.38		0.49	0.64	0.33	0.76			
V		0.33		0.27		0.42										
Cu	0.85		-0.28		0.52		0.80			0.71	0.52	0.42	0.75	0.65		

Table 6.5. Correlation between meteorological factors and trace elements

Parameters	Fe	Ca	Al	S	K	Mg	Ti	Mn	Zn	Ba	As	Cd	Ni	Pb	Sb	V	Co	Cu
Wind	-0.36	-0.15	0.03	0.-16	-0.26	-0.07	0.03	-0.36	-0.35	-0.06	-0.17	-0.36	-0.38	-0.53	-0.49	-0.28	-0.36	-0.64
Temperature	-12	0.14	0.17	-0.01	-0.52	0.09	0.16	-0.24	-0.24	-0.14	-0.13	-0.29	0.03	-0.47	-0.44	0.45	0.05	-0.14
Radiation	-22	0.25	0.25	00	-0.37	0.11	0.24	-0.21	-0.21	-0.13	-0.11	-0.23	-0.05	-0.49	-0.41	0.16	-0.13	-0.26
humidity	0.11	-0.08	-0.08	-0.09	0.23	-0.04	-0.05	0.28	-0.14	0.10	0.29	0.18	0.10	0.36	0.31	-0.16	0.04	0.22
rainfall	-0.22	0.03	0.05	-0.32	-0.06	-0.03	-0.12	-0.14	0.28	-0.15	-0.08	-0.13	0.02	-0.19	-0.14	-0.15	-0.06	-0.14

6.7. Health risk assessment

Health risk due to trace element exposure was calculated using USEPA human health evaluation methods (USEPA, 2001). Elements entered into human body through three exposure pathways a) ingestion, b) dermal contact, and c) inhalation (Ferreira-Baptista and Miguel, 2005; Kurt-Karakus, 2012). The Potential exposure doses through inhalation are calculated from the following equations

a) Daily potential exposure dose through inhalation, $LADD_{inh}$

$$LADD_{inh} = \frac{C \times InhR \times EF \times ED}{BW \times AT} \qquad \text{(Eq 6.2)}$$

Details of the parameter used in the equations (Eq 6.2) have been given in table 6.6. Finally, the cancer risk (CR) of the exposure of elements is estimated and this value is acceptable for the value lower than 1.0×10^{-6} to 1.0×10^{-4}.

Health risk characterization has been calculated from the equations described below:

$$CR = LADD_{inh} \times CSF_{inh} \qquad \text{(Eq 6.3)}$$

Here, LADD = average daily exposure dose of trace elements through ingestion, dermal contact and inhalation pathways (mg/kg/day)
RfD = reference dose; CSF= cancer slope factor $(mg/kg/day)^{-1}$.

All the above calculations have been done in this study by following USEPA method and published documents (Čupr et al., 2013; Lee et al., 2006; US EPA, 2011; Wcisło et al., 2002; Liu et al., 2015). The average daily exposure doses of trace elements through inhalation pathways are provided in Table 6.7. The daily exposure doses showed variation and followed the orders Ca>Al> S> K> Mg> Fe>Zn> Ba> Ni> As> Mn> Pb> Ti> Cd> Sb> V> Co> Cu. The exposure doses of trace elements through inhalation pathways were much higher for children as compared to adults. It is not possible to calculate HI values for all the measured trace elements as the USEPA has not estimated RfD values for all the elements. The recommended values for RfD used in this study has been given in Table 6.8 whereas the calculated CR values were given in Table 6.9.

Table 6.6. Recommended values of the parameters used to calculated the daily exposure dose of trace elements in $PM_{2.5}$

Parameter	Definition	Value	References
C	Average concentration of HMs in APM (mg/kg)		Hu et al. (2012)
EF	Exposure frequency (days/year)	180	USEPA(2004)
ED	Exposure duration (year)	24 (adults), 6 (children)	USEPA(2004)
CF	Conversion factor	10^{-6} (kg/mg)	USEPA(2004)
BW	Body weight (kg)	70 (adults), 15 (children)	USEPA(2004)
AT	Averaging time (days)	Non-carcinogens, AT=ED*365 days/year	USEPA(2004)
		Carcinogens, AT=70*365 days/year	Du et al. (2013)
InhR	Inhalation rate (m^3/day)	7.63 (adults), 20 (children)	USEPA (2009)

Table 6.7. Calculated daily exposure doses of trace elements through inhalation pathways

	Adult	Children
	$LADD_{inh}$	$LADD_{inh}$
Fe	6.3×10^{-7}	1.7×10^{-9}
Ca	3.3×10^{-7}	8.9×10^{-9}
Al	2.0×10^{-7}	5.5×10^{-9}
S	2.5×10^{-7}	6.8×10^{-9}
K	1.4×10^{-7}	3.8×10^{-9}
Mg	1.4×10^{-7}	3.9×10^{-9}
Ti	1.9×10^{-9}	5.2×10^{-11}
Mn	2.8×10^{-9}	7.7×10^{-11}
Zn	1.4×10^{-8}	3.7×10^{-10}
Ba	4.2×10^{-9}	1.1×10^{-10}
As	2.7×10^{-10}	7.4×10^{-12}
Cd	6.5×10^{-11}	1.8×10^{-12}
Ni	3.8×10^{-9}	1.0×10^{-10}
Pb	2.0×10^{-9}	5.6×10^{-11}
Sb	5.0×10^{-10}	1.4×10^{-11}
V	3.0×10^{-10}	8.2×10^{-12}
Co	4.3×10^{-11}	1.2×10^{-12}
Cu	1.4×10^{-9}	3.9×10^{-11}

Table 6.8. Recommended values in equations of the health risk characterization of elements in atmospheric particulate matter

	Zn	Pb	Cd	Ni	Mn	Cr	Cu
RfD-ADD$_{inh}$	3.01×10^{-1}	3.52×10^{-3}	1.00×10^{-3}	5.04×10^{-3}	1.84×10^{-3}	6.00×10^{-5}	1.20×10^{-2}
RfD-CSF$_{inh}$			6.30×10^{0}	8.40×10^{-1}		4.20×10^{1}	

Table 6.9. Characterization of risk of trace elements in PM$_{2.5}$.

	Mn	Zn	Cd	Ni	Pb	Cu
Adult CR			1.29×10^{-10}	1.0×10^{-9}		
Children CR			1.13×10^{-11}	1.50×10^{-12}		

The cancer risk of Cd and Ni has been estimated from the average daily exposure doses through inhalation pathway and the values of cancer risk for both the trace elements are below the acceptable limit of European Union (10^{-6} to 10^{-4} per year: EC, 2001), indicated that these two elements are not responsible for carcinogenic risk.

6.8. Conclusion

The mean concentration of $\sum_{18}$ trace element was 3382 ng m^{-3} and it ranged from 1326-17205 ng m^{-3}. Among 18 elements the most abundant elements are Fe, Ca, Al, S, K, Mg and Zn. Most of the elements showed the highest concentration in VI as compared to others. Concerning temporal trends, the elements like Fe, K, Zn, Ba, Pb, Sb and Cu showed the highest mean concentrations during winter months whereas, the highest concentration was recorded for Ca, Al, Mg, Ti, Mn, Cd, V and Co during the summer months. Several elements such as S, Ti, Zn, As and Ni showed almost similar concentrations throughout the year. The highest values during winter month may be due to the biomass burning for household heating and cooking as well as the atmospheric stability and lower mixing layers resulting in pollutant accumulation at ground level. On the contrary, vehicular traffic may be responsible for the higher concentration of several elements especially V, Cd and Ni. Relationship among trace

element and meteorological factors such as wind, temperature, solar radiation, humidity and precipitation revealed that these relationships follow the same pattern like OC-EC and PAHs. Most of the metals showed negative relationship with temperature and wind velocity may be due to the presence of lower pollutant dispersions with stable atmospheric condition during winter. Enrichment factor was determined and it revealed that S, Zn, As, Cd, Pb and Sb are the most enriched elements and originated from the emissions of various anthropogenic activities whereas Fe, Al, Ti, Mn, Mg, V and Co are the low enriched elements, supposed to be originated from soil or road dust suspension. Health risk associated with trace element exposure was calculated using USEPA human health evaluation methods and it is apparent that the exposure doses of trace elements through inhalation pathways were much higher for children than adults.

CHAPTER 7

POSSIBLE SOURCES

7.1.   Factor Analysis (FA)

To find possible sources of $PM_{2.5}$, a statistical procedure named factor analysis was performed to identify number of factors and species profile of each source. Main principle of the FA is to reduce the number of variables keeping original information. Before FA analysis, missing values was substituted with LOD/2 and then both Kaiser-Myer-Olkin (KMO) for sampling adequacy and Bartlett's test for homogeneity of variance were performed to test the suitability of the data for FA test. Generally, a KMO value over 0.6 and a level of significance for Bartlett's test below 0.5 reveal there is a reasonable amount of correlation in the data, thus suitable for FA analysis. Factor analysis was conducted separately for all the measurement sites. In this study, KMO was 0.76 and *p value* for Bartlett's test was lower than 0.05 (*p=0.000*), indicating data are correlated enough for FA analysis. Factors were identified using varimax rotation method based on eigen-value, scree plot, variability in the number of factors and sensibility of each variable to factor loading. Variables were considered as a sources when factor loading were>0.65 and moderately loading (0.50-0.65). Before factor analysis, Principle Component Analysis (PCA) was performed and we observed that all the PAHs congeners are highly correlated and fall into same group and therefore we have used sum of PAHs congeners ($\sum_8$PAHs) instead of all PAHs congeners separately. To perform FA analysis, OC, EC, PAHs, trace elements and ions data (which was analysed by another team member of our group) were used to get a complete scenario of the origin of the pollutants. Potential sources of atmospheric $PM_{2.5}$ were identical separately for all six measurement sites as they have distinct geomorphological characteristic. Variables with loading in factor analysis of all the measurement sites have been given in Table 7.1-7.6.

Table 7.1. Shows the variable with loading in factor analysis in BL. Variables with loading factors >0.65 are red colored and variables with loading factors 0.5-0.65 are blue colored

Element	Factor 1	Factor 2	Factor 3
OC	**0.85**	0.18	0.26
EC	**0.73**	-0.04	0.25
PAH	**0.81**	-0.27	0.17
NO_3^-	**0.87**	0.24	0.09
PO_4^{-2}	**-0.66**	0.17	-0.48
SO_4^{-2}	0.10	**0.92**	0.04
Na^+	0.64	0.31	0.20
NH_4^+	0.58	**0.66**	0.13
K^+	**0.89**	0.08	0.24
Ca^{+2}	0.06	**0.69**	-0.13
Fe	-0.36	0.37	-0.35
Ca	-0.13	-0.39	**-0.67**
Al	-0.13	-0.06	**-0.95**
S	0.15	**0.90**	0.08
K	**0.86**	0.02	-0.26
Ti	-0.50	0.13	-0.42
Mn	-0.16	0.52	-0.59
Zn	0.41	0.21	0.13
Ba	0.02	0.09	0.13
As	0.40	-0.14	0.44
Ni	-0.16	-0.01	-0.60
Pb	**0.73**	0.50	-0.02
Sb	0.59	0.47	0.01
V	-0.39	0.56	-0.03
Cu	-0.25	0.29	0.31
%Variance	34	17	9
Cumulative variance	34	51	60
Source	Biomass burning and Road traffic	Secondary Sulphates	Crustal

Table 7.2. Shows the variable with loading in factor analysis in TV. Variables with loading factors >0.65 are red colored and variables with loading factors 0.5-0.65 are blue colored.

Element	Factor 1	Factor 2
OC	**0.94**	0.25
EC	**0.77**	-0.22
PAH	**0.85**	-0.28
NO_3^-	**0.70**	0.32
PO_4^{-2}	-0.29	-0.14
SO_4^{-2}	0.07	**0.88**
Na^+	-0.14	-0.20
NH_4^+	0.46	**0.72**
K^+	**0.97**	0.05
Ca^{+2}	**0.66**	0.41
Fe	0.56	0.49
Ca	-0.22	0.37
Al	-0.37	0.47
S	0.21	**0.87**
K	**0.68**	0.37
Mn	0.45	0.48
Zn	0.33	0.16
As	-0.30	0.34
Ni	-0.07	0.27
Pb	**0.80**	0.47
Sb	**0.66**	0.23
V	-0.29	0.45
%Variance	36	15
Cumulative variance	36	51
Source	Biomass burning and Road traffic	Secondary Sulphates

Table 7.3. Shows the variable with loading in factor analysis in VI. Variables with loading factors >0.65 are red colored and variables with loading factors 0.5-0.65 are blue colored.

Element	Factor 1	Factor 2
OC	**0.97**	-0.00
EC	**0.70**	-0.03
PAH	**0.72**	-0.08
Cl	**0.88**	0.07
NO_3^-	0.62	-0.25
PO_4^{-2}	**-0.74**	0.27
SO_4^{-2}	0.52	0.33
Na^+	0.50	-0.15
NH_4^+	**0.69**	-0.13
K^+	**0.96**	-0.02
Ca^{+2}	0.55	0.04
Fe	-0.10	**0.92**
Ca	0.02	0.17
Al	-0.57	0.41
S	0.63	0.28
K	**0.67**	0.31
Mg	-0.08	0.17
Ti	0.31	0.42
Mn	0.11	**0.93**
Zn	**0.74**	0.06
Ba	0.15	-0.01
As	**0.81**	0.36
Ni	-0.15	**0.91**
Pb	**0.91**	0.10
Sb	**0.89**	-0.02
V	-0.04	**0.95**
Cu	0.32	**0.88**
%Variance	38	19
Cumulative variance	38	37
Source	Biomass burning and Road dust	Heavy oil

Table 7.4. Shows the variable with loading in factor analysis in PD. Variables with loading factors >0.65 are red colored and variables with loading factors 0.5-0.65 are blue colored.

Element	Factor 1	Factor 2	Factor 3
OC	**0.88**	0.21	0.29
EC	**0.67**	0.05	0.03
PAH	**0.84**	0.16	-0.15
Cl	**0.90**	0.11	0.11
NO_3^-	0.49	0.62	0.37
PO_4^{-2}	-0.36	0.36	-0.57
SO_4^{-2}	0.24	-0.03	**0.86**
Na^+	-0.16	0.45	-0.59
NH_4^+	0.47	0.47	0.63
K^+	**0.92**	0.17	0.13
Ca^{+2}	0.58	-0.23	0.16
Fe	**0.83**	-0.02	0.27
Ca	-0.21	**-0.87**	0.12
Al	-0.20	**-0.84**	0.06
S	0.25	-0.05	**0.82**
K	**0.86**	-0.32	0.16
Ti	0.16	**-0.67**	0.26
Mn	**0.90**	0.14	0.09
Zn	0.39	0.11	-0.08
Ba	0.31	0.03	0.30
As	0.47	0.57	0.35
Cd	0.46	-0.02	0.15
Ni	0.28	-0.29	0.19
Pb	**0.86**	0.26	0.25
Sb	**0.81**	0.09	0.37
V	-0.32	-0.12	0.51
Cu	**0.80**	0.16	0.15
%Variance	42	14	8
Cumulative variance	42	56	64
Source	Biomass burning and Road traffic	Crustal	Secondary sulphate

Table 7.5. Shows the variable with loading in factor analysis in VE. Variables with loading factors >0.65 are red colored and variables with loading factors 0.5-0.65 are blue colored.

Element	Factor 1	Factor 2	Factor 3
OC	**0.91**	0.29	0.07
EC	**0.85**	-0.06	0.01
PAH	**0.88**	-0.10	0.24
Cl	**0.89**	-0.06	-0.06
NO_3^-	0.52	0.53	0.15
PO_4^{-2}	-0.65	-0.21	-0.49
SO_4^{-2}	-0.02	**0.87**	-0.15
Na^+	**0.70**	0.27	0.34
NH_4^+	0.35	**0.80**	0.04
K^+	**0.93**	0.13	0.14
Ca^{+2}	**0.67**	0.10	-0.20
Fe	**0.84**	0.14	-0.25
S	0.14	**0.90**	-0.17
K	**0.91**	0.16	0.03
Ti	0.27	0.43	-0.48
Mn	**0.87**	0.13	-0.07
Zn	**0.84**	0.26	0.09
Ba	0.41	0.44	0.28
As	0.12	0.21	-0.19
Cd	-0.01	0.51	0.20
Ni	0.11	0.09	**-0.72**
Pb	**0.74**	0.41	-0.07
Sb	**0.71**	0.37	0.04
V	-0.35	0.30	**-0.69**
Cu	**0.73**	0.14	-0.46
%Variance	47	13	8
Cumulative variance	47	60	68
	Biomass burning and Road traffic	Secondary sulphate	Heavy oil

Table 7.6. Shows the variable with loading in factor analysis in RO. Variables with loading factors >0.65 are red colored and variables with loading factors 0.5-0.65 are blue colored.

Element	Factor 1	Factor 2
OC	**0.87**	0.22
EC	**0.68**	-0.05
PAH	**0.79**	-0.21
Cl	**0.73**	0.01
NO_3^-	**0.79**	0.15
PO_4^{-2}	-0.23	-0.09
SO_4^{-2}	0.37	0.57
Na^+	0.22	-0.22
NH_4^+	**0.77**	0.32
K^+	**0.93**	0.04
Ca^{+2}	0.30	0.14
Fe	**0.75**	0.28
Ca	-0.07	**-0.85**
Al	-0.09	**-0.87**
S	0.42	0.53
K	**0.81**	-0.49
Ti	0.02	-0.40
Mn	**0.95**	0.04
Zn	**0.88**	0.01
Ba	-0.07	0.26
As	0.29	0.09
Ni	-0.02	-0.13
Pb	**0.89**	0.07
Sb	**0.73**	0.17
V	-0.36	0.46
Cu	**0.67**	0.35
%Variance	39	12
Cumulative variance	39	51
Source	Biomass burning and Road traffic and secondary nitrate	Crustal and secondary sulphate

The first factor for all the sites includes OC, EC, PAHs, K^+ and also Pb. K^+ is the biomarker of biomass burning whereas OC concentration comes from household heating and cooking especially in winter. Moreover, EC is originated from gasoline and diesel powered vehicles followed by Pb (Cheng et al., 2010). Therefore this factor is designated as biomass burning and vehicular traffic.

The second factor of BL, TV, VE and RO and third factor of PD comprised of sulphate and sulphur which are predominant sources of secondary sulphate (Bove et al., 2014; Masiol et al., 2012). The 3rd factor of BL and second factor of PD and RO consists of primarily Ca, Al and and secondarily Ni and links to typical crustal origin (Rampazzo et al., 2008).

The second factor for VI and third factor for VE are comprised of nickel and vanadium and these elements are present in crude oil (Lewan, 1984) and biomarker for fossil fuel or heavy oil combustion processes (Moreno et al., 2010) such as petroleum refineries (Bosco et al., 2005), coke production (Moreno et al., 2007), heavy fuel oil broilers (Sippula et al., 2009) and shipping emissions (Becagli et l., 2012).

CHAPTER 8

CONCLUSION

PM$_{2.5}$ samples (n=360) were collected from April 2012 to February 2013 at six provinces in the Veneto region, to determine the chemical composition, the factors affecting organic and inorganic particulate matter variations and to find the sources of PM$_{2.5}$. Sixty samples per province were analysed in every alternate month (April, June, August, October, December and February): 10 samples per station in 10 consecutive days of the months selected.

PM$_{2.5}$ concentration fluctuated from 3.0 µg m^{-3} to 82.6 µg m^{-3} with a value (mean±standard deviation) of 24±17 µg m^{-3}. Concentrations were predominantly higher in the colder months than in the warmer ones. The OC concentration ranged from 0.98 µg m^{-3} to 22.34 µg m^{-3}, while the mean value was 5.48 µg m^{-3}, contributing 79% of the total carbon. EC concentrations fluctuated from 0.19 to 11.90 µg m^{-3} with an annual mean value of 1.31 µg m^{-3} (19% of the total carbon). The monthly OC concentration gradually increased from April to December. The EC did not vary in accordance with OC. However the highest values for both parameters were recorded in the cold period. Although there were concentration differences in OC among the provinces, these were not statistically significant as tested by the Kruskal–Wallis one-way analysis of variance. The OC/EC ratios ranged between 0.71 to 15.38 with a mean value of 4.54, which is higher than the values observed in most of the other European cities. Statistically significant correlations between OC and EC were found in all the monitored months except in October and December. Statistically significant meteorological factors controlling OC and EC were investigated by fitting linear models and using a robust procedure based on weighted likelihood. Temperature and wind velocity turned out to be statistically significant, with a multiple R^2 value of 0.79. The secondary organic carbon (SOC) was calculated from the EC tracer method. The SOC contributed for 69% of the total OC during the study period and this was confirmed by both the approaches OC/EC minimum ratio and regression. CPF (conditional probability function) and CBPF (conditional bivariate probability function) plots indicate that both biomass & wood burning and vehicular traffic are probably the main local sources for carbonaceous particulate matter emissions in two selected cities. Finally, a cluster analysis on the back-trajectories of air masses from different regions of Europe revealed no significant contributions in the levels of OC and EC. A limited influence of trans-boundary transports on the levels of carbonaceous PM$_{2.5}$ in the Veneto was therefore inferred.

Considering PAHs, the total concentration of 8 particulate PAHs ranged from 0.2 to 70.4 ng m^{-3} with a mean value of 11.5 ng m^{-3}. The mean BaP concentration was 2.0 ng m^{-3}, contributing 17.4% to the total PAHs which is two-times higher than limit set by the European Union. PAHs concentration across the region follow same pattern with maxima during colder months and minima in warm period. In this study, PAHs showed an inverse relationship with temperature, solar radiation, wind speed and ozone. The results of this study suggest that biomass burning for household heating and cooking followed by volatile PAHs absorption on particle due to lower atmospheric temperature and atmospheric stability are the main reasons for increasing PAHs concentration in winter. Health risk was evaluated by lifetime lung cancer risk (LCR), showed potential carcinogenic risk from the airborne BaP$_{TEQ}$ which is six fold higher in cold period as compared to the warm season. Gas-phase PAHs (P) concentrations were calculated and it could be concluded that there is tiny difference between P (particulate) data and G+P (gas+particulate) data set in Veneto region. Finally, local source emission was studied by conditional biovariate probability function and results revealed that local emissions especially domestic heating and road transport emissions were responsible for higher PAHs and PM$_{2.5}$ mass.

For elements, the mean concentration of $\sum_{18}$ trace element was 3382 ng m^{-3} and it ranged from 1326-17205 ng m^{-3}. Among 18 elements the most abundant elements are Fe, Ca, Al, S, K, Mg and Zn. Most of the elements showed the highest concentration in VI as compared to others. Several elements such as Fe, K, Zn, Ba, Pb, Sb and Cu showed highest mean concentrations during winter months whereas, the highest concentration was recorded for Ca, Al, Mg, Ti, Mn, Cd, V and Co during the summer months. Several elements such as S, Ti, Zn, As and Ni showed almost similar concentrations throughout the year. The highest values during winter month may be due to the biomass burning for household heating and cooking as well as the atmospheric stability and lower mixing layers resulting in pollutant accumulation at ground level. It is obvious from the correlation among trace elements and meteorological factors such as wind, temperature, solar radiation, humidity and precipitation that these relationships follow the same pattern like OC-EC and PAHs.

Enrichment factor was determined and it revealed that elements such as S, Zn, As, Cd, Pb and Sb are the most enriched elements and originated from the emissions of various

anthropogenic activities. Health risk, evaluated as the lifetime lung cancer risk (LR), and showed the cancer risks of Cd and Ni have been estimated from the average daily exposure doses through inhalation pathway and the values of cancer risk for both the elements are below the acceptable limit of European Union. The main factors for the increased organic compound concentrations and trace elements are biomass burning for household heating and cooking, followed by vehicular traffic, oil combustion and crustal.

Finally, $PM_{2.5}$ concentrations varied from 3.0 µg m^{-3} to 83 µg m^{-3} with a mean value of 24 ± 17 µg m^{-3}. Total carbon and inorganic ions (trace elements and ion) together contributed for almost 79% to the total $PM_{2.5}$ whereas organic compounds (TC and PAHs) contributed for 28% to the total $PM_{2.5}$. Therefore, OC, EC and trace elements are significant contributors to the total $PM_{2.5}$. Finally, the findings of this research work may be used as baseline data for the Italian Government as well as European community. Moreover, it also suggests to take necessary actions at both local and regional level to control fine particulate matter as $PM_{2.5}$ concentrations in four cities exceeded the annual mean concentration limit set by the 2008/50/EC directive: annual mean value 25 µg m^{-3} which will be met by 2015.

REFERENCES

Abdalmogith SS, Harrison RM. 2005. The use of trajectory cluster analysis to examine the long-range transport of secondary inorganic aerosol in the UK, Atmospheric Environment., 39, 6686–6695.

Adriano DC. 2001. Trace Elements in Terrestrial Environments: Biogeochemistry, Bioavailability, and Risks of Metals. Springer, New York.

Agostinelli C. 2001. Test of hypotheses based on the weighted likelihood methodology. Statistica Sinica 11, 499-514.

Agudelo-Castaňeda DM, Teixeira EC. 2014. Seasonal changes, identification and source apportionment of PAH in $PM_{1.0}$. Atmospheric Environment 96, 186-200.

Allen AG, Nemitz E, Shi JP, Harrison RM, Greenwood JC. 2001. Size distributions of trace metals in atmospheric aerosols in the United Kingdom, Atmospheric Environment 35, 4581–4591.

Almeida SM, Pio CA, Freitas MC, Reis MA, Trancoso MA. 2005. Source apportionment of fine and coarse particulate matter in a sub-urban area at the Western European Coast. Atmospheric Environment 39, 3127-3138.

Alves C. 2008. Characterisation of Solvent Extractable Organic Constituents in Atmospheric Particulate Matter: an Overview. Anais da Academia Brasileira de Ciências 80, 21–82.

Alves CA, Gomes J, Nunes T, Duarte M, Calvo A, Custódio,D, et al. 2015. Size-segregated particulate matter and gaseous emissions from motor vehicles in a road tunnel. Atmospheric Research 153, 134-144.

Andreae MO. 2001. The Dark Side of Aerosols. Nature 409, 671-672

Arey J, Atkinson R. 2003. Photochemical reactions of PAHs in the atmosphere. In: Douben, P.E.T. (Ed.), PAHs: an Ecotoxicological Perspective. Wiley, Chichester, pp. 47-63.

ARPA (Agenzia Regionale Prevenzione e Ambiente dell'Emilia Romagna). 2005. Caratterizzazione chimico-fisica del particolato atmospherico nelle classi deimensionali tra 10 e 0.4 µm.

ARPAV (Agenzia Regionale per la Protezione Ambientale del Veneto). 2007. Studio pilota sulla caratterizzazione del PM_{10} in provincia di Venezia.

Ashbaugh II, Malm WC, Sadeh WZ. 1985. A residence time probability analysis of sulfur concentrations at Grand Canyon national park. Atmospheric Environment 19 (8), 1263-1270.

Atkinson R, Arey J. 2003. Atmospheric degradation of volatile organic compounds. Chemical Reviews 103, 4605–4638.

ATSDR (Agency for Toxic Substances and Disease Registry). 1995. Toxicological profile for polycyclic aromatic hydrocarbons (PAHs). US Department of Health

and Human Services, Public Health Service. Atlanta, GA. /http://www. atsdr.cdc.gov/toxprofiles/tp69.htmlS.

ATSDR (Agency for Toxic Substances and Disease Registry). 2005. Toxicology profile for polyaromatic hydrocarbons. ATSDR's Toxicological Profiles on CD-ROM, CRC Press, Boca Raton, FL.

Ayrault S, Senhou A, Moskura M, Gaudry A. 2010. Atmospheric trace element concentrations in total suspended particles near Paris, France. Atmospheric Environment 44, 3700‐3707.

Baek SO, Field RA, Goldstone ME, Kirk PW, Lester JN, Perry, R. 1991. A review of atmospheric polycyclic hydrocarbons: Sources, fate and behavior. Water Air & Soil Pollution 60, 279-300.

Bahry PS, Zakaria MP, Abdullah AM, Abdullah DZ, Sakari M, Chandru K, Shahbazi A. 2009. Forensic characterization of polycyclic aromatic hydrocarbons and hopanes in aerosols from peninsular Malaysia. Environmental Forensics 10, 240-252.

Baker J. 2010. A cluster analysis of long range air transport pathways and associated pollutant concentrations within the UK. Atmospheric Environment. 44, 563–571.

Bari MA, Baumbach G, Kuch B, Scheffknecht G. 2010. Particle-phase concentrations of polycyclic aromatic hydrocarbons in ambient air of rural residential areas in southern Germany. Air Quality Atmosphere and Health 3, 103–116.

Baumard P, Budzinski H, Garrigues P, Dizer, H, Hansen PD. 1999. Polycyclic aromatic hydrocarbons in recent sediments and mussels (Mytilus edulis) from Western Baltic Sea: occurrence, bioavailability and seasonal variations. Marine Environmental Research 47, 17–47.

Baumgardner D, Popovicheva O, Allan J, Bernardoni V, Cao J, Cavalli et al. 2012. Soot reference materials for instrument calibration and intercomparisons: a workshop summary with recommendations. Atmospheric Measurement Techniques 5, 1869-1887.

Becagli S, Sferlazzo DM, Pace G, Sarra AD, Bommarito C, Calzolai G, et al. 2012. Evidence for heavy fuel oil combustion aerosols from chemical analyses at the island of Lampedusa: a possible large role of ships emissions in the Mediterranean. Atmospheric Chemistry and Physics 12 (7), 3479-3492.

Begum BA, Biswas SK, Markwitz A, Hopke PK. 2010. Identificaiton of sources of fine and course particulate matter in Dhaka, Bangladesh. Aerosol and Air Quality Research 10, 345-353.

Belis CA, Cancelinha J, Duane M, Forcina V, Pedroni V, Passarella R, et al. 2011. Sources for PM air pollution in the Po Plain, Italy: I. Critical comparison of

methods for estimating biomass burning contributions to benzo(a)pyrene. Atmospheric Environment 45 (39), 7266-7275.

Bengtsson L, Roeckner E, Stendel M. 1999. Why is the global warming proceeding much slower than expected? Journal of Geophysical Research 104, 3865-3876.

Berggren D, Bergkvist B, Falkengrengrerup U, Folkeson L, Tyler G. 1990. Metal Solubility and Pathway in Acidified Forest Ecosystems of South Sweden. Science of the Total Environment 96, 103-114.

Bernstein JA, Alexis N, Barnes C, Bernstein IL, Nel A, Peden D, Diaz-Sanchez D, Tarlo SM, Williams PB. 2004. Health effects of air pollution. Journal of Allergy and Clinical Immunology 114 (5),1116-1123.

Bigi A, Ghermandi G, Harrison RM. 2012. Analysis of the air pollution climate at a background site in the Po valley. Journal of Environmental Monitoring 14, 552-563.

Bilos C, Colombo JC, Skorupka CN, Rodriguez Presa MJ. 2001. Sources, distribution and variability of airborne trace metals in La Plata City area, Argentina. Environmental Pollution 111, 149-158.

Birch ME, Cary RA. 1996. Elemental carbon-based method for monitoring occupational exposures to particulate diesel exhaust. Aerosol Science and Technology 25, 221-241.

Bond, T.C., Bergstrom, R.W., 2006. Light absorption by carbonaceous particles: an investigative review. Aerosol Science and Technology 40, 27-67.

Borbély-Kiss I, Koltay E, Szabó GY, Bozó L, Tar K. 1999.Composition and sources of urban and rural atmospheric aerosol in Eastern Hungary. Journal of Aerosol Science 30, 369–391.

Bosco ML, Varrica D, Dongarra G. 2005. Case study: inorganic pollutants associated with particulate matter from an area near a petrochemical plant. Environmental Research 99, 18-30.

Boström CE, Gerde P, Hanberg A, Jernström B, Johansson C, Kyrklund T. et al. 2002. Cancer risk assessment, indicators, and guidelines for polycyclic aromatic hydrocarbons in the ambient air. Environmental Health Perspectives 110, 451-488.

Bove MC, Brotto P, Cassola F, Cuccia E, Massabo D, Mazzino A, et al. 2014. An integrated $PM_{2.5}$ source apportionment study: Positive Matrix Factorisation vs. the chemical transport model CAMx. Atmospheric Environment 94, 274-186.

Brown AS, Brown RJ. 2012. Correlations in polycyclic aromatic hydrocarbon (PAH) concentrations in UK ambient air and implications for source apportionment. Journal of Environmental Monitoring 14, 2072–2082.

Brunelli A. 2009. Characterization of gaseous and particulate matter ($PM_{2.5}$) in a suburban industrial site in the Venice area. Thesis degree in Environmental Science. Ca Foscari University of Venice.

Cabada J, Pandis SN, Subramanian R, Robinson AL, Polidori A, Turpin B. 2004. Estimating the secondary organic aerosol contribution to $PM_{2.5}$ using the EC tracer method. Aerosol Science and Technology 38, 140–55.

CAFÉ. 2011. CAFE reference documents. Available from: http://ec.europa.eu/environment/archives/cafe/general/keydocs.htm. Accessed 27 Sep 2014.

Callèn M, Lòpez JM, Iturmendi A, Mastral AM. 2013. Nature and sources of particle associated polycyclic aromatic hydrocarbons (PAH) in the atmospheric environment of an urban area. Environmental Pollution 183,166-174.

Calvo AI, Alves C, Castro A, Pont V, Vicente AM, Fraile R. 2013. Research on aerosol sources and chemical composition: Past, currrent and emerging issues. Atmospheric Research 120-121, 1-28.

Campen MJ, Nolan JP, Schladweiler MCJ, Kodavanti UP, Evansky PA, Costa D.L, Watkinson WP. 2001. Cardiovascular and thermoregulatory effects of inhaled PM-associated transition metals: a potential interaction between nickel and vanadium sulfate. Toxicological Sciences 64, 243–252.

Caricchia AM, Chiavarini S, Pezza M. 1999. Polycyclic aromatic hydrocarbons in the urban atmospheric particulate matter in the city of Naples (Italy). Atmospheric Environment 33, 3731–3738.

Carslaw DC, Beevers SD, Bel MC. 2007. Risks of exceeding the hourly EU limit value for nitrogen dioxide resulting from increased road transport emissions of primary nitrogen dioxide. Atmospheric Environment 41, 2073-2082.

Carslaw DC. 2014. The openair manual — open-source tools for analysing air pollution data. Version 10th June 2014, King's College London.

Castro LM, Pio CA. Harrison RM, Smith DJT. 1999. Carbonaceous aerosol in urban and rural European atmospheres: estimation of secondary organic carbon concentrations. Atmospheric Enviornment 33, 2771–81.

Chan YC, Simpson RW, Mctainsh GH, Vowles PD, Cohen DD, Bailey GM. 1999. Source Apportionment of Visibility Degradation Problems in Brisbane (Australia) Using the Multiple Linear Regression Techniques. Atmospheric Environment 33, 3237-3250.

Cheng J, Yuan T, Wu O, Zhao W, Xie H, Ma Y, et al. 2007. PM_{10}-bound polycyclic aromatic hydrocarbons (PAHs) and cancer risk estimation in the atmosphere surrounding an industrial area of Shanghai, China. Water Air & Soil Pollution 183, 437–446.

Cheng Y, Lee SC, Ho KF, Chow JC, Watson JG, Louie PKK, et al. 2010. Chemically-speciated on-road PM2.5motor vehicle emission factors in HongKong. Science of the Total Environment 408, 1621–1627.

Chetwittayachan T, Shimazaki D, Yamamoto K. 2002. A comparison of temporal variation of particle-bound polycyclic aromatic hydrocarbons (pPAHs) concentration in different urban environments: Tokyo, Japan, and Bangkok, Thailand. Atmospheric Environment 36, 2027–2037.

Choi J, Heo J, Ban S, Yi S, Zoh K, 2013. Source apportionment of $PM_{2.5}$ at the coastal area in Korea. Science of the Total Environment 447, 370-380.

Colbeck I, Lazaridis M. 2010. Aerosols and Environmental pollution. Naturwissenschaften 97, 117–131.

Cox A. 1989. The Elements : Their Origin, Abundance, and Distribution. Oxford University Press, UK.

Crosier J, Allan JD, Coe H, Bower KN, Formenti P, Williams PI. 2007. Chemical composition of summertime aerosol in the Po Valley (Italy), northern Adriatic and Black Sea. Quarterly Journal of the Royal Meteorological Society 133, 61–75.

Cuccia E, Massaò D, Ariola V, Bove MC, Fermo P, Piazzalunga A, Prati P. 2013. Size-resolved comprehensive characterization of airborne particulate matter. Atmospheric Environment 67, 14-26.

Čupr P, Flegrová Z, Franců J, Landlová L, Klánov, J. 2013. Mineralogical, chemical and toxicological characterization of urban air particles. Environmental International 54, 26–34.

Ćwiklak K, Pastuszka JS, Rogula-Kozłowska R. 2009. Influence of traffic on particulate-matter polycyclic aromatic hydrocarbons in urban atmosphere of Zabrze, Poland. Polish Journal of Environmental Studies 18, 579–585.

Dan M, Zhuang G, Li X, Tao H, Zhuang Y. 2004. The characteristics of carbonaceous species and their sources in $PM_{2.5}$ in Beijing. Atmospheric Environment 38(21), 3443–3452.

de la Campa AS, Pio C, de La Rosa JD, Querol X, Alastuey A, González-Castanedo Y. 2009. Characterization and origin of EC and OC particulate matter near the Doñana National Park (SW Spain). Environmental Research 109(6), 671-681.

Delhomme O, Millet M. 2012. Characterization of particulate polycyclic aromatic hydrocarbons in the east of France urban areas. Environmental Science and Pollution Research 19, 1791-1799.

Devries W, Bakker DJ. 1996. Manual f(Agency for Toxic Substances and Disease Registry). or Calculating Critical Loads of Heavy Metals for Soils and Surface

Waters. Report 114, DLO, Winland Staring Center, Wageningen, The Netherlands.

Di Giuseppe F, Riccio A, Caporaso L, Bonafe G, Gobbi GP, Angelini F. 2012. Automatic detection of atmospheric boundary layer height using ceilometers backscatter data assisted by a boundary layer model. Q J R. Meteorol Soc 138, 649-663.

Dockery DW, Pope CA, Xu XP, Spengler JD, Ware JH, Fay ME, Ferris BG, Speizer FE. 1993. An association between air-pollution and mortality in six US cities. The New England Journal of Medicine 329, 1753-1759.

Dockery DW, Pope, CA. 1994. Acute Respiratory Effects of Particulate Air Pollution. Annual Review of Public Health 15, 107-132.

Donaldson K, Brown DM, Mitchell C, Dineva M, Beswick PH, Gilmour P, MacNee W. 1997. Free radical activity of PM_{10}. Iron-mediated generation of hydroxyl radicals. Environmental Health Perspective 105, 1285–1290.

Donaldson K, Tran CL, MacNee W. 2002. Deposition and effects of fine and ultrafine particles in the respiratory tract. European Respiratory Monograph 21, 77–92.

Draxler RR, Rolph G.D. 2013. HYSPLIT (HYbrid Single-Particle Lagrangian Integrated Trajectory) Model access via NOAA ARL READY Website (http://www.arl.noaa.gov/HYSPLIT.php). NOAA Air Resources Laboratory, College Park, MD.

Draxler RR, Rolph GD, 2011. HYSPLIT (Hybrid Single–Particle Lagrangian Integrated Trajectory) Model, http://ready.arl.noaa.gov/HYSPLIT.php, accessed in February 2013.

Du YR, Gao B, Zhou HD, Ju XX, Hao H, Yin SH. 2013. Health risk assessment of heavy metals in road dusts in urban parks of Beijing, China. Procedia Environmental Science. 18, 299–309.

Duan F, He K, Ma Y, Jia Y, Yang F, Lei Y, et al. 2005. Characteristics of carbonaceous aerosols in Beijing, China. Chemosphere 60, 355–364.

Duan JC, Tan JH, Wang SL, Hao JM, Chai FH, 2012. Size distributions and sources of elements in particulate matter at curbside, urban and rural sites in Beijing. Journal of Environmental Science 24, 87-94.

Duce RA, Mohnen VA. 1983. Organic material in the global troposphere. Reviews of Geophysics 21, 921-952.

Durant J, Busby W, Lafleur A, Penman B, Crespi C. 1996. Human cell mutagenicity of oxygenated, nitrated and unsubstituted polycyclic aromatic hydrocarbons associated with urban aerosols. Mutation Research/Genetic Toxicology 371, 123-157.

EC (European Commission), 2008. Directive 2008/50/EC of the European Parliament and of the Council of 21 May 2008 on ambient air quality and cleaner air for Europe (OJ L 152, 11.6.2008, p. 1–44) (http://eur-lex.europa. eu/LexUriServ/LexUriServ.do?uri=OJ:L:2008:152:000   1:0044:EN:PDF) accessed 14 May 2013.

EC (European Commission). 2001. Polycyclic Aromatic Hydrocarbons (PAH) Position Paper (July 2001) (Prepared by the Working Group on Polycyclic Aromatic Hydrocarbons).

EC (European Commission). 2004. Directive 2004/107/EC of the European Parliament and of the Council of 15 December 2004 relating to arsenic, cadmium, mercury, nickel and polycyclic aromatic hydrocarbons in ambient air.

EEA (European Environmental Agency). 2013b. L'aria che respiriamo. Migliorare la qualità dell'aria in Europa.

EEA (European Environmental Agency). 2013a. Status of black carbon monitoring in ambient air in Europe. EEA Technical report, No 18/2013. eea.europa.eu. Denmark.

Elbayoumi M, Ramli NA, Yusuf NFFM, Madhoun WA. 2013. Spatial and seasonal variation of particulate matter (PM_{10} and $PM_{2.5}$) in Middle Eastern classrooms. Atmospheric Environment 80, 389-397.

Esteve W, Budzinski H, Villenave E. 2006. Relative rate constants for the heterogeneous reactions of NO_2 and OH radicals with polycyclic aromatic hydrocarbons adsorbed on carbonaceous particles. Part 2: PAHs adsorbed on diesel particulate exhaust SRM 1650a. Atmospheric Environment 40, 201-211.

Evagelopoulos V, Albanis TA, El K, Zoras S. 2010. Particle-associated polycyclic aromatic hydrocarbons near power plants as determined by large volume injection—GC/MS. Chemosphere 80:235–240.

Fang GC, Chang KF, Lu C, Bai H. 2002. Toxic equivalency factors study of polycyclic aromatic hydrocarbons (PAHs) in Taichung City, Taiwan. Toxicology and Industrial Health 18, 279-288.

Farao C. 2014. Development of analytical methodologies for the monitoring of the atmospheric particulate matter. La Sapienza University in Rome.

Ferreira-Baptista L, Miguel ED. 2005. Geochemistry and risk assessment of street dust in Luanda, Angola: a tropical urban environment. Atmospheric Environment 39, 4501–4512.

Ferrero L, Perrone MG, Petraccone S, Sangiorgi G, Ferrini BS, Lo Porto C, et al. 2010. Vertically resolved particle size distribution within and above the mixing layer over the Milan metropolitan area. Atmospheric Chemistry and Physics 10, 3915–3932.

Fertmann F, Tesseraux I, Schümann M, Neus H. 2002. Evaluation of ambient air concentrations of polycyclic aromatic hydrocarbons in Germany from 1990 to 1998. Journal of Exposure Analysis and Environmental Epidemiology 12, 115-123.

Fujii T, Hayashi S, Hogg JC, Mukae H, Suwa T, Goto Y, Vincent R, Eden SF. 2002. Interaction of alveolar macrophages and airway epithelial cells following exposures to particulate matter produces mediator that stimulate the bone marrow. American journal of respiratory cell and molecular biology 27, 34-41.

Galarneau E. 2008. Source specificity and atmospheric processing of airborne PAHs: implications for source apportionment. Atmospheric Environment 42, 8139-8149.

Gao J, Tian H, Cheng Ke, Lu L, Wang Y, Wu Y, et al. 2014. Seasonal and spatial variation of trace elements in multi-size airborne particulate matters of Beijing, China: Mass concentration, enrichment characteristics, source apportionment, chemical speciation and bioavailability. Atmospheric Environment 99, 257-265.

Gao Y, Nelson ED, Field MP, Ding Q, Li H, Sherrell RM, et al. 2002. Characterization of atmospheric trace elements on PM2.5 particulate matter over the NewYork–New Jersey harbor estuary. Atmospheric Environment 36, 1077–1086.

Garçon G, Dagher Z, Zerimech F, Ledoux F, Courcot D, Aboukais A, Puskaric E, Shirali P. 2006. Dunkerque City air pollution particulate matter-induced cytotoxicity, oxidative stress and inflammation in human epithelial lung cells (L132) in culture. Toxicology in Vitro 20, 519–528.

Gelencsér A. 2004. Carbonaceous aerosols. Springer, Netherlands, pp. 350.

Geng N, Wang J, Xu Y, Zhang W., Chen C, Zhang R, 2.013. PM$_{2.5}$ in an industrial district of Zhengzhou, China: Chemical composition and source apportionment. Particuology 11, 99-109.

Giannoni M, Martellini T, Bubba MD, Gambaro A, Zangrando R, Chiari M., et al. 2012. The use of levoglucosan for tracing biomass burning in PM2.5 samples in Tuscany (Italy). Environmental Pollution 167, 7-15.

Gilardoni S, Vignati E, Cavalli F, Putaud JP, Larsen BR, Karl M, et al. 2011. Better constraints on sources of carbonaceous aerosols using a combined C-14-macro tracer analysis in a European rural background site. Atmospheric Chemistry and Physics 11, 5685-5700.

Garcia VC, Gego E, Lin S, Pantea C, Rappazzo K, Wootten A, Rao ST. 2011. An evaluation of transported pollution and respiratory– related hospital admissions in the state of New York. Atmospheric Pollution Research 2, 9-15.

Grimmer G, Jacob J, Naujack KW. 1983. Profile of the polycyclic aromatic compounds from crude oils—inventory by GC GC-MS. PAH in environmental materials, part 3. Fresenius Journal for Analytical Chemistry 316, 29–36.

Grivas G, Chaloulakou A, Samara C, Spyrellis N. 2004. Spatial and temporal variation of PM_{10} mass concentrations within the greater area of Athens, Greece. Water, Air, and Soil Pollution 158, 357–371.

Gu ZL, Qiu J, Zhao YZ, Hou XP. 2008. Analysis on Dust Devil Containing Loess Dusts of Different Sizes. Aerosol and Air Quality Research 8, 65-77.

Guo H, Lee SC, Ho KF, Wang XM, Zou SC. 2003. Particle-associated polycyclic aromatic hydrocarbons in urban air of Hong Kong. Atmospheric Environment 37, 5307–5317.

Gupta AK, Karar K, Srivastava A. 2007. Chemical mass balance source apportionment of PM10 and TSP in residential and industrial sites of an urban region of Kolkata, India. Journal of Hazardous Materials 142, 279 – 287.

Halasinski TM, Salama F, Allamandola LJ. 2005. Investigation of the ultraviolet, visible, and near-infrared absorption spectra of hydrogenated polycyclic aromatic hydrocarbons and their cations. Astrophysical Journal 628, 555–566.

Hamed A, Joutsensaari J, Mikkonen S, Sogacheva L, Dal Maso M, Kulmala M, et al. 2007. Nucleation and growth of new particles in Po Valley, Italy.

Hamilton RS, Mansfield TA. 1991. Airborne particulate elemental carbon, its sources, transport, contribution to dark smoke and soiling, Atmospheric Environment, 25A, 715-723.

Hao YC, Guo ZG, Yang ZS, Fang M, Feng JL. 2007. Seasonal variations and sources of various elements in the atmospheric aerosols in Qingdao, China. Atmospheric Research 85, 27 – 37.

Harrison RM, Yin J. 2008. Sources and processes affecting carbonaceous aerosol in central England. Atmospheric Environment 42(7), 1413–1423.

Harrison RM, Yin J. 2010. Chemical speciation of $PM_{2.5}$ particles at urban background and rural sites in the UK atmosphere. Journal of Environmental Monitoring 12, 1404-1414.

Harrison RM., Yin J. 2000. Particulate matter in the atmosphere: which particle properties are important for its effects on health? The Science of the Total Environment 249, 85-101.

Hauck H, Berner A, Frische,r T, Gomiscek B, Kundi M, Neuberger M, Puxbaum H, Preining O, and AUPHEP-Team. 2004. AUPHEP-Austrian project on health effects of particulates – general overview, Atmospheric Environment 38, 3905-3915.

155

He J, Fan S, Meng O, Sun Y, Zhang J, Zu F. 2014. Polycyclic aromatic hydrocarbons (PAHs) associated with fine particulate matters in Nanjing, China: Distributions, sources and meteorological influences. Atmospheric Environment 89, 207-215.

Hellén H, Hakola S, Haaparanta S, Pietarila H, Kauhaniem, M. 2008. Influence of residential wood combustion on local air quality. Science of the Total Environment 393, 283-290.

Hester RE, Harrison RM. 2009. Air quality in urban environment. Royal Society of Chemistry: Cambrige, UK.

Hildemann LM, Markowski GR, Cass GR. 1991. Chemical composition of emissions from urban sources of fine organic aerosol. Environmental Science and Technology 25, 744–759.

Hitzenberger R, Jennings SG, Larson SM, Dillner A, Cachier H, Galambos Z, et al. 1999. Intercomparison of measurement methods for black carbon aerosols. Atmospheric Environment 33, 2823–2833.

Hitzenberger R, Jennings SG, Larson SM, Dillner A, Cachier H, Galambos Z, Rouc A, Spain, TG. 1999. Intercomparison of measurement methods for black carbon aerosols. Atmospheric Environment 33, 2823–2833.

Hu X, Zhang Y, Ding Z, Wang T, Lian H, Sun Y et al. 2012. Bioaccessibility and health risk of arsenic and heavy metals (Cd, Co, Cr, Cu, Ni, Pb, Zn and Mn) in TSP and PM2.5 in Nanjing, China. Atmospheric Environment 57, 146–152.

Hu Y, Bai Z, Zhang L, Wang X, Zhang L, Yu Q, and Zhu T. 2007. Health risk assessment for traffic policemen exposed to polycyclic aromatic hydrocarbons (PAHs) in Tianjin, China. Science of the Total Environment 382, 240-250.

Huang W, Cao J, Tao Y, Dai L, Lu S E, Hou B et al. 2012. Seasonal variation of chemical species associated with Short-Term mortality effects of PM2.5 in Xi'an, a central city in China. American Journal of Epidemiology 175(6), 556–566.

Hudson G J, Da X. 1996. Volatility and size of cloud condensation nuclei. Journal of Geophysical Research 101, 4435−4442.

Hussein, T., Puustinen, A., Aalto, P.P., Makela, J.M., Hameri, K., Kulmala, M., 2004. Urban aerosol number size distributions. *Atmospheric Chemistry and Physics* 4, 391-411.

ICAO. 2005. International Civil Aviation Organization. Information Paper CAEP-SG/20082-IP/05.

Iijima A, Sato K, Fujitani Y, Fujimori E, Saito , Tanabe K, et al. 2009. Clarification of the predominant emission sources of antimony in airborne particulate matter

and estimation of their effects on the atmosphere in Japan. Environmental Chemistry 6, 122-132.

IPCC. 2001. Climate Change 2001: The Scientific Basis. Contribution of Working Group I to the Third Assessment Report of the Intergovernmental Panel on Climate Change [Houghton, J.T., Y. Ding, D.J. Griggs, M. Noguer, P.J. van der Linden, X. Dai, K. Maskell, and C.A. Johnson (eds.)]. Cambridge University Press, Cambridge, United Kingdom and New York, NY, USA, 881pp.

IPCC. 2007. Climate Change 2007. The physical science basic. Contribution of working group I to the fourth assessment report of the Intergovernmetnal Panel on Climate Change, Solomon, S., Qin, D., Manning, M., Chen, Z., Marquis, M., Averyt, K.B., Tignor, M., and Miller, H.L. (Eds.), Cambrige, United Kingdom and New York, USA, 996, pages.

Ito K, Mathes R, Ross Z, Nadas A, Thurston G, Matte T. 2011. Fine particulate matter constituents associated with cardiovascular hospitalizations and mortality in New York City. Environmental Health Perspectives 119, 467–73.

Jacobson MC, Hansson HC; Noone KJ. Charlson RJ. 2000. Organic atmospheric aerosols: Review and state of the science. Reviews of Geophysics 38(2), 267-294.

Jaenicke R. 2005. 8 Global aerosols, In: Landolt-Bornstein, Numerical Data and Functional Relationships in Science and Technology, Group V: Geophysics, Volume 6, Observed Global Climate, Hantel M. (Ed.), Springer, Berlin, pp. 81-89.

Japer SM, Bracaczec WW, Jr Gorsea RA, Norbeck JM, Pierson WR. 1986. The concentration of elemental carbon to the optical properties of rural atmospheric aerosols. Atmospheric Environment 20, 1281-1289.

Jedynska A, Hoek G, Eeften, M, Cyrys J, Keuken M, Ampe C, et al. 2014. Spatial variations of PAH, hopanes/steranes and EC/OC concentrations within and between European study areas. Atmospheric Environment 87, 239-248.

Kameda Y, Shirai J, Komai T, Nakanishi J, Masunaga S. 2005. Atmospheric polycyclic aromatic hydrocarbons: size distribution, estimation of their risk and their depositions to human respiratory tract. Science of the Total Environment. 340, 71–80.

Kanakidou M, Tsigaridis K, Dentener FJ, Crutzen PJ. 2000. Human-activity-enhanced formation of organic aerosols by biogenic hydrocarbon oxidation. Journal of Geophysical Research: Atmospheres 105(D7), 9243-9254.

Karanasiou AA, Sitaras IE, Siskos PA, Eleftheriadis K. 2007. Size Distribution and Sources of Trace Metals and n-alkanes in the Athens Urban Aerosol During Summer. Atmospheric Environment 41, 2368-2381.

Karthikeyan S, Joshi UM, Balasubramanian R 2006. Microwave assisted sample preparation for determining water-soluble fraction of trace elements in urban airborne particulate matter: evaluation of bioavailability. Analytica Chimica Acta 576, 23-30.

Katsouyanni K, Touloumi G, Samoli E, Gryparis A, Le Tertre A, Monopolis Y, et al. 2001. Confounding and effect modification in the short-term effects of ambient particles on total mortality: results from 29 European cities within the APHEA2 project. Epidemiology 12(5), 521-531.

Kaufman Y, Tanre D, Boucher O. 2002. A satellite view of aerosols in the climate system, Nature, 419, 215-223.

Kavouras IG, Koutrakis P, Tsapakis M, Lagoudaki E, Stephanou EG, Von Baer D, Oyola P. 2001. Source apportionment of urban particulate aliphatic and polynuclear aromatic hydrocarbons (PAHs) using multivariate methods. Environmental Science and Technology 35, 2288–2294.

Khalili NR, Scheff PA, Holsen TM. 1995. PAH source fingerprints for coke ovens, diesel and gasoline engines, highway tunnels, and wood combustion emissions. Atmospheric Environment 29, 533–542.

Khan MF, Latif MT, Lim CH, Amil N, Jaafar SA, Dominick D, et al. 2015. Seasonal effect and source apportionment of polycyclic aromatic hydrocarbons in $PM_{2.5}$. Atmospheric Environment 106, 178-190.

Kim BM, Teffera S, Zeldin MD. 2000. Characterization of $PM_{2.5}$ and PM_{10} in the south coast air basin of Southern California: Part 1—spatial variations. Journal of the Air and Waste Management Association 50, 2034–2044.

Kim E, Hopke PK, Edgerton ES. 2003. Source identification of Atlanta aerosol by positive matrix factorization. Journal of the Air & Waste Management Association 53, 731-739.

Kim E, Hopke PK, Kenski DM, Koerber M. 2005. Sources of fine particles in a rural Midwestern U.S. area. Environmental Science & Technology 39, 4953-4960.

Kitazawa A, Amagai T, Ohura T. 2006. Temporal trends and relationships of particulate chlorinated polycyclic aromatic hydrocarbons and their parent compounds in urban air. Environmental Science & Technology 40, 4592–4598.

Koelemeijer RBA, Homan CD, Matthijsen J. 2006. Comparison of spatial and temporal variations of aerosol optical thickness and particulate matter over Europe. Atmospheric Environment 40, 5304–5315.

Kurt-Karakus PB. 2012. Determination of heavy metals in indoor dust from Istanbul, Turkey: estimation of the health risk. Environmental International 50, 47–55.

Larsen BR, Gilardoni S, Ktenstrom K, Niedzialek, J, Jimenez J, Belis CA. 2012. Sources for PM air pollution in the Po Plain, Italy: II. Probabilistic uncertainty characterization and sensitivity analysis of secondary and primary sources. Atmospheric Environment 50, 203-213.

Lee DS, Garland JA, Fox AA. 1994. Atmospheric concentrations of trace elements in urban areas of the United Kingdom. 1994. Atmospheric Environment 28, 2691-2713. 2015.

Lee SW, Lee BT, Kim JY, Kim KW, Lee JS. 2006. Human risk assessment for heavy metals and as contamination in the abandoned metal mine areas, Korea. Environmental Monitoring and Assessment 119, 233–244.

Lewan MD. 1984. Factors controlling the proportionality of vanadium to nickel in crude oils. Geochim. Cosmochim. Acta 48 (11), 2231-2238.

Li P, Han B, Huo J, Lu B, Ding X, Chen L, et al. 2012. Characterization, meteorological influences and source identification of carbonaceous aerosols during the autumn-winter period in Tianjin, China. Aerosol and Air Quality Research 12, 283-294.

Li Z, Porter EN, Sjodin A, Leedham LL, Lee S, Russell AG, Mulholland JA. 2009. Characterization of $PM_{2.5}$-bound polycyclic aromatic hydrocarbons in AtlantadSeasonal variations at urban, suburban, and rural ambient air monitoring sites. Atmospheric Environment 43, 4187-4193.

Lim H, Turpin B. 2002. Origins of primary and secondary organic aerosol in Atlanta: results of time-resolved measurements during the Atlanta Supersite experiment. Environmental Science and Technology 36, 4489–4496.

Lima ALC, Farrington JW, Reddy CM. 2005. Combustion- derived polycyclic aromatic hydrocarbons in the environment— a review. Environmental Forensics 6, 109–131.

Liu X, Zhai Y, Zhu Y, Liu Y, Chen H, Li P, et al. 2015. Mass concentration and health risk assessment of heavy metals in size-segregated airborne particulate matter in Changsha. Science of the Total Environment 517, 215-221.

Lonati G, Giuglian M, Butelli P, Romele L, Tardivo R. 2005. Major chemical components of $PM_{2.5}$ in Milan (Italy). Atmospheric Environment 39, 1925–1934.

Lonati G, Ozgen S, Giugliano M. 2007. Primary and secondary carbonaceous species in $PM_{2.5}$ samples in Milan (Italy). Atmospheric Environment 41 (22), 4599–4610.

Lyamani H, Olmo FJ, Alcàntara A, Alados-Arboledas L. 2006. Atmospheric aerosols during the 2003 heat wave in southeastern Spain II: microphysical columnar properties and radiative forcing. Atmospheric Environment 40, 6465–6476.

Maenhaut W, Francois F, Cafmeyer J, Okunade O. 1996. Size-fractionated aerosol composition at Gent, Belgium. Results from one-year study, Nuclear Instruments and Methods in Physics Research, B109/110, 476-481.

Malaguti A, Mircea M, Torretta TMGL, Piersanti A, Salvi S, Zanini G, et al. 2013. Fine carbonaceous aerosol characteristics at a coastal rural site in the Central Mediterranean as given by OCEC online measurement. Journal of Aerosol Sciences 56, 78-87.

Malm WC. 2000. Introduction to Visibility. Cooperative Institute for Research in the Atmosphere (CIRA), Ft. Collins, Colorado.

Manahan SE. 1993. Fundamentals of environmental chemistry. six edition, Lewis publishers, Michigan, USA. pp 844.

Manahan SE. 1994. Environmental Chemistry. sixth ed. Lewis Publisher, New York.

Manahan SE. 2009. Environmental Chemistry, ninth ed. CRC Press, New York.

Marino F, Cecinato A, Siskos PA. 2000. Nitro-PAH in ambient particulate matter in the atmosphere of Athens. Chemosphere 40, 533–537.

Markatou M, Basu A, Lindsay BG. 1998. Weighted likelihood estimating equations with a bootstrap root search. Journal of the American Statistical Association 93, 740-750.

Martellini T, Giannoni M, Lepri L, Katsoyiannis A, Cincinelli A. 2012. One year intensive PM2.5 bound polycyclic aromatic hydrocarbons monitoring in the area of Tuscany, Italy. Concentrations, source understanding and implications. Environmental Pollution 164, 252-258.

Masiol M, Agostinelli C, Formenton G, Tarabotti E, Pavoni B. 2014. Thirteen years of air pollution hourly monitoring in a large city: Potential sources, trends, cycles and effects of car-free days. Science of the Total Environment 494–495, 84–96.

Masiol M, Centanni E, Squizzato S, Hofer A, Pecorari E, Rampazzo G, Pavoni B. 2012b. GC-MS analyses and chemometric processing to discriminate the local and long-distance sources of PAHs associated to atmospheric PM2.5. Environmental Science and Pollution Research 19 (8), 3142-3151.

Masiol M, Formenton G, Pasqualetto A, Pavoni B. 2013. Seasonal trends and spatial variations of PM_{10}-bounded polycyclic aromatic hydrocarbons in Veneto region, Northeast Italy. Atmospheric Environment 79, 811-821.

Masiol M, Hofer A, Squizzato S, Piazza R, Rampazzo G, Pavoni B. 2012c. Carcinogenic and mutagenic risk associated to airborne particle-phase polycyclic aromatic hydrocarbons: A source apportionment. Atmospheric Environment 60, 375–382.

Masiol M, Rampazzo G, Ceccato D, Squizzato S, Pavoni B. 2010. Characterization of PM_{10} sources in a coastal area near Venice (Italy): An application of factor-cluster analysis. Chemosphere 80, 771–778.

Masiol M, Squizzato S, Ceccato D, Rampazzo G, Pavoni B. 2012a. A chemometric approach to determine local and regional sources of PM_{10} and its geochemical composition in a coastal area. Atmospheric Environment 54, 127–133.

Mastral AM, Lopez, JM, Callen, MS, García T, Murillo R, Navarro MV. 2003. Spatial and temporal PAH concentrations in Zaragoza, Spain. Science of the Total Environment 307, 111-124.

Mather TA, Pyle DM, Oppenheimer C. 2003. Tropospheric volcanic aerosol, Volcanism and the Earth's Atmosphere, Geophysical Monograph 139, 189-212.

Matthias-Maser S, Bogs B, Jaenicke R. 2000. The size distribution of primary biological aerosol particles in cloud water on the mountain Kleiner Feldberg/Taunus (FRG). Atmospheric Research 54:1-13.

Mauderly JL, and Chow JC. 2008, 'Health effects of organic aerosols', *Inhalation Toxicology* (20) 257– 288. Borbély-Kiss I, Koltay E, Szabó GY, Bozó L, Tar K (1999): Composition and sources of urban and rural atmospheric aerosol in Eastern Hungary. Journal of Aerosol Science 30, 369–391.

Ministry of the Environment. 2013. Ministry of the Environment, Land and Sea. Available at: http://www.minambiente.it.

Mitra AP, Morawska L, Sharma C, Zhang J. 2002. Chapter two: methodologies for characterization of combustion sources and for quantification of their emissions. Chemosphere 49, 903-922.

Mohapatra KD, Biswal SK. 2014. Effect of particulate matter (PM) on plants, climate and ecosystem and human health. International Journal of Advanced Technology in Engineering and Science 2(4), 118-129.

Molinaroli E, Masiol M. 2006. Particolato atmosferico e ambiente mediterraneo. Il caso delle polveri sahariane [Atmopheric particulate matter and the Mediterranean environment. The Saharan dust case of study]. Aracne Editrice, Rome, Italy, pp. 224. [Book, in Italian].

Moreno T, Alastuey A, Querol X, Font O, Gibbons W. 2007. The identification of metallic elements in airborne particulate matter derived from fossil fuels at Puertollano, Spain. International Journal of Coal Geology 71, 122-128.

Moreno T, Querol X, Alastuey A, de la Rosa J, Sanchez de la Campa AM, Minguillon M, et al. 2010. Variations in vanadium, nickel and lanthanoid element concentrations in urban air. Science of the Total Environment 408 (20), 4569-4579.

Na K, Sawan, AA, Song C, Cocker DR. 2004. Primary and secondary carbonaceous species in the atmosphere of Western Riverside County, California. Atmospheric Environment 38 (9), 1345–1355.

NARSTO. 2004. Particulate Matter Science for Policy Makers: A NARSTO Assessment. P. McMurry, M. Shepherd and J. Vickery, eds. Cambridge University Press, Cambridge, England.

Neff JM. 1979. Polycyclic Aromatic Hydrocarbons in the Aquatic Environment. Sources, Fates and Biological Effects. Applied Science Publication, London, pp. 1–262.

Nisbet C, LaGoy P. 1992. Toxic equivalency factors (TEFs) for polycyclic aromatic hydrocarbons (PAHs). Regulatory Toxicology and Pharmacology 16, 290-300.

Novakov T, Corrigan CE, Penner JE, Chuang CC, Rosario O, Mayol-Bracero O. 1997. Organic aerosols in the Caribbean trade winds: A natural source? Journal of Geophysical Research, 102, 21307-21313.

NTP (National Toxicology Program). 2005. Report on Carcinogens, eleventh ed. Public Health Service, US Department of Health and Human Services, Washington, DC.

Oberdörster G. 2000. Toxicology of Ultrafine Particles: In Vivo Studies. Philosophical Transaction of the Royal Society A 358, 2719-2740.

Odum JR, Jungkamp TPW, Griffin RJ, Flagan RC. Seinfeld J.H. 1997. The atmospheric aerosol-forming potential of whole gasoline vapor. Science 276(5309), 96-99.

Omar NYMJ, Mon TC, Rahman NA, Abas MRB. 2006. Distributions and health risks of polycyclic aromatic hydrocarbons (PAHs) in atmospheric aerosols of Kuala Lumpur, Malaysia. Science of the Total Environment 369, 76-81.

PAHs position paper. 2001. Ambient air pollution by polycyclic aromatic hydrocarbons (PAH). Office for Official Publications of the European Communities, Luxembourg.

Pakkanen TA, Loukkola K, Korhonen CH, Aurela M, Makela T, Hillamo RE, Aarnio P, Koskentalo T, Kousa A, Maenhaut W. 2001. Sources and chemical composition of atmospheric fine and coarse particles in the Helsinki area. Atmospheric Environment 35, 5381-5391.

Pandey PK, Patel KS, Lenicek J. 1999. Polycyclic aromatic hydrocarbons: need for assessment of health risks in India? Study of an urban-industrial location in India. Environmental Monitoring and Assessment 59, 287–319.

Pandis SN, Harley RH, Cass GR, Seinfeld JH. 1992. Secondary organic aerosol formation and transport. Atmospheric Environment 26A, 2269-2282.

Pankow JF, 1994a. An absorption-model of gas-particle partitioning of organic-compounds in the Atmosphere. Atmospheric Environment 28, 185-188.

Pankow JF. 1987. Review and comparative analysis of the theories of partitioning between the gas and aerosol particulate phases in the atmosphere. Atmospheric Environment 21, 2275-2283.

Pankow JF. 1994b. An absorption-model of the gas aerosol partitioning involved in the formation of secondary organic aerosol. Atmospheric Environment 28, 189-193.

Park SS, Kim YJ, Kang C.H. 2002. Atmospheric polycyclic aromatic hydrocarbons in Seoul, Korea. Atmospheric Environment 36, 2917–2924.

Penner JE, Eddleman H, Novakov T. 1993. Towards the Development of a Global Inventory for Black Carbon Emissions. Atmospheric Environment 27A, 1277-1295.

Perrone MR, Piazzalunga A, Prato M, Carofalo I. 2011. Composition of fine and coarse particles in a coastal site of the central Mediterranean: Carbonaceous species contributions. Atmospheric Environment 45, 7470-7477.

Petaloti C. Triantafyllou A, Kouimtzis T, Samara C. 2002. Trace elements in atmospheric particulate matter over a coal burning power production area of western Macedonia, Greece. Chemosphere 65, 2233-2243.

Peters A, Wichmann HE, Tuch T, Heinrich J, Heyder J. 1997. Respiratory Effects are Associated with the Number of Ultrafine Particles. American Journal of Respiratory and Critical Care Medicine 155, 1376-1383.

Pindado O, Perez R, Garcia S, Sanchez M, Galan P, Fernandez M. 2009. Characterization and Sources Assignation of PM2.5 Organic Aerosol in a Rural Area of Spain. Atmospheric Environment 43, 2796–2803.

Pirovano G, Colombi C, Balzarini A, Riva GM, Gianelle V, Lonati, G. 2015. PM2. 5 source apportionment in Lombardy (Italy): Comparison of receptor and chemistry-transport modelling results. Atmospheric Environment 106, 56-70.

Pope CA, Burnett RT, Thun MJ. Calle EE, Krewski D, Ito K, Thruston GD. 2002. "Lung Cancer, Cardiopulmonary Mortality, and Long-Term Exposure to Fine Particulate Air Pollution." Journal of the American Medical Association 287(9): 1132-1141.

Pope CA, Burnett RT, Thurston GD, Thun MJ, Calle EE, Krewski D, Godleski JJ. 2004. Cardiovascular mortality and long-term exposure to particulate air pollution: epidemiological evidence of general pathophysiological pathways of disease. Circulation 109(1), 71-77.

Pope CA, Dockery DW. 2006. Health effects of fine particulate air pollution: lines that connect. Journal of the Air and Waste Management Association 56(6), 709–742.

Pope CA, Thun MJ, Namboodiri MM, Dockery DW, Evans JS, Speizer FE, Heath CW. 1995. "Particulate Air Pollution as a Predictor of Mortality in a Prospective Study of U.S. Adults." American Journal of Respiratory and Critical Care Medicine 151: 669-674.

Poschl U. 2002. Formation and decomposition of hazardous chemical components contained in atmospheric aerosol particles, Journal of Aerosol Medicine, 15, 203-212.

Poschl U. 2005. Atmospheric aerosols: Composition, transformation, climate and health effects. Angewandte Chemie, International, Edition 44, 7520-7540.

Putaud JP, Raes F, van Dingenen R, Bruggemann E, Facchini MC, Decesari S, et al., 2004. A European aerosol phenomenology — 2: Chemical characteristics of particulate matter at kerbside, urban, rural and background sites in Europe. Atmospheric Environment 38, 2579–95.

Putaud JP, Van Dingenen R, Alastuey, Bauer H, Birmili W, Cyrys J, et al. 2010. A European aerosol phenomenology – 3: Physical and chemical characteristics of particulate matter from 60 rural, urban, and kerbside sites across Europe. Atmospheric Environment 44, 1308–1320.

Puxbaum H, Caseiro A, Sánchez-Ochoa A, Kasper-Giebl A, Claeys M,Gelencser A, et al. 2007. Levoglucosan levels at background sites in Europe for assessing the impact of biomass combustion on the European aerosol background. Journal of Geophysical Research 112. doi:10.1029/2006JD008114.

Raes F, Van Dingenen R, Vignati E, Wilson J, Putaud JP, Seinfeld JH Adams P. 2000. Formation and cycling of aerosols in the global troposphere, Atmospheric Environment, 34, 4215-4240.

Rajsic S, Mijic Z, Tasic M, Radenkovic M, and Joksic J. 2008. Evaluation of the levels and sources of trace elements in urban particular matter. Environmental Chemistry Letters 6, 95-100.

Ramanathan V, Crutzen PJ, Kiehl JT, Rosenfeld D. 2001 Aerosols, Climate, and the Hydrological Cycle. Science 294, 2119-2124.

Rampazzo G, Masiol M, Visin F, Rampado E, Pavoni B. 2008. Geochemical characterization of PM10 emitted by glass factories in Murano, Venice (Italy). Chemosphere 71, 2068-2075.

Ravindra K, Benc L, Wauters E, de Hoog J, Deutsch F, Roekens E, et al. 2006. Seasonal and sitespecific variation in vapour and aerosol phase PAHs over

Flanders (Belgium) and their relation with anthropogenic activities. Atmospheric Environment 40, 771–785.

Ravindra K, Sokhi R, Van Grieken R. 2008. Atmospheric polycyclic aromatic hydrocarbons: source attribution, emission factors and regulation. Atmospheric Environment. 42, 2895-2921.

Ringuet J, Albinet A, Leoz-Garziandia E, Budzinski H, Villenave E. 2012. Reactivityof polycyclic aromatic compounds (PAHs, NPAHs and OPAHs) adsorbed on natural aerosol particles exposed to atmospheric oxidants. Atmospheric Environment 61, 15-22.

Robinson AL, Donahue NM, Rogge WF. 2006a. Photochemical oxidation and changes in molecular composition of organic aerosol in the regional context. Journal of Geophysical Research 111, D03302.

Robinson AL, Subramanian R, Donahue NM, Bernardo-Bricker A, Rogge WF. 2006b. Source apportionment of molecular markers and organic aerosols 1. Polycyclic aromatic hydrocarbons and methodology for data visualization. Environmental Science and Technology 40, 7813–7820.

Robock A. 2011. Surface Cooling due to Forest Fire Smoke, Journal of Geophysical Research 96(11), 20869-20878.

Rogula-Kozłowska W, Klejnowski K, Rogula-Kopiec P, Ośródka L, Krajny E, et al. 2014. Spatial and seasonal variability of the mass concentration and chemical composition of PM2.5 in Poland. Air Quality Atmosphere and Health 7, 41–58.

Rolph GD. 2013. Real-time Environmental Applications and Display System (READY) Website (http://www.ready.noaa.gov). NOAA Air Resources Laboratory, College Park, MD.

Saarnio K, Sillanpää M, Hillamo R, Sandell E, Pennanen AS, Raimo O. 2008. Polycyclic aromatic hydrocarbons in size-segregated particulate matter from six urban sites in Europe. Atmospheric Environment 42, 9087–9097.

Saarnio K. Aurela M, Timonen H, Saarikoski S, Teinila K, Makela T, et al. 2010. Chemical composition of fine particles in fresh smoke plumes from boreal wild-land fires in Europe. Science of the Total Environment 408, 2527-2542

Salam A, Hossain T, Siddique MNA, Alam SAM. 2008. Characteristics of atmospheric trace gases, particulate matter, and heavy metals pollution in Dhaka, Bangladesh. Air Quality Atmospheric and Health 1, 101-109.

Salma I, Chi X, Maenhaut W. 2004. Elemental and organic carbon in urban canyon and background environments in Budapest, Hungary. Atmospheric Environment 38, 27–36.

Samet J, Wassel R, Holmes KJ, Abt E, Bakshi K. 2005. Research priorities for airborne particulate matter in the United States. Environ Science and Technology 39(14):299A-304A.

Sandrini N, Fuzzi S, Piazzalunga A, Prati P, Bonasoni P, Cavalli F, et al. 2014. Spatial and seasonal variability of carbonaceous aerosol across Italy. Atmospheric Environment

Schauer JJ, Kleeman MJ, Cas, GR, Simoneit BRT. 2002. Measurement of emissions from air pollution sources. 5. C1–C32 organic compounds from gasoline-powered motor vehicles. Environmental Science and Technology 36, 1169–1180.

Schauer JJ, Kleeman MJ, Cass GR, Simoneit BRT. 2001. Measurement of emissions from air pollution sources. 3. C1–C29 organic compounds from fireplace combustion of wood. Environmental Science and Technology 35, 1716–1728.

Schenone G, Lorenzini G. 1992. Effects of regional air pollution on crops in Italy. Agriculture Ecosystem & Environment 38, 51–59.

Schmauss A.1920. Die chemie des nebels der wolken und des regens. Die Unschau 24:61–63.

Schulz H, Harder V, Ibald-Mulli A, Khandoga A, Koenig W, Krombach F, Radykewicz R, Stampft A, Thorand B, and Peters A. 2005. Cardiovascular effects of fine and ultrafine particles. Journal of Aerosol Medicine 18, 1-22.

Schwartz J, Dockery DW, Neas LM. 1996. Is Daily Mortality Associated Specifically with Fine Particles? Journal of Air and Waste Management Association 46, 927-939.

Schwartz J, Dockery DW. 1992. Increased Mortality in Philadelphia Associated with Daily Air Pollution Concentrations. American Review of Respiratory Disease 145, 600-604.

Schwartz J. 1994. Air-Pollution and Daily Mortality - a Review and Meta Analysis. Environmental Research 64(1): 36-52.

Schwarz J, Chi X, Maenhaut W, Civis M, Hororka J, Smolik J. 2008. Elemental and organic carbon in atmospheric aerosols at downtown and suburban sites in Prague. Atmospheric Research 90, 287-302.

Seinfeld JH, Pandis SN. 1998. Atmospheric Chemistry and Physics: From Air Pollution to Climate Change. John Wiley, New York.

Seinfeld JH, Pandis SN. 2006. Atmospheric Chemistry and Physics: From Air Pollution to Climate Change. John Wiley & Sons Inc, New York.

Sippula O, Hokkinen J, Puustinen H, Yli-Pirila P, Jokiniemi J. 2009. Comparison of particle emissions from small heavy fuel oil and wood-fired boilers. Atmospheric Environment 43 (32), 4855-4864.

Šišović A, Vađić Ž, Šega K, Bešlić I, Vađić V. 2005. Comparison between PAH mass concentrations measured in PM_{10} and $PM_{2.5}$ particle fractions. Bulletin of Environmental Contamination and Toxicology 75, 121–126.

Smith KR. 1987. Biofuels, Air Pollution, and Health—a Global Review. Plenum Press, New York.

Soclo H, Garrigues P, Ewald M. 2000. Origin of polycyclic aromatic hydrocarbons (PAHs) in coastalmarine sediments: case studies in Cotonou (Benin) and Aquitaine (France) areas. Marine Pollution Bulletin 40, 387–396.

Sogacheva L, Hamed A, Facchini MC, Kulmala M, Laaksonen A. 2007. Relation of air mass history to nucleation events in Po Valley, Italy, using back trajectories analysis.

Sohrabpour M, Mirzaee H, Rostami S, Athari M. 1999. Elemental concentration of the suspended particulate matter in the air of Tehran. Environment International 25, 75‐81.

Spurny KR. 2001. Historical Aspects of Aerosols. In: Baron PA and Willeke K (Eds) Aerosol measurement: Principles, techniques and applications. John wiley & Sons Inc., New York.

Squizzato S, Masiol M, Brunelli A, Pistollato S, Tarabotti E, Rampazzo, et al. 2012a. Factors determining the formation of secondary inorganic aerosol: a case study in the Po Valley (Italy). Atmospheric Chemistry and Physics 12, 16377–16406.

Squizzato S, Masiol M, Innocente E, Pecorari E, Rampazzo G, Pavoni B. 2012b. A procedure to assess local and long-range transport contributions to $PM_{2.5}$ and secondary inorganic aerosol. Journla of Aerosol Science 46, 64-75.

Squizzato S. 2011. Particulate matter and secondary particulate inorganic: distribution and origin in the Venice area. PhD thesis in Environmental Sciences. Ca Foscari University of Venice.

Sternbeck J, Sjodin A, Andrèasson K. 2002. Metal emissions from road traffic and the influence of resuspension-results from two tunnel studies. Atmospheric Environment 36, 4735-4744.

Stohl A. 1998. Computation, accuracy and applications of trajectories—a review and bibliography. Atmospheric Environment 32, 947–966.

Stracquadanio M, Apollo G, Trombini C. 2007. A Study of $PM_{2.5}$ and $PM_{2.5}$-Associated Polycyclic Aromatic Hydrocarbons at an Urban Site in the Po Valley (Bologna, Italy).

Taylor BN, Kuyatt CE. 1994. Guidelines for evaluation and expressing the uncertainty of NIST measurement results. US Government Printing Office, Washington DC,

Taylor SR. 1964. Abundances of chemical elements in the continental crust, a new table. Geochimica et cosmochimica acta XXVIII, 1273-1285.

Tecer LH, Tuncel G, Karaca F, Alagha O, Suren P, Zararsiz A, Kirmaz, R. 2012. Metallic composition and source apportionment of fine and coarse particles using positive matrix factorization in the southern Black Sea atmosphere. Atmospheric Research 118, 153-169.

Tham YWF. Takeda K, Sakugawa H. 2008. Polycyclic aromatic hydrocarbons (PAHs) associated with atmospheric particles in Higashi Hiroshima, Japan: Influences of meteorological conditions and seasonal variations. Atmospheric Research 88, 224-233.

Tie X, Wu D, and Brasseur G. 2009. Lung cancer mortality and exposure to atmospheric aerosol particles in Guangzhou, China, Atmospheric Environment 43, 2375-2377.

Tolis EI, Saraga DE, Lytra MK, Papathanasiou ACh, Bougaidis PN, Prekas-Patronakis OE, et al. 2015. Concentration and chemical composition of $PM_{2.5}$ for a one-year period at Thessaloniki, Greece: A comparison between city and port area. Atmospheric Environment 113, 197-207.

Tsapakis M, Stephanou EG. 2005. Occurrence of gaseous and particulate polycyclic aromatic hydrocarbons in the urban atmosphere: study of sources and ambient temperature effect on the gas/particle concentration and distribution. Environmental Pollution 133, 147–156.

Turpin BJ, Huntzicker JJ. 1995. Identification of secondary organic aerosol episodes and quantification of primary and secondary organic aerosol concentrations during SCAQS. Atmospheric Environment 29, 3527–44.

Uria-Tellaetxe I, Carslaw DC, 2014. Conditional bivariate probability function for source identification. Environmental Modelling & Software 59, 1-9.

USEPA (United States Environmental Protection Agency). 2001. Risk Assessment Guidance for Superfund:Volume III — Part A, Process for Conducting Probabilistic Risk Assessment Office of Emergency and Remedial Response. U.S. Environmental Protection Agency,Washington, D.C., p. 20460.

USEPA (United States Environmental Protection Agency). 2004. Risk Assessment Guidance for Superfund Volume I: Human Health Evaluation Manual (Part E, Supplemental Guidance for Dermal Risk Assessment). Office of Superfund Remediation and Technology Innovation, Washington, D.C.

USEPA (United States Environmental Protection Agency). 2009. Risk Assessment Guidance for Superfund Volume I: Human Health Evaluation Manual (Part F,

Supplemental Guidance for Inhalation Risk Assessment). Office of Superfund Remediation and Technology Innovation, Washington, D.C.

USEPA (United States Environmental Protection Agency). 2011. Exposure Factors Handbook: 2011 Edition.National Center for Environmental Assessment, Washington, D.C. (EPA/600/R-09/ 052F. Available from the National Technical Information Service, Springfield, VA, and online at http://www.epa.gov/ncea/efh).

Vardoulakis S, Kassomenos P. 2008. Sources and factors affecting PM_{10} levels in two European cities: Implications for local air quality management. Atmospheric Environment 42, 3949-3963.

Venkataraman C, Friedlander SK. 1994. Size distribution of polycyclic aromatic hydrocarbons and elemental carbon 2. Ambient measurements and effects of atmospheric processes, Environmental Science and Technology 28, 563-572.

Viana M, Lopex JM, Querol X, Alastuey A, Garcio D, Blanco-Beras G, et al. 2008a. Tracers and impact of open burning of rice straw residues on PM in Eastern Spain, Atmospheric Environment 42, 1941:1957.

Viana M, Maenhaut W, Brink HM, Chi X, Weijers E, Querol X, et al. 2007. Comparative analysis of organic and elemental carbon concentrations in carbonaceous aerosols in three European cities. Atmospheric Environment 41, 5972–5983.

Viana M, Querol X, Alastuey A, Ballester F, Llop S. 2008b. Characterizing exposure to PM aerosols for an epidemiological study. Atmospheric Environment 42, 1552–1568.

Viidanoja J, Sillanpa, M, Laakia J, Kerminen V, Hillamo R, Aarnio,P, Koskentalo T. 2002. Organic and black carbon in $PM_{2.5}$ and PM_{10}: 1 year of data from an urban site in Helsinki, Finland. Atmospheric Environment 36, 3183–3193.

Villar-Vidal M, Lertxundi A, de Dicastillo MDML, Alvarez JI, Marina LS, Ayerdi M, et al. 2014. Air Polycyclic Aromatic Hydrocarbons (PAHs) associated with PM2.5 in a North Cantabric coast urban environment. Chemosphere 99, 233-238.

Wang W. 2010. Inorganic and organic speciation of atmospheric aerosols by ion chromatography and aerosol chemical mass closure. PhD thesis. University of Gent.

Watson JG, Chow JC, Houck JE. 2001. $PM_{2.5}$ chemical source profiles for vehicle exhaust, vegetative burning, geological material, and coal burning in northwestern Colorado during 1995, Chemosphere 43(8), 1141–1151.

Watson JG. 2002. Visibility: Science and Regulation. Journal of Air & Waste Management Association 52, 628-713.

Wayne RP, Barnes I, Biggs P, Burrows JP, Canosa-Mas CE, Hjorth J, et al. 1991. The nitrate radical: Physics, chemistry and the atmosphere. Atmospheric Environment 25A, 1-203.

Wcisło E, Ioven D, Kucharski R, Szdzuj J. 2002. Human health risk assessment case study: an abandoned metal smelter site in Poland. Chemosphere 47, 507–515.

Wedepohl KH. 1995. The composition of the continental crust. Geochimica et cosmochimica acta, Vol. 59 (7), 1217-1232.

WHO (World Health Organization). 1987. Air Quality Guidelines for Europe WHO Regional Publication, European Series No. 23. World Health Organization, Copenhagen.

WHO (World Health Organization). 2000. Air quality guidelines for Europe. 2nd ed. Copenhagen: WHO Regional Publications; European Series No. 91.

Whytlaw-Gray R, Speakman JB, Campbell JHP. 1923. Smokes part I—a study of their behaviour and a method of determining the number of particles they contain. Proceedings of the Royal Society of London A 102, 600–615.

Wilson WE, Chow JC, Claiborn C, Fusheng W, Engelbrecht J, Watson JG. 2002. Monitoring of particulate matter outdoors. Chemosphere 49, 1009-1043.

World Health organization (WHO). 2002. World Health Report 2002: Reducing Risks, Promoting Life. http://www.who.int/whr/en/S.

Xie M, Barsanti KC, Hannigan MP, Dutton SJ, Vedal S. 2013. Positive matrix factorization of PM2.5-eliminating the effects of gas/particle partitioning of semivolatile organic compounds. Atmospheric Chemistry and Physics 13, 7381-7393.

Xu X, Barsha NAF, Li J. 2008. Analyzing Regional Influence of Particulate Matter on the City of Beijing, China. Aerosol and Air Quality Research 8, 78-93.

Yamasaki H, Kuwata K, Miyamoto H. 1982. Effects of temperature on aspects of airborne polycyclic aromatic hydrocarbons, Environmental Science and Technology 16, 189-194.

Yttri KE, Aas W, Bjerke A, Cape JN, Cavalli F, Ceburnis D, et al. 2007. Elemental and organic carbon in PM10: a one year measurement campaign within the European Monitoring and Evaluation Programme EMEP. Atmospheric Chemistry and Physics 7, 5711-5725.

APPENDICES

Appendix- 3
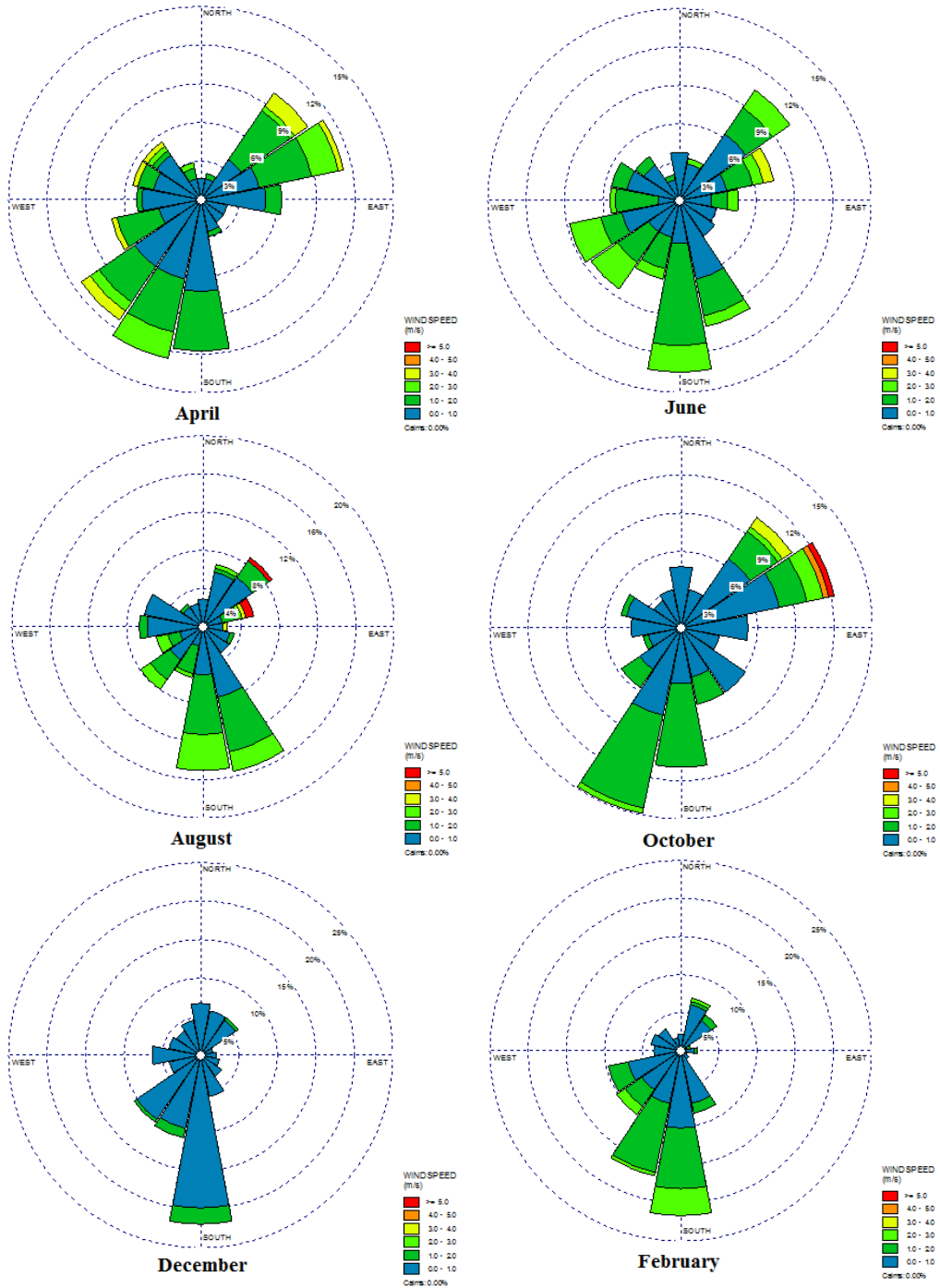
Figure A-3.1.Wind-rose of Belluno
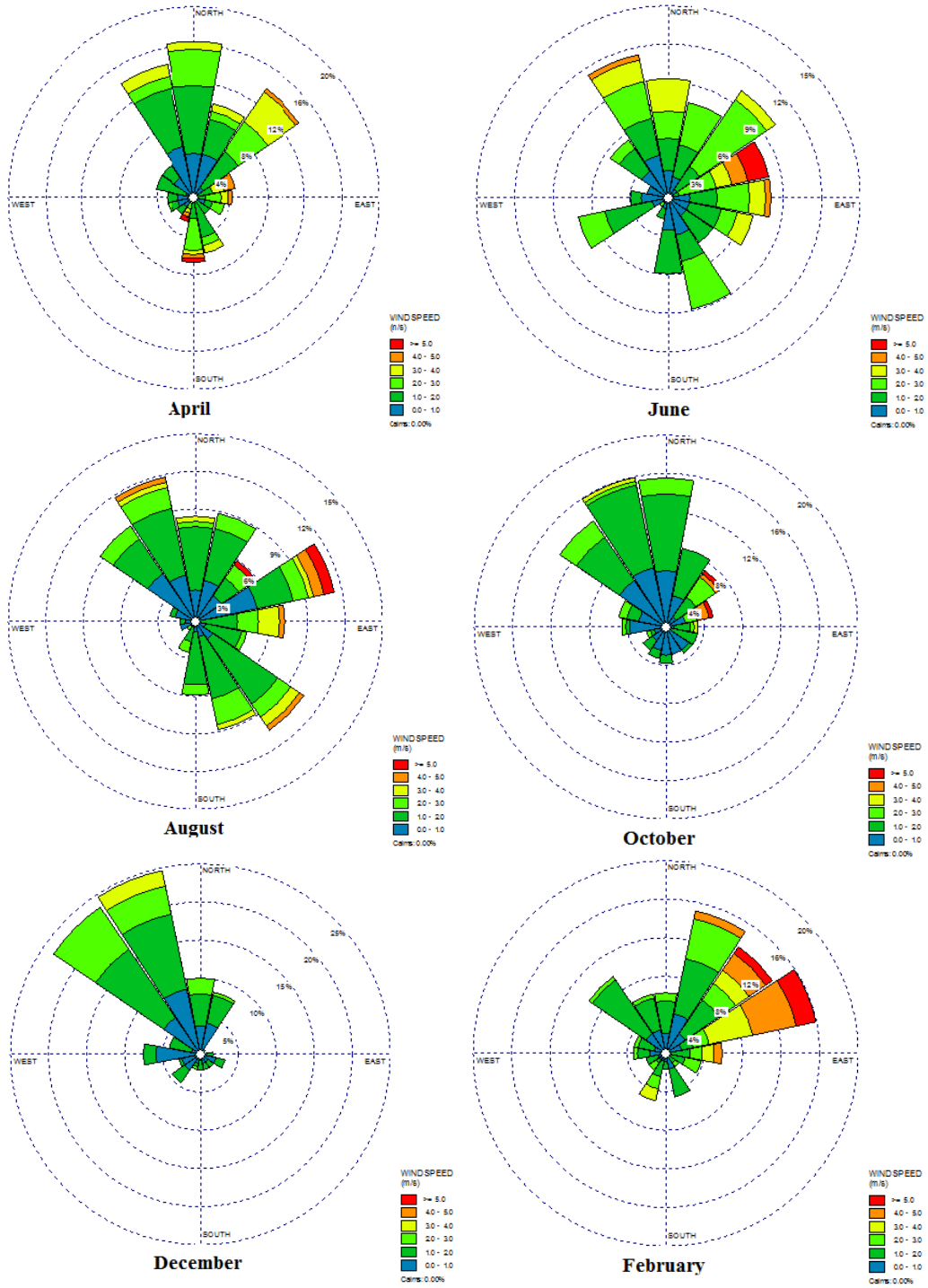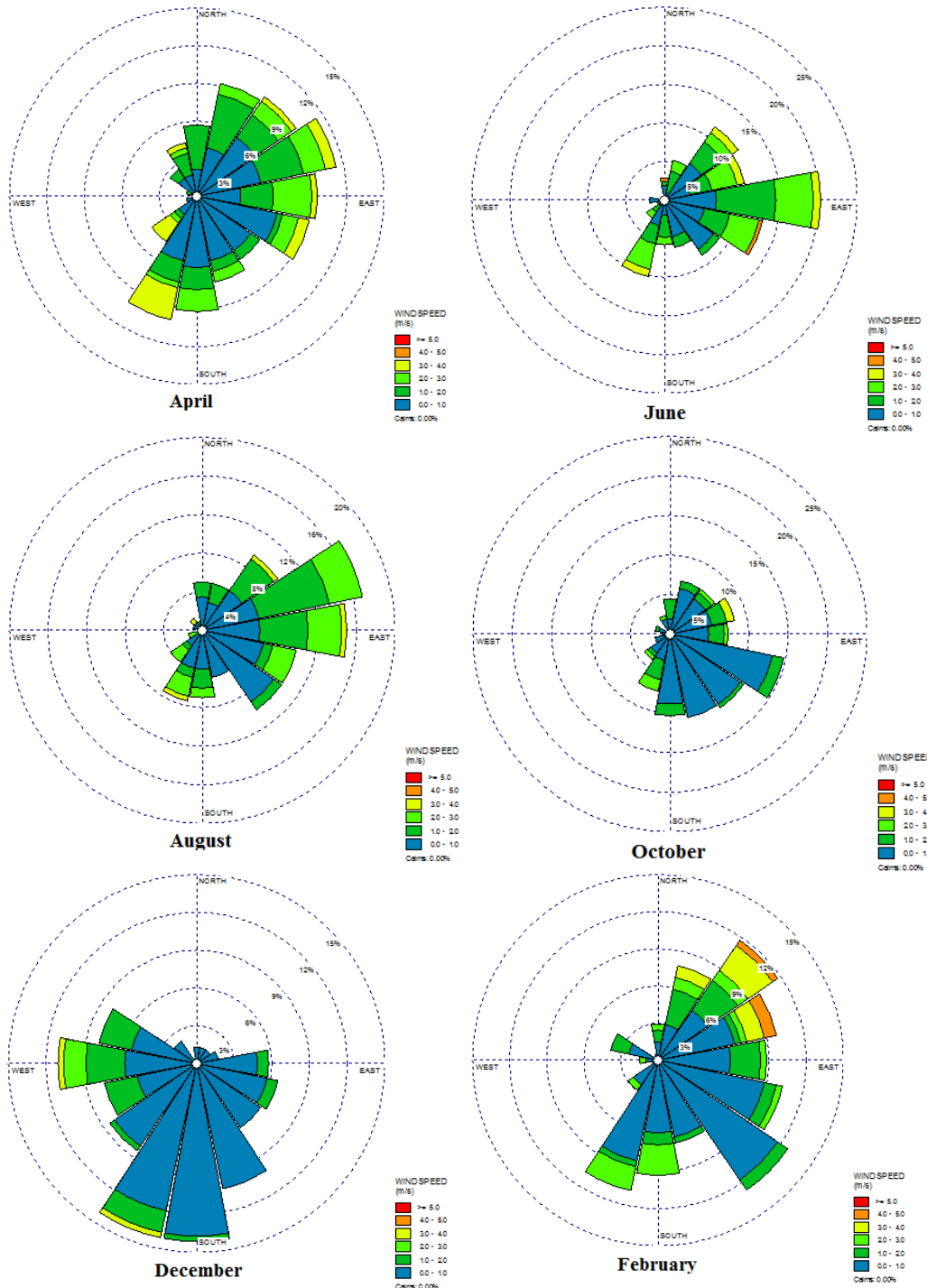
Figure A-3.2. Wind-rose of Treviso
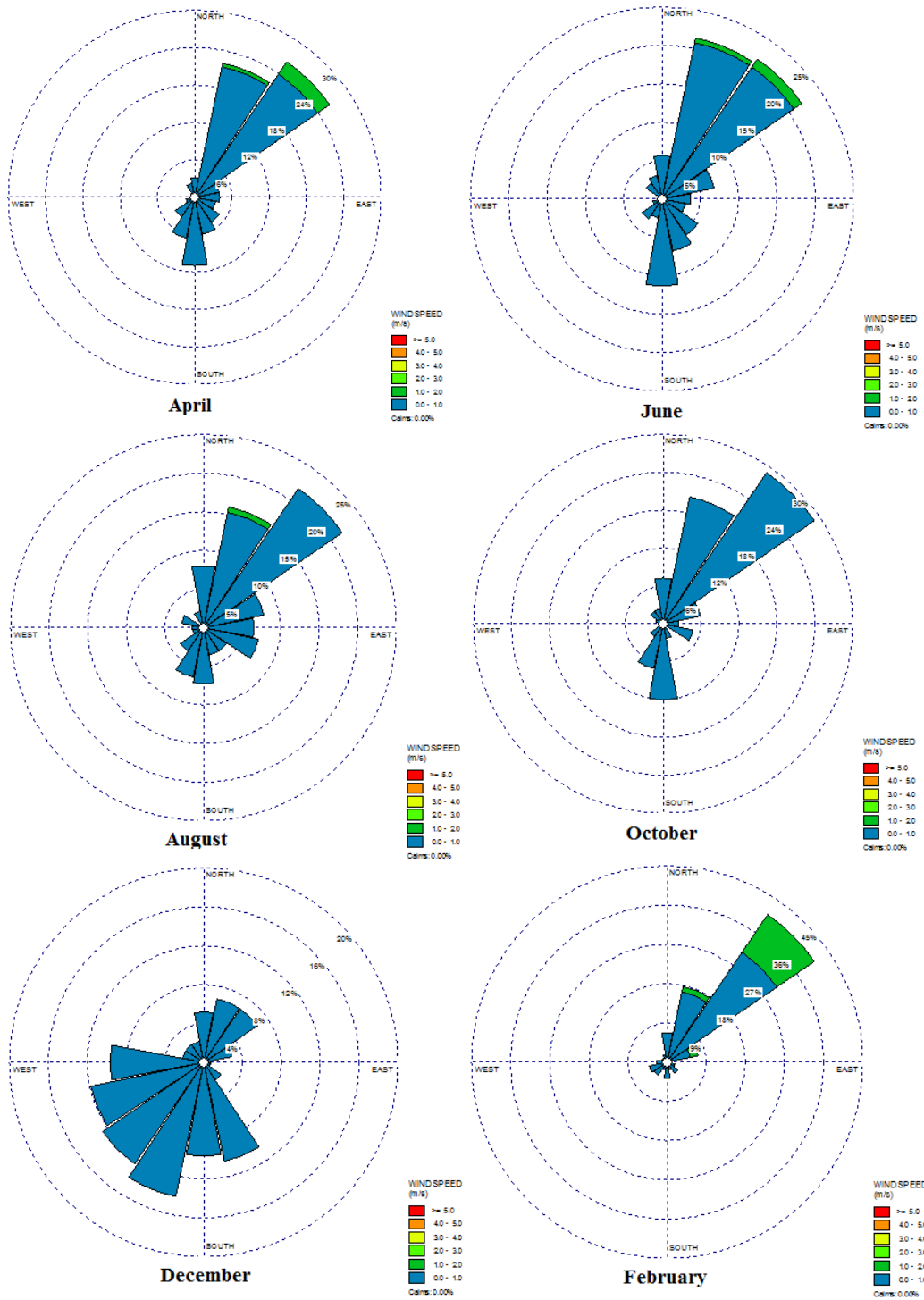
Figure A-3.3. Wind-rose of Vicenza

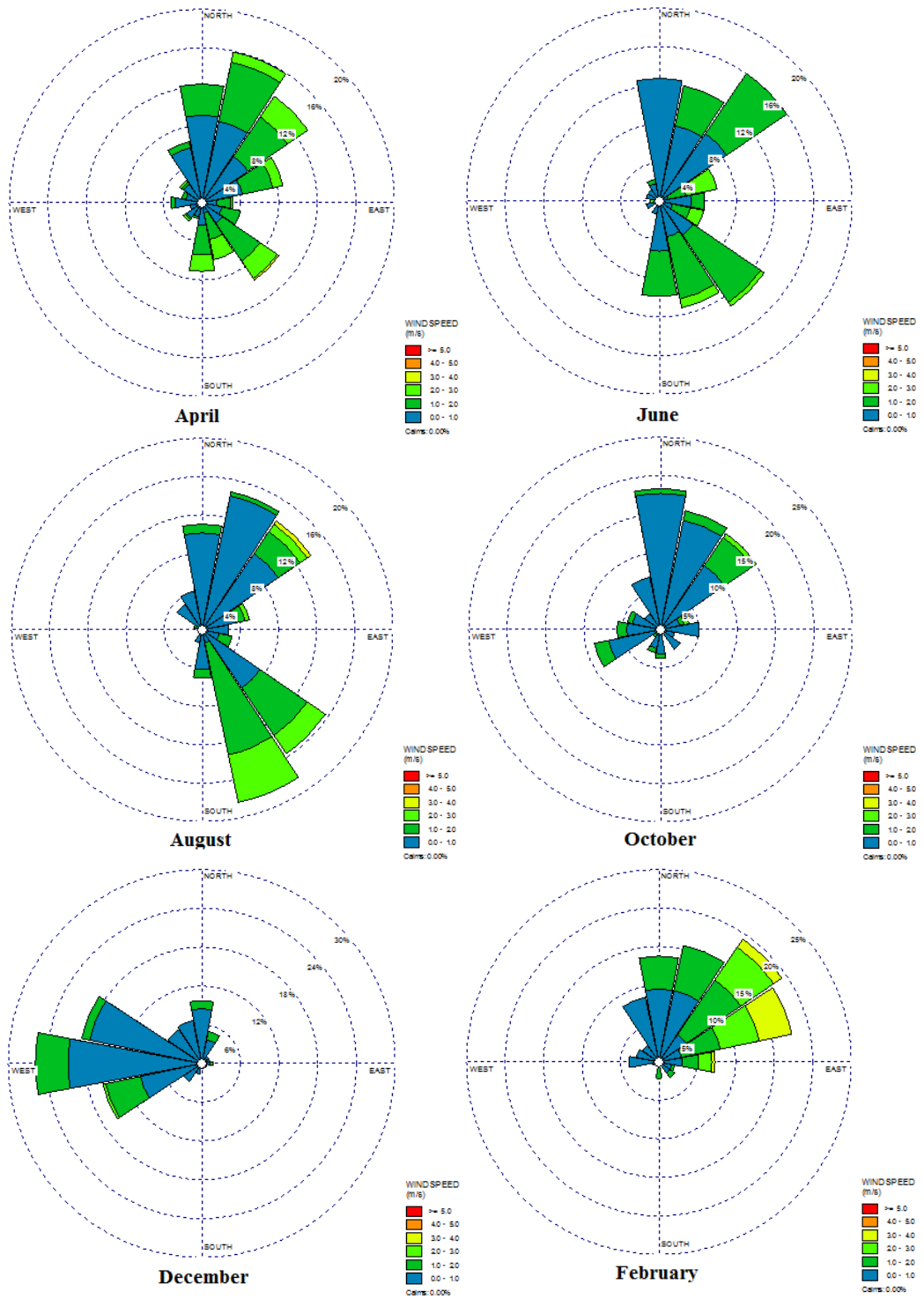Figure A-3.4. Wind-rose of Padova

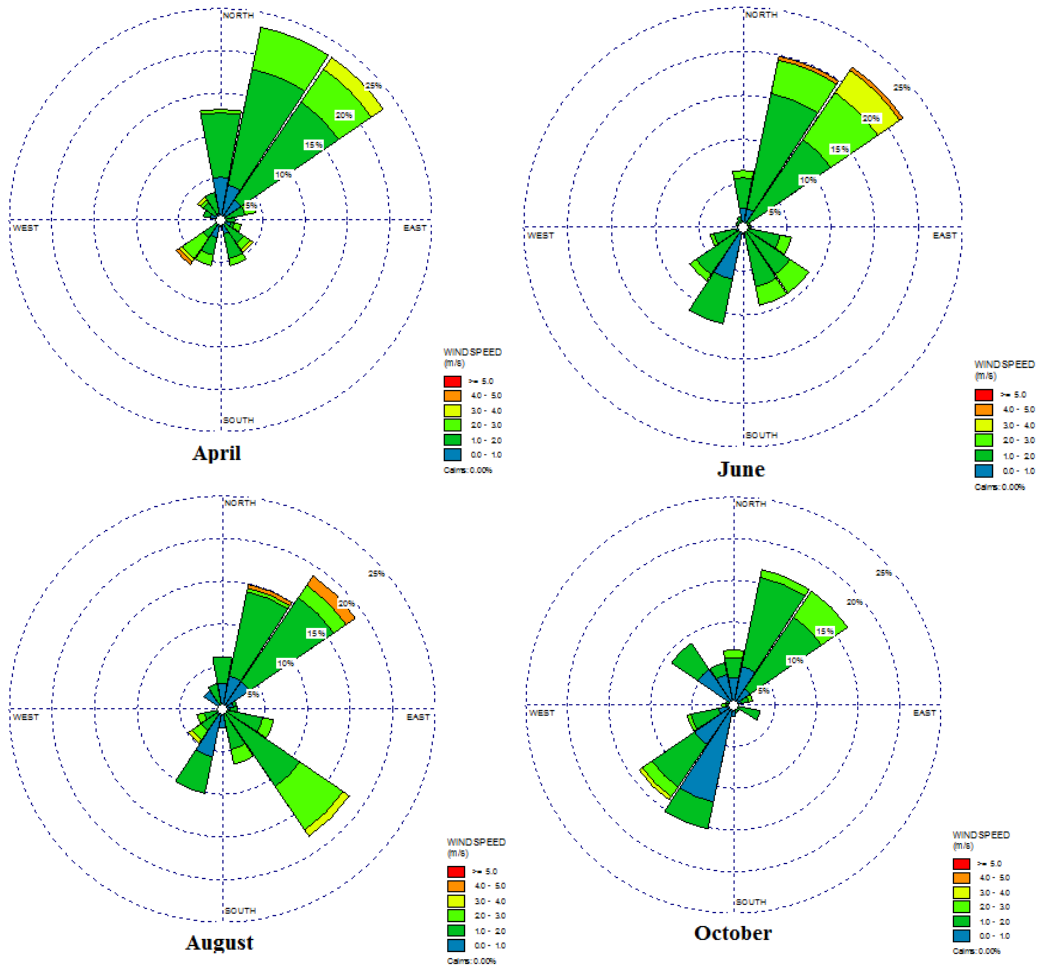Figure A-3.5. Wind-rose of Venice

Figure A-3.6. Wind-rose of Rogivo

Appendix – 4

Table A-4.1. The *p-value* and level of significance of the parameters of model

	Estimate	Std. Error	t-value	P-value	Level of significance
Intercept	0.388	0.051	7.588	0000	***
logEC	0.323	0.051	6.326	0000	***
Month_Feb	0.556	0.045	12.199	0000	***
Month_Jun	-0.003	0.061	-0.051	0.959	
Month_Aug	0.048	0.067	0.714	0.008	
Month_Oct	0.080	0.030	0.629	0000	**
Month_Dec	0.588	0.055	10.548	0000	***
Temp	0.007	0.004	1.875	0.06 1	.
Wind	-0.109	0.014	-7.575	3.73×10^{-13} ***	***

Here, *** is the 0.1 % level of significance and ** is the 1% level of significance

Figure A-4.1. Weights of the root

Here, model identified three outliers
219: Measurement station Padova 39 (Octber 20, 2012): Relative Humidity (91.4%):
220: Measurement station Padova 40 (October 21, 2012) Relative Humidity (91.6%)
279: Measurement station Venice 39 (October 20,) Relative Humidity (95.5%)
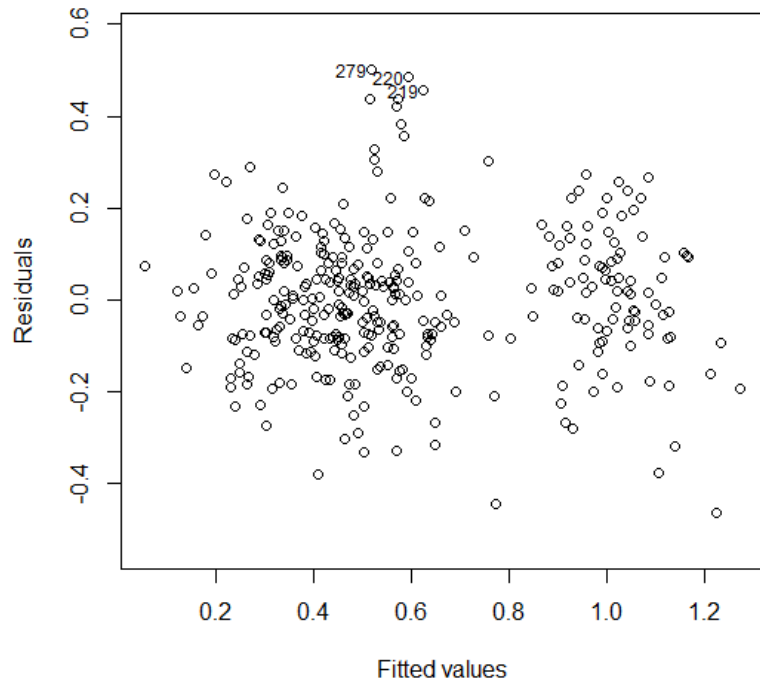
Figure A-4.2. Fitted values vs Residuals
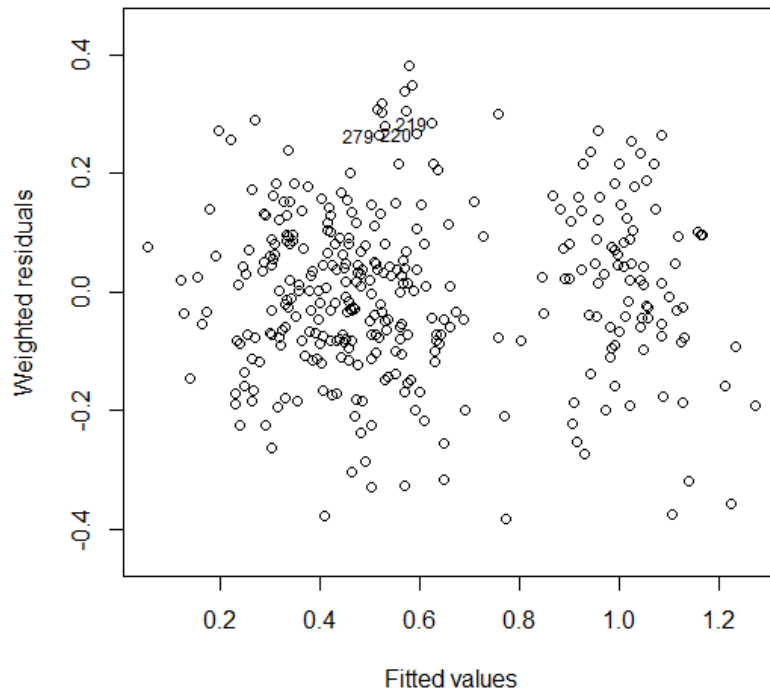
Figure A-4.3. Fitted values vs Weighted residuals

Figure A-4.4. City maps with highlighted sources
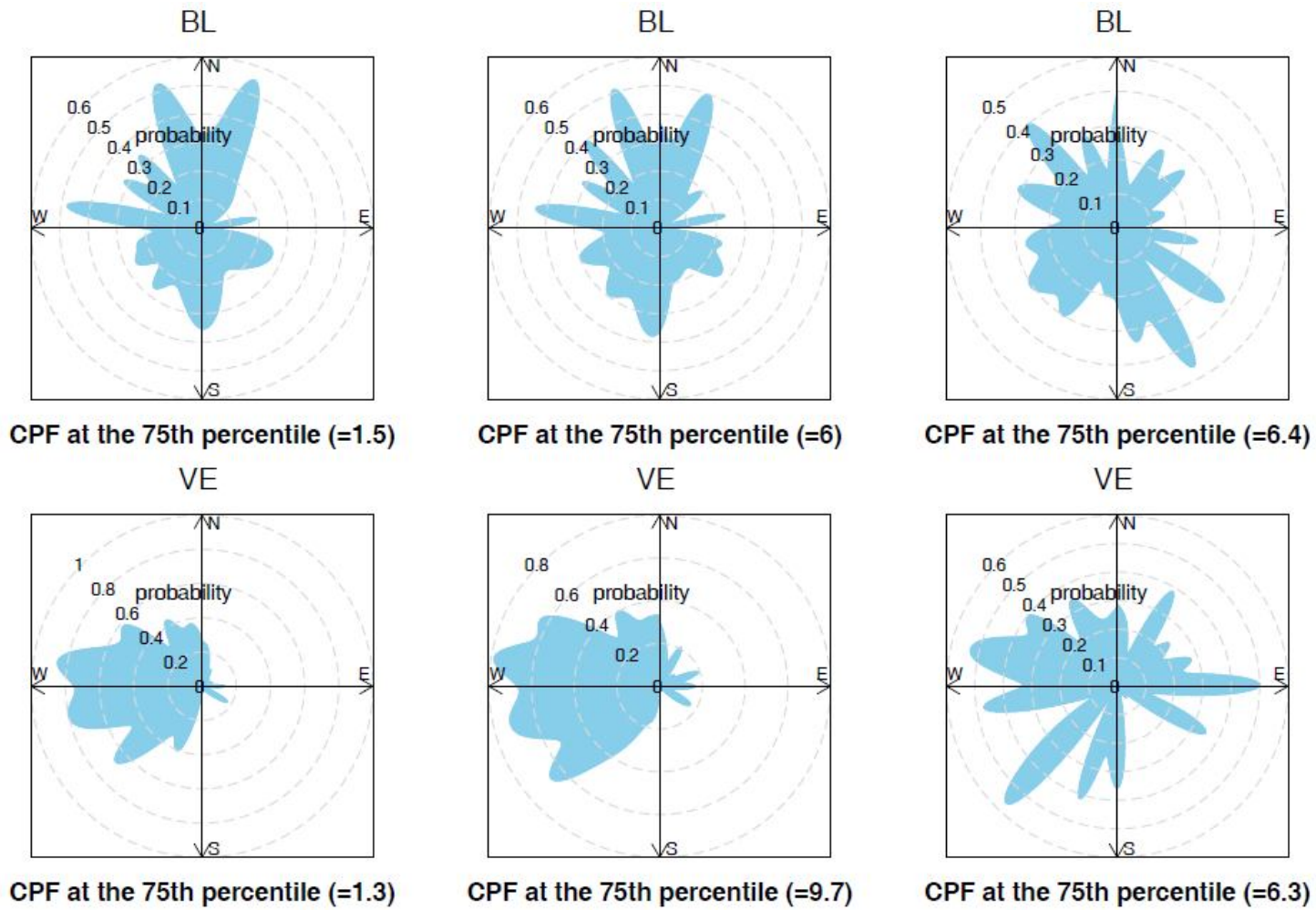
Figure A-4.5. CPF plots for EC, OC concentrations and OC/EC ratios in BL and VE
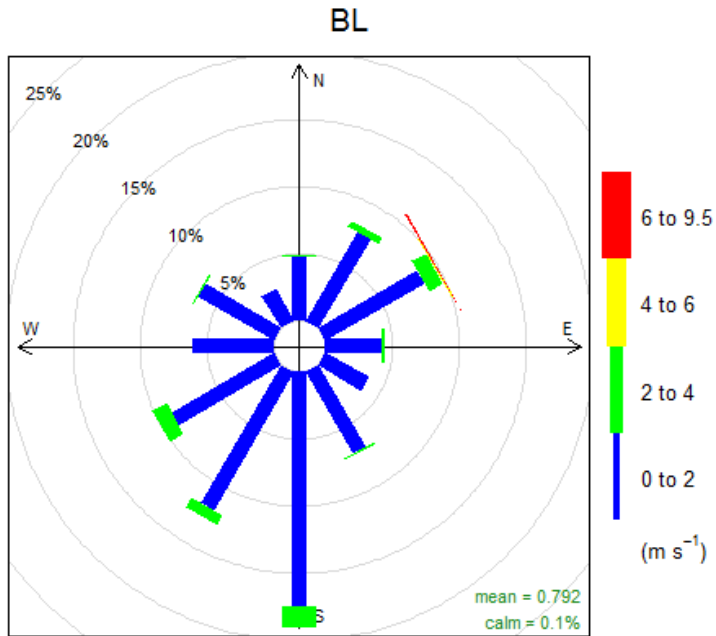
(a)
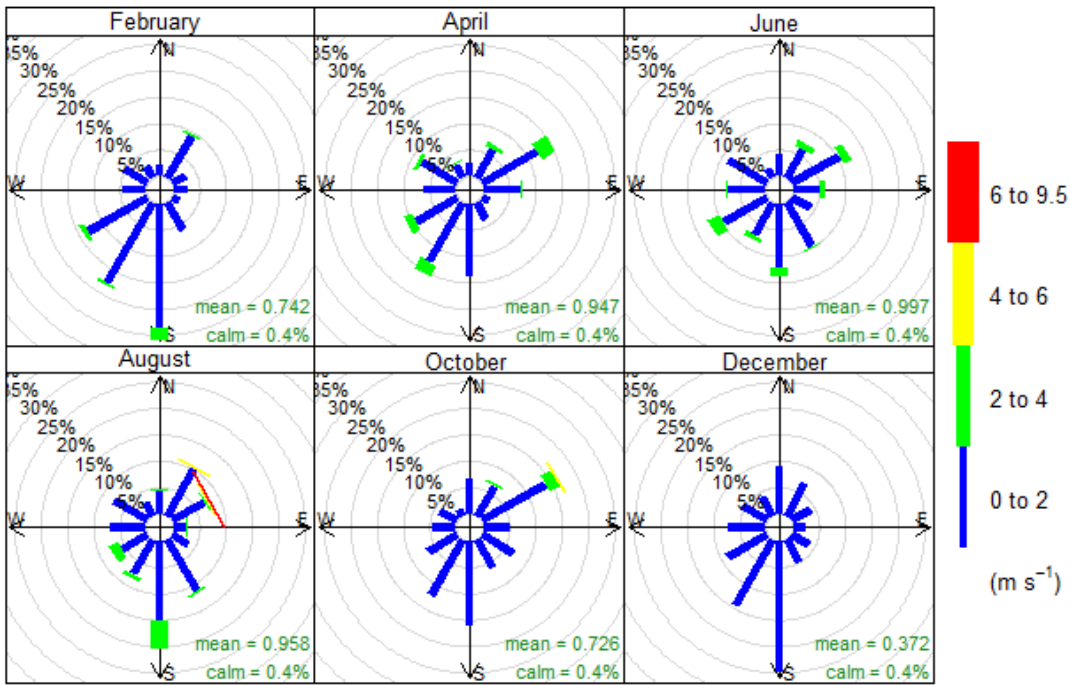
(b)

Figure A-4.6. Wind rose showing (a) annual and (b) monthly wind speed and direction frequencies at Belluno.
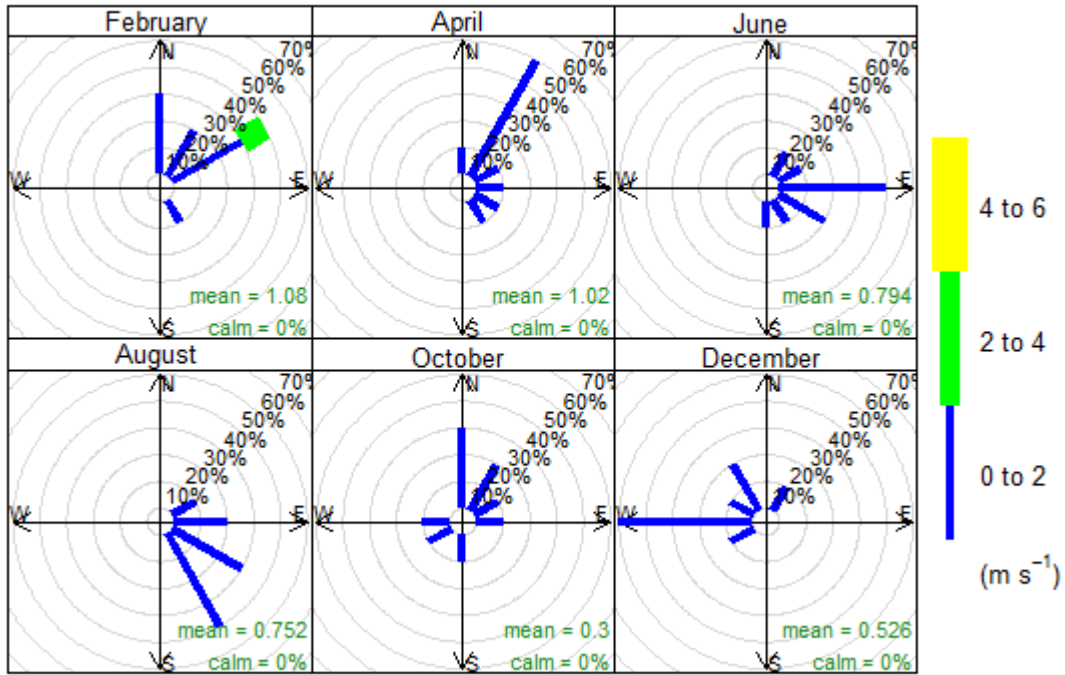
Figure A-4.7. Wind rose showing the monthly wind speed and direction frequencies at Venice.

Appendix – 5

Table A-5.1. Spearman's rank correlations (bottom-left) and Kruskal-Wallis analysis of variance (top-right) calculated for the PAHs levels among sites.

	Provinces					
	BL	TV	VI	PD	VE	RO
BL	-	0.22	0.000	0.08	0.01	0.000
TV	0.90		0.79	1.0	1.0	0.09
VI	0.84	0.95		1.0	1.0	1.0
PD	0.82	0.92	0.97		1.0	0.21
VE	0.82	0.92	0.95	0.95		1.0
RO	0.79	0.85	0.89	0.91	0.84	

Table A-5.2. Carcinogenic and Mutagenic values used for the congeners

Congeners	TEFs[a]	MEFs[b]
BaA (ng m^{-3})	0.1	0.082
Chry (ng m^{-3})	0.01	0.017
BbF (ng m^{-3})	0.1	0.25
BkF (ng m^{-3})	0.1	0.11
BaP (ng m^{-3})	1	1
IP (ng m^{-3})	0.1	0.31
DBahA (ng m^{-3})	1	0.29
BghiP (ng m^{-3})	0.01	0.19

[a] Nisbet and LaGoy (1992); [b] Durant et al. (1996)
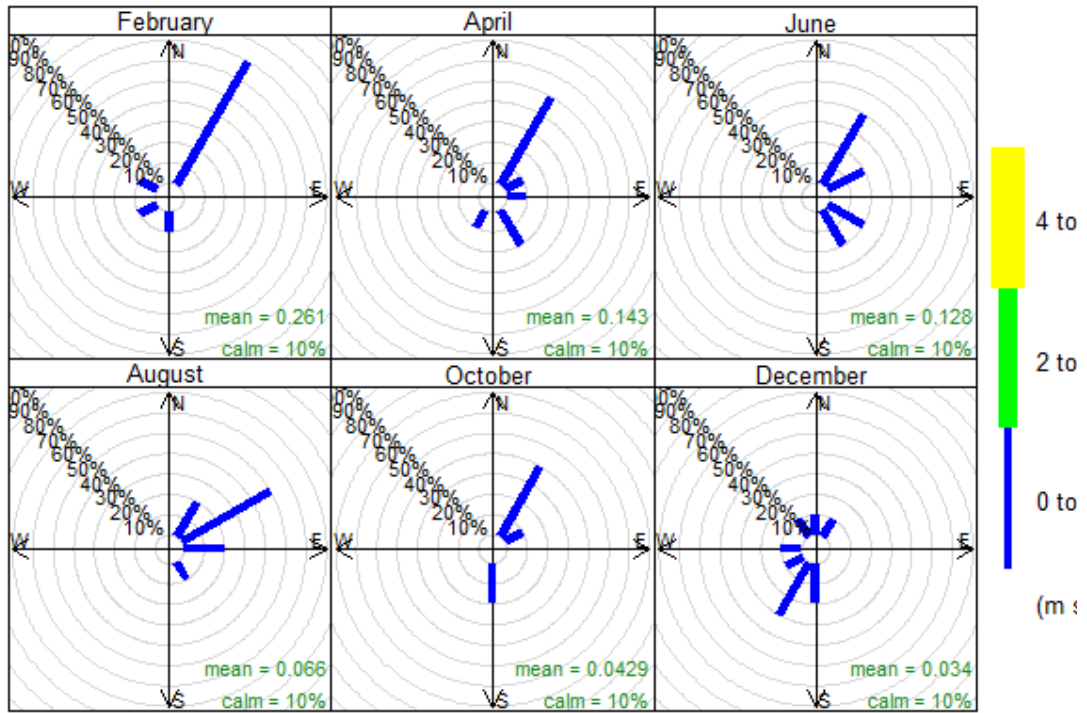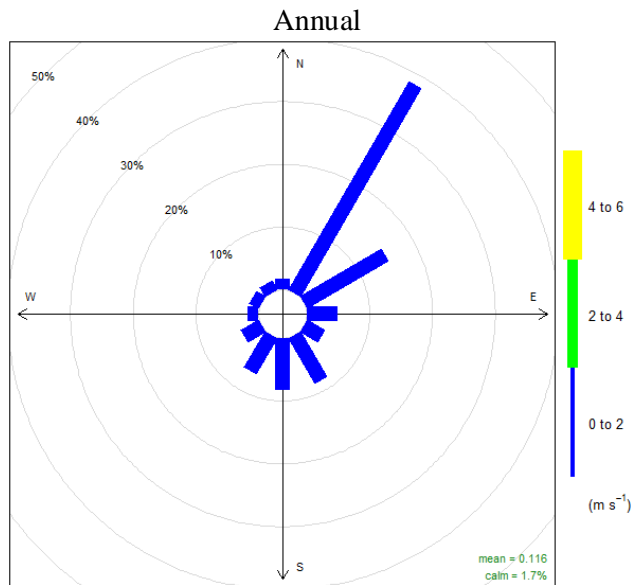
Figure A-5.1. Wind rose showing the wind speed and direction frequencies at Padova.
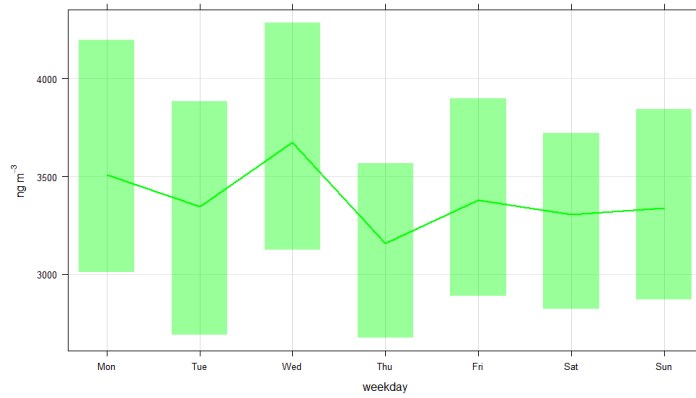
Appendix 6

Figure A-6.1. The concentration of metal ($\sum_{18}$ between week and weekend over Veneto region.

References

Durant, J., Busby, W., Lafleur, A., Penman, B., Crespi, C., 1996. Human cell mutagenicity of oxygenated, nitrated and unsubstituted polycyclic aromatic hydrocarbons associated with urban aerosols. Mutation Research/Genetic Toxicology 371, 123-157.

Nisbet, C., LaGoy, P., 1992. Toxic equivalency factors (TEFs) for polycyclic aromatic hydrocarbons (PAHs). Regulatory Toxicology and Pharmacology 16, 290-300.

Estratto per riassunto della tesi di dottorato

L'estratto (max. 1000 battute) deve essere redatto sia in lingua italiana che in lingua inglese e nella lingua straniera eventualmente indicata dal Collegio dei docenti.
L'estratto va firmato e rilegato come ultimo foglio della tesi.

Studente: MD. BADIUZZAMAN KHAN_____ matricola: 956030

Dottorato: Scienze Ambientali **/** Environmental Science

Ciclo: XXVIII_____

Titolo della tesi[1]: Inorganic and Organic Pollutants in Atmospheric Aerosols: Chemical Composition and Source Apportionment

Inquinanti inorganici ed organici nell'aerosol atmosferico: composizione chimica e identificazione/quantificazione delle fonti di inquinamento

Abstract:

In Italiano: Questo lavoro è il primo condotto in Veneto, Italia, con la collaborazione di ARPAV, che riguarda importanti inquinanti organici (OC / EC e IPA) e inorganici (elementi in tracce), che sono stati caratterizzati per un periodo di tempo relativamente lungo, al fine di quantificare i contributi per la formazione del PM2.5 a scala regionale. I campioni (n=360) sono stati raccolti da sei grandi città situate in 6 province da aprile 2012 a febbraio 2013. I risultati mostrano che OC, EC, IPA ed elementi in tracce hanno concentrazioni maggiori durante i mesi invernali in tutte le stazioni di campionamento: l'atmosfera stabile, il minore spessore dello strato di mescolamento e la temperatura giocano un ruolo importante per l'accumulo di inquinanti. I parametri meteorologici, soprattutto la velocità del vento e la temperatura, hanno una significativa influenza sull'accumulo di sostanze inquinanti provenienti da fonti locali. Infine, le possibili fonti di particolato sono state caratterizzate usando una procedura basata su Conditional Bivariate Probability Function, Diagnostic ratios and Factor Analysis. I risultati indicano che la combustione di biomassa per il riscaldamento domestico e la cottura, seguiti da traffico veicolare, combustione di petrolio e la risospensione di elementi crostali sono le principali fonti di particolato nella regione Veneto.

In English: This work is the first one conducted in the Veneto region, Italy, with the collaboration of ARPAV and includes important organic (OC/EC and PAHs) and inorganic (trace elements) pollutants, which were characterized for a relatively long period of time in order to quantify the source contributions of $PM_{2.5}$ at regional scale. Samples (n=360) were collected from six major cities located in 6 Provinces during April 2012 - February 2013. Results show that OC, EC, PAHs and trace elements exhibited higher concentrations during winter months in all measurement sites, suggesting that a stable atmosphere and a lower mixing layer play an important role for the accumulation of pollutants. Meteorological parameters, especially wind velocity and temperature, significantly influence pollutant accumulation from local sources. Finally, the possible sources of particulate matter have been characterized using procedures like Conditional Bivariate Probability Function, Diagnostic ratios and Factor Analysis and results indicate that biomass burning for household heating and cooking, followed by vehicular traffic, oil combustion and resuspension of crustal elements are the main sources of particulate matter in the Veneto region.

Firma dello student
___ _____

---

[1] Il titolo deve essere quello definitivo, uguale a quello che risulta stampato sulla copertina dell'elaborato consegnato.